6.07 Magmatism, Magma, and Magma Chambers

B. D. Marsh, Johns Hopkins University, Baltimore, MD, USA

© 2007 Elsevier B.V. All rights reserved.

6.07.1 Introduction

Magmatism is directly linked to tectonism. Where there is no tectonic activity, as in continental shield regions, there is no magmatism. Tectonic activity is a clear sign of convection in the mantle and often the crust, although the associated length scales may be much different. Relative to conduction of heat, convection moves material at rapid rates. This manifests itself in the inability of rock to cool easily during convection, which, coupled with the condition that much of the lower crust and mantle is already near melting, brings on melting as rock is adiabatically convected through a solidus. Convection through a phase boundary is the major process of producing magma on Earth. This form of melting is progressive, and instabilities associated with the field of affected rock, which depend on the size of the field, the degree of melting, and the nature of the melt itself, simultaneously arise to collect and transport the magma upward to Earth's surface. Most magmas thus arise through partial melting of source or parent rock. The collected magma may contribute to volcanism or, perhaps more often, become stalled at depth in plutonism. This overall process is called 'magmatism'. This is the process that has given rise to the diversity of rocks on Earth's surface and perhaps also to the very structure of Earth itself. Within any process of magmatism there are certain physical and chemical processes that are truly fundamental to shaping the behavior and outcome of the magma and it is these that are considered herein.

Volcanoes on a planet reflect the physical processes at depth of magma production, collection, and transport. This is in contrast to magma produced *in situ* through an externally applied heat source as in partial melting of granitic continental crust by emplacement of higher-temperature basaltic magma in underplating (Bergantz, 1989) or prolonged heating of wall rock on the conduit of a volcanic system. Meteorite impact is also an effective means of magma production. The Sudbury melt sheet of Ontario, some 35 000 km^3 of magma, was produced in 5 min by a 10–12 km bolide 1.85 Ga. Wholesale melting of continental crust produced a magma superheated to ~1700°C, which is never found in endogenetic magmatism. Only the prolific volcanism of Io, due to viscous dissipation in tidal pumping by Jupiter, is similarly superheated. The most voluminous and steady magmatisms of Earth, like those of the ocean ridges and Hawaii, erupt magma at or near the liquidus, but never superheated. The low crystallinity of these magmas reflects this high-temperature eruptive state, whereas many island arc magmas, especially the andesitic ones, can be of high crystallinity; the most dangerous ones flirt with the point of critical crystallinity at 55 vol.%. As the phenocryst content approaches maximum packing at critical crystallinity the magma becomes a dilatant solid, expanding upon shear. The volcano becomes, in effect, corked or plugged, and can only erupt explosively. High-temperature, low-crystallinity basaltic magmas are not generally explosive, but the exceeding mobility of the lavas is dangerous. Cinder cone volcanism, commonly areally sporadic and associated with alkali basalts, is just the reverse. The early phase of volcanism is explosive, almost regardless of crystal content, but the associated lavas are sluggish and immobile. Explosiveness can thus reflect an enhanced volatile content, high crystallinity, or high silica content.

The pattern and style of magmatism intimately reflect the nature of the causative process. Globally widespread magmatism, as on Io, reflects planetwide melting as in tidal pumping or a heavy impact flux.

Linear arrays or strings of magmatism, as along ocean ridges, island arcs, and some ocean islands, reflect melting associated with thermoconvective flows tightly focused within the phase field of the source rock. That is, either the thermal regime or the source material (or both) is spatially focused. Areally widespread, small-volume magmatism as, for example, that of cinder cone fields, reflects a pervasive, marginally focused convective flow, much like a broad low-pressure system in the atmosphere, where melting instabilities are mainly due to local irregularities in the source rock detailed composition. Typical convective flows of this nature are the broad, gently upwelling flows associated with the wedge flows driven by subduction. Widespread, but voluminous magmatisms, as in the silicic volcanism of the western United States over the past 50 My, reflect convective stretching and destabilization of the continental lithosphere. The asthenosphere thermal regime is, in effect, brought to the Moho where vast regions of continental crust of irregular thickness are accessible to melting.

Volcanoes themselves, as opposed to impact melt sheets, reflect deep-seated, endogenetic processes, and in a simple way the volcanic edifice is a measure of the hydrostatic (i.e., magmastatic) head of the system. The size of volcanoes also reflects the activity or strength of the system, the mobility of the source relative to the surface plate, the strength (and thus age) of the local lithosphere, and the intensity of the gravitational field. The largest volcanoes in the solar system are in the Tharsis Bulge region of Mars. Olympus Mons is 30 km tall and 850 km in basal diameter. Martian gravity is weak, the lithosphere is very old and strong, and the source has evidently been immobile relative to the surface plate. For a given areal extent, the volcanoes of Venus are the shortest, reflecting the high-temperature, weak nature of the Venuisian lithosphere. This is broadly similar to the volcanoes within the rift zones of Iceland, where isostasy is rapid ($\sim$1 km My^{-1}) due to the thin, hot, and weak crust.

The plumbing of magmatic systems begins in the source region and ends at a volcano or pluton. Knowledge of the structure of volcanoes and plutons comes mainly from direct observations of field relations in deeply eroded terrains. The deeper source regions can be sensed, in terms of depth, degree of melting upon extraction, and source material, through geochemistry. Detailed knowledge of the physical state of these systems comes mainly from modeling and rare, well-exposed crustal rocks. Hypocenter distributions, particularly in active, voluminous systems, like Hawaii, are valuable in inferring the deeper geometric form, extent, and sense of connection between eruptions and deep transport. Some styles of harmonic tremor, which sometimes occurs during eruptive stages, seem to indicate the pre-eruptive state of magma held in vertically oriented cylindrical conduits. Ground deformation associated with tumescence prior to eruption consistently indicates through elastic modeling a local, near-surface staging region, which is commonly identified with the concept of a magma chamber. This is reinforced by the very nature and pervasiveness of plutons. Overall, the most commonly held conceptualization of a generic magmatic plumping system has a deep source region linked to a near-surface magma chamber through a poorly discerned transport region. Aside from the gross inferences from seismic studies, the intervening plumbing linking source to near surface, the ascent path, has been difficult to ascertain. Although magma perhaps spends most of its life in this part of the system, it has, *per force*, been largely ignored physically and chemically due to lack of a clear and detailed conception of this important feature. This basic magmatic architecture, source, ascent path, chamber, and pluton or volcano, is found in different forms in most magmatic systems (see Figure 1).

Magma chamber is a particularly important concept. Volcanologists use the mechanics of magma chambers to handle all the major and subtle chemical and textural transitions necessary to link one lava to another. Successive lavas may give a time record of the operation of a magma chamber, although the actual chamber can never be sensed. Plutons are, in a strong sense, actual magma chambers, but the sense of how they operated in real time has been largely lost through protracted crystallization and annealing, and the nature of the connection of plutons to either volcanoes or to the deeper, ascent path of the system is not at all clear.

6.07.2 The Nature of Magma

Magma is a viscous fluid consisting most often of polymerized silicate melt, crystals, dissolved gasses, and sometime bubbles and foreign chunks of crystals and rocks. Of all the fluids provided by Nature, magma is perhaps the most intriguing. In traversing the melting range, a span of $\sim$200°C, magma viscosity increases by a factor of 10^{18} (MKS or CGS), which is the largest change of any physical parameter for this temperature change. Crystals spontaneously

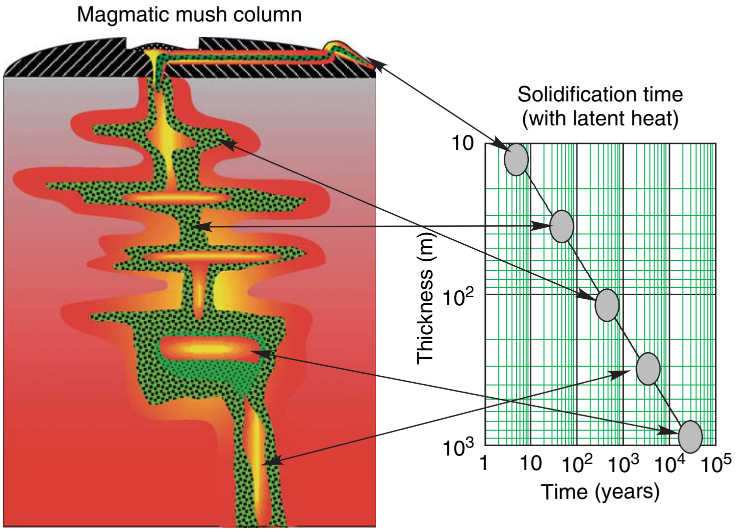

Figure 1 Magmatic systems (left) are an integrated collection of sills and connecting conduits linking a source region to the near surface and volcanic centers. The thermal timescales (right) for solidification vary throughout the system due to the local thermal regime and the length scale of the system.

nucleate and grow, modifying both the local buoyancy and melt composition, furnishing swarms of particles of a wide range of sizes that sort by size and density and stick together, welding tightly to form strong, truss-like, networks at many degrees of crystallinity.

6.07.2.1 Transport Characteristics

Heat and mass transport are slow in magma. Thermal (K) and chemical (D) diffusivities are small (typically $\sim 10^{-2}$ and $\sim 10^{-6}\,\mathrm{cm^2\,s^{-1}}$, respectively) and kinematic viscosity (v) is large, making the Prandtl ($Pr = v/K$), Schmidt ($Sc = v/D$), and Lewis ($Le = K/D$) numbers each large as opposed to molten metals with small Pr. That is, vorticity, heat, and mass can each be described by an equation of the form

$$\frac{\partial A}{\partial t} = \mathrm{B}\frac{\partial^2 A}{\partial X_i^2} \qquad [1]$$

where A is vosticity, temperature, or mass concentration, B is kinematic viscosity, thermal diffusivity, or mass diffusivity, and X_i is a spatial dimension. A scaling analysis of this equation relates the characteristic distance (δ) of diffusion associated with each of these processes to the transport property B and time (t), yielding

$$\delta = C(Bt)^{1/2} \qquad [2]$$

where C is a constant near unity in magnitude. The dimension δ is a measure of the diffusive layer thickness during the flow of momentum, heat, or mass. And the relative thicknesses of these layers is thus measured by

$$\frac{\delta_v}{\delta_T} \approx \frac{v}{K} = Pr\,(\text{Prandtl no.}) \qquad [3]$$

$$\frac{\delta_v}{\delta_D} \approx \frac{v}{D} = Sc\,(\text{Schmidt no.}) \qquad [4]$$

$$\frac{\delta_D}{\delta_T} \approx \frac{D}{K} = Le\,(\text{Lewis no.}) \qquad [5]$$

Notice also that $Pr = Sc\,Le$.

As an example of the value of these relative measures, for magma with a kinematic viscosity of $10^2\,\mathrm{cm^2\,s^{-1}}$ moving 1 km along a wall at the rate of $0.1\,\mathrm{cm\,s^{-1}}$, the momentum boundary thickness will be about 400 m. The thermal boundary layer will have a thickness of about 4 m, and the mass boundary layer thickness will be about 4 cm.

With Pr being a measure of the relative thicknesses of viscous or momentum to thermal boundary layers, momentum boundary layers are much thicker than thermal boundary layers, making the boundary layer approach for momentum transfer in fluid mechanics generally not a useful approach, unlike in metallurgy where Pr is small. Thermal boundary layer approaches, on the contrary, are highly valuable. Similarly, from the Schmidt and Lewis numbers, chemical boundary

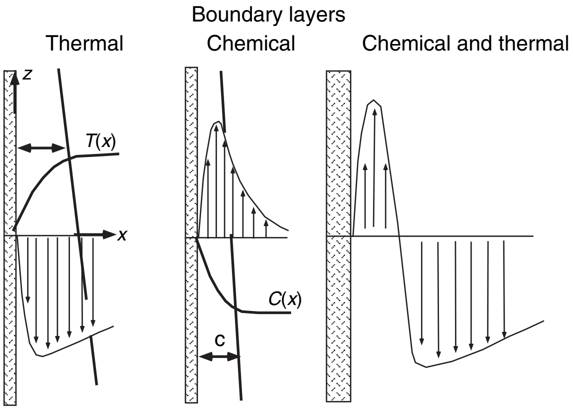

Figure 2 The types of boundary layers and their characteristic length scales operating in magmatic systems.

layers due to chemical diffusion are much thinner than both momentum and thermal boundary layers (see Figure 2). Diffusion halos about growing crystals, for example, are exceedingly thin and contamination by xenoliths affect only narrow margins. In many ways, this makes solving magmatic transport problems straightforward. Thin thermal and chemical boundary layers are embedded in wide shear zones where the variation in velocity is broad and gentle. We shall soon see, however, that the unusually strong effects of variable viscosity, as mentioned already, partly mitigate this attractive feature of many magmatic flows. Some of this viscosity effect comes from the increasing silica content of the melt as crystallization proceeds, but by far the most serious effect comes from the increasing concentration of crystals themselves and the interactions among these solids. These characteristics affect all aspects of magma generation, transport, differentiation, and eruption.

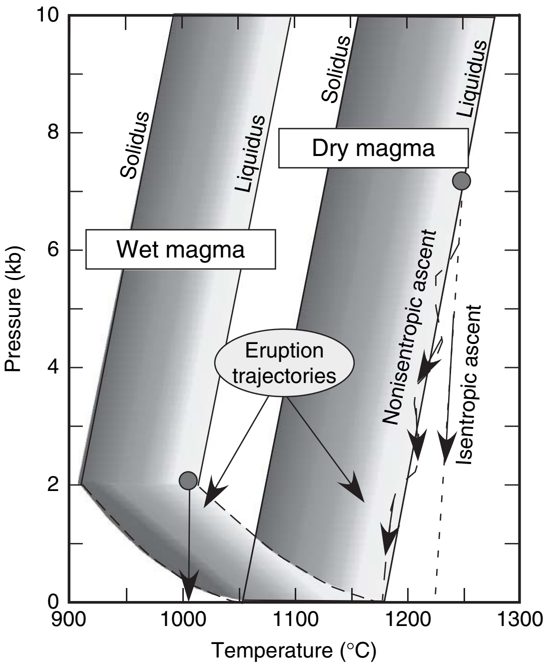

Figure 3 The general phase equilibria for basaltic magma as a function of pressure for dry and wet magmas. The adiabatic ascent path is indicated for the dry magma and also is the effect of rapid cooling due to superheating and convection. For the wet magma, the near surface liquidus may be below the 1-atm solidus temperature.

6.07.2.2 Phase Equilibria

The melting behavior of a typical basaltic magma, in terms of phase equilibria, as a function of pressure is shown by Figure 3. The high-temperature boundary beyond which (in temperature) no crystals exist is the 'liquidus' and the lower boundary below which the magma is completely solid, is the 'solidus'. In between these boundaries are phase fields delineating the stability of various mineral phases. Two magmas are indicated, one is free of dissolved water (dry magma) and the other (wet magma) contains a few percent dissolved water, where the point of saturation occurs at about 2 kb (0.2 GPa, 200 MPa). The solubility of water (and CO_2 and SO_2, the other principal volatile species) is directly proportional to the confining pressure, or depth in Earth, and there is also a point (~10–15 kb) at which no more water can be dissolved in the magma. At this point, the magma contains about 25 wt.% water, which is equivalent to the molar proportion of water in seawater (~96%). Magma in this condition, should it ever be achieved, is an aqueous solution with a silicate solute. At pressures above the indicated point of saturation at 2 kb, the wet magma is undersaturated with water and the phase diagram is geometrically similar to that of the dry magma, except that it is at a significantly lower temperature. This difference, as will be treated later, has a profound effect on the characteristics of eruption.

6.07.2.3 Solidification Fronts

Between the liquidus and solidus the magma is a physical and chemical mixture of liquid (melt) and crystals (and perhaps bubbles). The properties of this mixture are complex and exceedingly important at every stage of a magma's life in determining the set of dominant physical and chemical processes involved in shaping the magma's behavior. The buildup of crystals with decreasing temperature between the liquidus and solidus for typical basalts is shown by Figure 4. Nucleation and growth of crystals begins at the liquidus, by definition, and with decreasing temperature crystallinity (ϕ, or crystal fraction) at first builds up slowly and then more rapidly as crystallinity reaches 50 vol.% after which it again builds increasingly slowly with approach to the solidus. Near the liquidus, where crystallinity is low and crystals are small, the magma is a 'suspension'. Here the crystals can settle relative to one another without much hindrance from one another, but since they are small, settling is slow. This state holds to a crystallinity of about 25 vol.% where the viscosity of the mass (see below) has increased by a factor of 10 over that at the liquidus and the crystals now 'feel' the presence of one another as they move. Motion of a single crystal causes a shear flow extending out ~10 radii which entrains neighboring crystals. There is also some observational (Marsh, 1998) and experimental (Philpotts and Carroll, 1996) evidence that, especially in plagioclase-bearing basaltic magmas, a 'chicken-wire' network of crystals may develop that gives a certain structure and strength to the magma. Beyond the suspension zone where crystals are (ideally) still separated from one another is the 'mush' zone, which persists until the crystallinity reaches the state of maximum packing where the crystals are all touching. This occurs when crystallinity reaches about 55 vol.% ($\phi \sim 0.55$). At this point, the crystals are tacked together to form a solid framework of some strength (e.g., Marsh, 2002). In essence, the magma is now a rock and can no longer flow as a viscous fluid. The remaining melt, which is interstitial to the crystals, can still move, but as a porous or Darcian flow (e.g., Hersum *et al.*, 2005). Because of this overall strength, which is found in Hawaiian lava lakes to be drillable, this region is called the 'rigid crust'. These three zones, then, suspension, mush, and rigid crust, make up all magmatic 'solidification fronts'. A solidification front (see Figure 5) is the

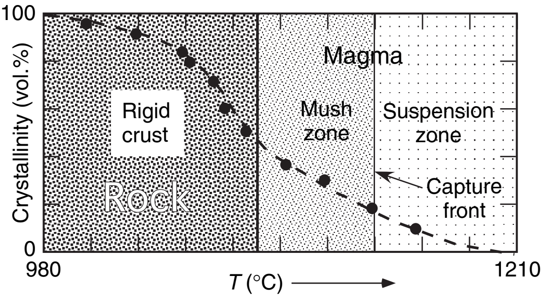

Figure 4 The variation of crystallinity in basaltic magma at any pressure as a function of temperature.

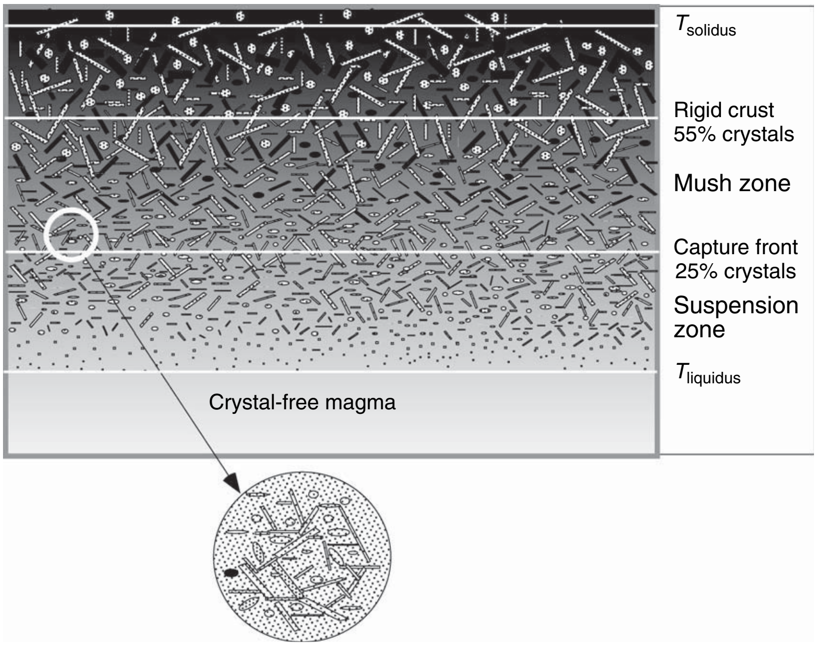

Figure 5 Upper solidification front propagating inward (down). The base or outermost edge of the front is defined by the solidus and the leading, innermost edge is the liquidus. The overall thickness of the front increases with time and the rate of thickening depends on the local thermal regime. The inset depicts the framework-like structure of the crystal at about 30% crystals.

active zone of crystallization that forms the perimeter of all magmas. Solidification fronts are dynamic in the sense that they continually move in response to the prevailing thermal regime or state of heat transfer from (or sometimes to) the magma. All crystallization, by definition, takes place within solidification fronts. And it is within these fronts that physical and chemical processes take place to modify magma composition and texture and the behavioral character of the magma is determined. Beyond the solidification fronts, in the magma interior, there are no new crystals and hence no processes operate there to separate crystals and melt (more below).

As magma approaches the point of maximum crystal packing, where $f \sim 0.55$, it undergoes a dramatic rheological transition. It becomes a dilatant solid, which means that the mass of crystals and melt upon being sheared expands as neighboring solids try to move outward and around one another to accommodate the shear. When this condition is reached for magma in the throat of a volcano, the volcano becomes plugged and can no longer emit lava. With continued cooling and crystallization in the magma below, gases exsolve that can build pressure to the point of catastrophic failure of the entire edifice. This condition will be discussed again shortly. The dynamics of solidification fronts measure the dynamics, especially the rate of cooling, of every magma from deep chambers to lava flows.

6.07.3 Crystals in Magma

All magmas can be separated into two groups according to the sources of the constituent crystals: (1) crystals grown in the present cycle of active solidification fronts, and (2) crystals inherited or entrained from prior crystallization events, including crystals from disaggregated wall rock. It is fundamental to the study of every magmatic rock to recognize the provenance of the constituent crystals. Crystals have historically been separated texturally into phenocrysts and groundmass. Phenocrysts are unusually large or otherwise distinctive crystals and groundmass is commonly tiny crystals interstitial to any phenocrysts. The distinction is most apparent in volcanic rocks, but is also often clear in many plutonic rocks and the textures are called porphyritic. It has long been assumed (e.g., Turner and Verhoogen, 1960; Carmichael *et al.*, 1974) that phenocrysts represent crystallization at depth under slow, protracted cooling, and groundmass crystals the latest rapid phase of cooling associated, in volcanic rocks, with eruptive processes or emplacement processes in plutons. The apparent sharp change in crystal size between phenocrysts and groundmass upon quantitative examination using measured crystal size distributions (CSDs) shows that most crystal population are actually continuous in size from phenocrysts to groundmass. This feature is characteristic of active crystallization where a time span of active nucleation has given rise to large crystals. Yet there are many magmas that have inherited crystals from earlier solidification events and these crystals are valuable indicators of dynamic processes involving crystal entrainment and transport. Recognizing the distinction between these two classes of crystals is of critical importance to understanding magmatic processes. Yet, it has proven elusive in some magmatic bodies to recognize imported crystals, which has led to faulty reasoning in deciphering magmatic history. These two regimes, which for convenience are hence forth referred to as phenocryst free and phenocryst bearing, are next considered in some detail to emphasize this importance, beginning first with crystallization controlled by solidification fronts.

6.07.3.1 Solidification Front Crystallization or Phenocryst-Free Magmas

Solidification fronts are packaged between the liquidus isotherm at the leading edge and the solidus isotherm at the trailing edge. Nuclei and superclusters already present begin to grow in earnest at the leading edge of the solidification front and these crystals continue to grow as the front passes through the region of melt. In the strictest sense, the melt is stationary and the solidification front moves through the melt transforming it into a crystalline mass. In the leading part of the solidification front, the suspension zone, crystals can settle easily without hindrance, but individual crystals are small and settle slowly. This settling is well described by Stokes' law:

$$V_s = C_s \frac{\Delta \rho g a^2}{\mu} \qquad [6]$$

where C_S is a constant ($\sim 2/9$) depending on the shape of the crystal, $\Delta\rho$ is density contrast, g is gravity, a is crystal radius, and μ is viscosity. To escape the solidification front, the crystal must settle faster than the rate of advancement of the solidification front itself. Early in the cooling history, especially for magma emplaced in cool upper crustal wall rock, solidification fronts move rapidly and it is impossible for newly formed crystals to escape. Only in very slow-moving solidification fronts are crystals sometimes able to escape. And if once a crystal becomes deeply embedded in a solidification front, melt viscosity and hindrance from neighboring crystals increase to the point that escape is not possible. The region where this transition occurs marks the boundary between the suspension and mush zones and is called the 'capture front'. Crystals outward of the capture front are trapped in the solidification front.

As cooling proceeds, the distance between these isotherms defining the solidification front increases with the square root of time, just as in any conductive process. That is, even though solidification fronts involve heat production from latent heat of crystallization, from solutions to Stefan-type problems (e.g., Carslaw and Jaeger, 1959; Mangan and Marsh, 1992; Turcotte and Schubert, 1982) the position $S(t)$ of the front is given exactly by:

$$S(t) = 2b(Kt)^{1/2} \qquad [7]$$

where b is a constant and K is thermal diffusivity. The rate of advance is given by the time derivative of this equation.

$$V_{\mathrm{F}} = \frac{\mathrm{d}S(t)}{\mathrm{d}t} = b\left[\frac{K}{t}\right]^{1/2} \qquad [8]$$

Equating this with the rate of crystal settling from Stokes' law gives a relation for minimum size crystal that can escape from the solidification front as a function of time. That is,

$$a(t) = \left[\frac{b}{C_{\mathrm{s}}}\frac{\mu(K/t)^{1/2}}{\Delta\rho g}\right]^{1/2} \qquad [9]$$

The larger the viscosity the larger the crystal must be to escape, and for density contrast it is just the reverse. The constant b measures the effect of latent heat relative to the enthalpy of the magma, and can be adequately represented from its original transcendental equation as (e.g., Zieg and Marsh, 2002)

$$b = \left[\frac{C_{\mathrm{P}}(T_{\mathrm{m}} - T_{\mathrm{w}})}{5H(\pi)^{1/2}}\right]^{2/5} \qquad [10]$$

where C_{P} is specific heat, T_{m} is magma initial temperature, T_{w} is wall rock initial temperature, and H is latent heat.

This measure of crystal size must be compared with the actual size crystal growing in the suspension zone as the solidification front thickens. This can be found by estimating how long taken by the capture front isotherm to traverse the suspension zone as a function of time. The position of the capture front isotherm is a large fraction ($f_{\mathrm{CF}} \sim 0.95$–$0.98$) of position of the leading edge of the solidification front given by eqn [7],

$$S(t) = 2bf_{\mathrm{CF}}(Kt)^{1/2} \qquad [11]$$

and the difference of these two equations gives an estimate of the thickness of the suspension zone

$$\Delta S(t) = (1 - f_{\mathrm{CF}})2b(Kt)^{1/2} \qquad [12]$$

The time spent traversing this zone is given by the quotient of [12] and [8],

$$\Delta t(t) = \frac{\Delta S(t)}{V_{\mathrm{F}}(t)} = 2(1 - f_{\mathrm{CF}})t \qquad [13]$$

The time for the solidification front to traverse the suspension zone is a linear function of time and independent of the thermal properties of the system. The size ($a(t)$) of a typical crystal grown during this time can be found using a general growth law for crystal growth. Although this choice is completely arbitrary, a convenient and realistic formula is the linear relation (e.g., Marsh, 1998; Zieg and Marsh, 2002),

$$a(t) = G\,\Delta t(t) = 2G(1 - f_{\mathrm{CF}})t \qquad [14]$$

Solving this equation simultaneously with that given by eqn [9] gives the time at which the first crystals escape from the solidification front,

$$t = \left[\frac{(b/C_{\mathrm{S}})\mu K^{1/2}}{(2G(1 - f_{\mathrm{CF}}))^2\,\Delta\rho g}\right]^{2/5} \qquad [15]$$

This time can also be inserted in to the growth law of eqn [14] to yield the size of the crystal at the time of escape, which is

$$a(t) = \left[\frac{(b/C_{\mathrm{S}})(2G(1 - f_{\mathrm{CF}}))^{1/2}\,\mu K^{1/2}}{\Delta\rho g}\right]^{2/5} \qquad [16]$$

The time of escape and size of crystal escaping are shown by **Figure 6**. The time of escape is sensitive to the growth rate. For a magma viscosity of 10^3 P where crystals are growing at $10^{-10}\,\mathrm{cm\,s^{-1}}$, escape begins after about 30 years and the crystal size (radius) is about 0.03 cm. As might be expected, the size of the crystal at first escape is relatively insensitive to growth rate. The time of escape is much more sensitive to

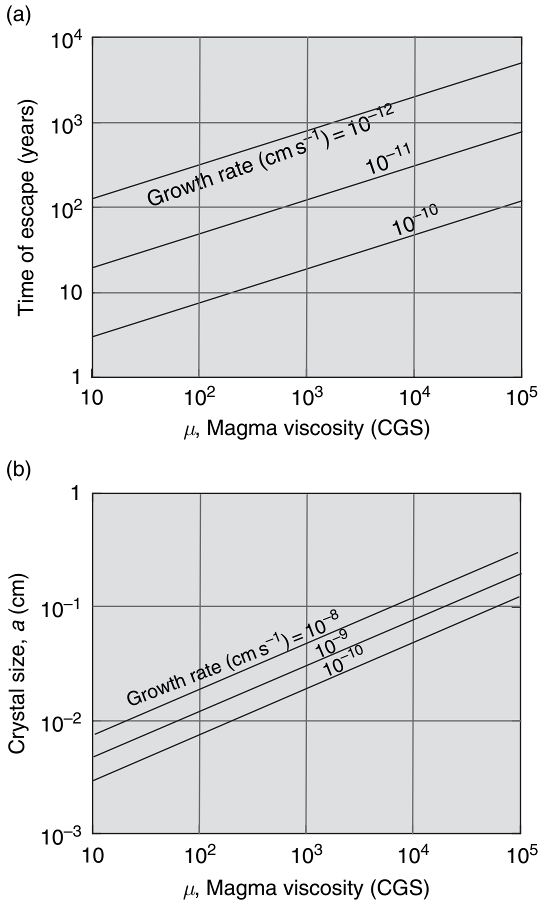

Figure 6 (a) The time of escape of a crystal from a solidification front as a function of magma viscosity and crystal growth rate. (b) The size of the first escaping crystal as a function of magma viscosity and crystal growth rate.

growth rate, which is understandable. The sooner a crystal can reach the critical size to sink faster than the rate of advancement of the capture front, the sooner it can escape. As magma viscosity increases, the time of first escape and the crystal size at escape each increase. For granitic magmas where the viscosity might be 10^5–10^6 P, escaping crystals must be about 1 cm in radius, which takes for the growth rates indicated on the order of 10^3–10^4 years. This indicates why differentiation by crystal escape from solidification fronts is unlikely in granitic magmas.

Crystal escape from solidification fronts is much more likely in basaltic magmas once the crystals reach about 0.1 mm in size, which can occur after about 30 years when the solidification front has a thickness of about 50 m, depending on the cooling regime. The question then arises what happens to these crystals once they escape the solidification front? Since the magma below the advancing front is the hottest part of the system, crystals entering this region will begin melting and dissolving back into the magma (see **Figure 7**). This process was examined by Mangan and Marsh (1992), who, through a different approach, found results similar to those above. Fractionation begins after about 25 years when capture front advancement has slowed to 1–2 m yr^{-1}. For intrusions thinner than about 30 m, this condition is never achieved and no escape is possible, but for magmatic sheets thicker than about 100 m this process may often occur. They also followed the course of the sinking crystals into the magma interior and estimated the time and distance settled for complete

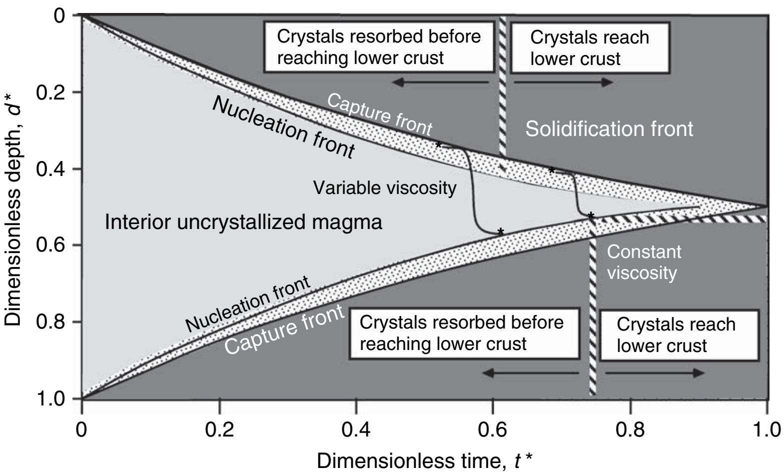

Figure 7 The thickening of upper and lower solidification fronts in a sheet-like body and their relationship to capturing settling crystals.

resorption. Survival through the hotter interior depends also on the proximity of the lower solidification front rising from the floor of the magma. Crystal accumulation on the floor of the magma chamber is not possible until the lower solidification front has advanced to intercept the descending crystals prior to resorption. Interception is unlikely until the magmatic sheet is about 75% solidified, where the depth of interception is about midway through the original magma (**Figure 7**). At best, a microcumulate layer may develop near the centerline of the body.

The net result of crystallization of a magma initially containing only nuclei and no large phenocrysts is a body of rock of essentially uniform composition and with a crystal size that increases inward in accord with the local growth or transit time of the solidification front. Many dolerite (diabase) sills throughout the world ranging in thickness from 1 to 350 m are often of uniform composition with a grain size that increases gradually in response to the slowing of the solidification front as it moves into the body from top and bottom. Actual CSDs can be calculated in detail to characterize this process (see Zieg and Marsh, 2002).

6.07.3.2 Phenocryst-Bearing Magma

That some magmas carry significant loads of large crystals that suddenly settle when the magma comes to rest upon emplacement and strongly chemically differentiate the magma became apparent with the controversy over the origin of the sequence of rock at Shonkin Sag laccolith in north-centeal Montana. It is also from early studies of this body that came the basic concepts on magmatic processes assumed to control magmatic chemical evolution. Although much more on this crucial history will be covered later, it is important here to consider this body to set the stage for understanding this large class of magmas, which often lead to exotically layered bodies.

Shonkin Sag is a relatively small circular laccolith, 70 m thick and 3 km in diameter. Yet, in spite of its small size, it is strongly differentiated (**Figure 8**). The obvious curiosity is that many much thicker and more areally extensive dolerite sills throughout the world, also of basaltic composition, show almost no differentiation. In the initial study of Shonkin Sag, Pirsson (1905) realized that a large mass of crystals had settled and formed a thick pile of cumulates on the floor. Many bodies show similar distributions of a thick pile of cumulate crystals on the floor. And most commonly it has been assumed, like Pirsson, that these crystals grew after emplacement in response to strong cooling from the roof of the sill and simply settled to the floor. When the body was restudied in the 1930s independently by C. S. J. Hurlbut (1939) at Harvard and J. D. Barksdale (1937) at Yale, a controversy sprung up. Hurlbut recognized that the initial magma carried a high population (~35 vol.%) of large crystals prior to emplacement. He realized that these crystals did not grow after

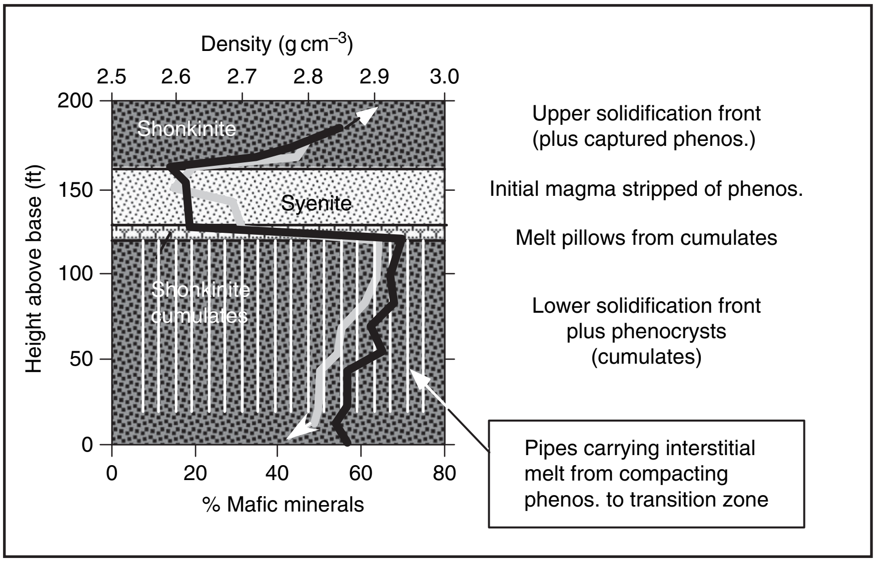

Figure 8 The stratigraphic field relations between rock types of Shonkin Sag laccolith.

emplacement and did not fall to the floor to form the thick pile of cumulates. They fell to the floor because they came in as essentially an instantaneous injection of phenocrysts into the system. This may be the origin of the extremely important idea of the role of magma in carrying crystals. Barksdale, on the other hand, was deeply impressed by the presence of what appeared to be an internal contact where the transition zone rocks (see **Figure 8**) directly overlay the basal cumulates. This feature in the field does, indeed, look very much like an internal contact that might be formed by the injection of a separate magma. This was the point of contention: Hurlbut said the entire stratigraphic distribution of rocks could be formed in place from an initially crystal-laden magma. Barksdale insisted that multiple injections of magma are necessary. These two points of view, *in situ* differentiation versus multiple injections, are still often points of contention in explaining igneous sequences. And, as will be seen here, there is clearly room and good reason for both views. In short, as the large load of phenocrysts was settling and accumulating in a thick pile on the laccolith floor, interstitial melt was forced upward through a series of pipe-like conduits (Marsh *et al.*, 1991). These pipes carried the melt up, expelling it on top of the compacting cumulate pile. Being too dense to rise higher in the sequence, the expelled essentially crystal-free melt established a series of overlapping pillows of melt forming the transition zone. The expelled melt being in the hottest part of the body, and multiply saturated because of its intimate prior contact with the cumulates crystallized into unusually coarse crystals. The net result is a layer of rock in sharp contrast to the texture of the underlying cumulates of clinopyroxene phenocrysts. For all intents, this looks like an internal contact from a separate injection of magma. And it is, but this is an auto- or internal injection. Barksdale was very impressed by this, and his arguments centered in many facets on this observation. It is important to note that, whereas the basic geologic observation is correct, it is the interpretation of this feature in terms of a magmatic process that is faulty. This is a fairly common pitfall in magmatology, and it appears even more strongly when the meaning of a thick cumulate pile of crystals on the floor of a magmatic body is interpreted (see below).

On more general grounds, when magma carrying phenocrysts is emplaced, there is a competition between the rate of crystal settling and the rate of solidification. Just as in the previous section when considering crystal capture and escape by the solidification front, the same process operates here except with crystals distributed vertically throughout the body a large population of crystals escape capture and settle freely into the lower, upcoming solidification front. Consider some end-member situations for magma laden with crystals emplaced as a sheet shown by **Figure 9**. If the magma could cool instantaneously regardless of its thickness, which physically is impossible, all the crystals would be trapped in place before they could settle any distance at all. The final distribution of crystals would be uniform from top to bottom throughout the sheet. At the other extreme, if the body did not crystallize at all, all the crystals would settle to the floor and form a thick pile of constant abundance like a bed of clastic sedimentary rock. Although very thin (∼1 m) and very thick (hundreds of meters) sheets of magma may approximate these extremes, actual magmas are somewhere in between these two extremes. Inward advancing solidification fronts from the top and bottom compete with crystal settling. The initial advance of the upper and lower solidification fronts is infinitely rapid, which is what leads to the fine-grained chilled margins around igneous bodies, and any phenocrysts near the margins are immediately captured. But because the rate of solidification front advance decreases inversely with distance into the body (i.e., from eqn [2] an isotherm advance velocity (V) can be formed that leads to $V \sim K/Z$, where K is thermal diffusivity and Z is distance into the body), more and more crystals escape capture with depth and all crystals initially in the center of the body settle into the lower rising solidification front. The net result is an S-shaped profile of phenocryst abundance vertically through the body (see **Figure 9**). This basic form of phenocryst distribution is seen in many magmatic sheets and it is a clear indication of solidification of a phenocryst-charged body of magma. Moreover, there are many variations on this basic theme, and one readily accessible system of this nature that was studied in real time is Kilauea Iki Lava Lake in Hawaii.

6.07.3.2.1 *Kilauea Iki Lava Lake*

Lava lakes form at Hawaii when erupting magma fills naturally occurring pits or sink holes due to collapsing deeper lava tubes. Kilauea Iki Lava Lake formed from the 1959 eruption of a crystal (olivine)-laden basalt, filling a ∼2-km-wide pit to a depth of about 125 m (e.g., Helz, 1986; Helz *et al.*, 1989). Because the eruptive flux repeatedly waxed and waned during

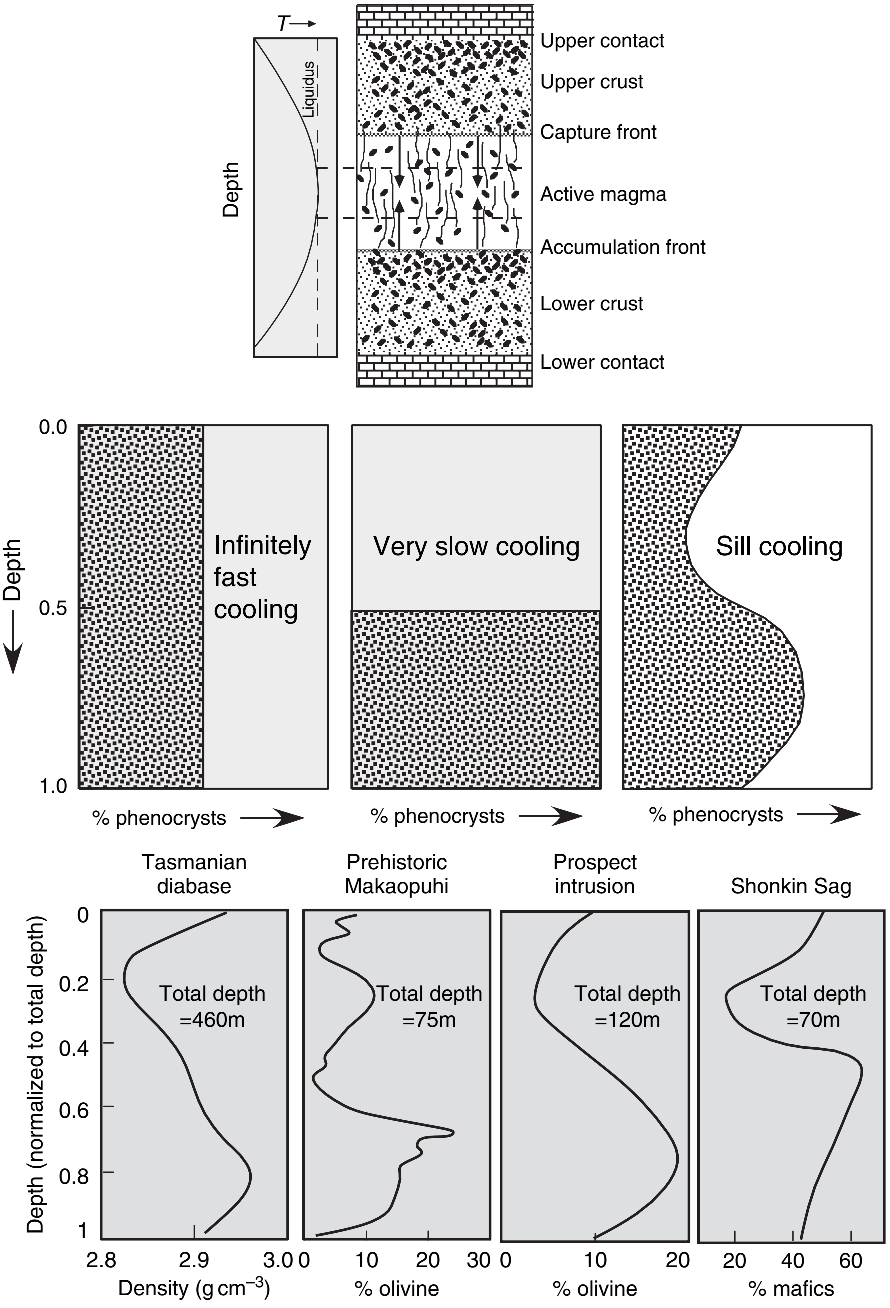

Figure 9 The process of settling of phenocrysts leading to formation of various final distributions of crystals. (a) A schematic depiction of the process. (b) The formation of idealized or end-member distributions. (c) Actual distributions of crystals observed in some intrusions.

filling, the load of large olivine crystals delivered to the lava lake also varied over time. Murata and Richter (1966) found that the magnitude of the eruptive flux at Kilauea is proportional to the size and the abundance of olivine crystals entrained by the erupting magma. In other words, the bigger the eruptive flux and the stronger the eruption, the more and the larger the olivine carried by the erupting magma. This is like a river in flood stage. The bigger and more dramatic the flood, the bigger the bedload of solids that it can move, and the larger the size of the individual solids that can be moved. The olivines entrained are not necessarily phenocrysts but are all sorts of crystals that are found in the plumbing system; some are phenocrysts from earlier magmatic events, others are xenocrysts from peridotitic wall rock, and everything in between. When the crystals in a single sample are examined they go from Fo_{75} to Fo_{92}, and the latter compositions are clearly from mantle wall rock (e.g., Maaloe *et al.*, 1989, 1992). At Hawaii, these crystals are called 'tramp' crystals to reflect their perhaps vagrant and varied origins (e.g., Wright and Fiske, 1971). Tramp crystals are found in systems all over the world at, for example, Jan Mayen (Imsland, 1984), Reunion (Upton and Wadsworth, 1967), and the Ferrar dolerites (see below). Considering that all magmas everywhere must ascend and erupt through crystalline mantle and crust wall rock, which are in effect gravel piles, every magmatic system should contain tramp crystals.

The surprising aspect of magma carrying this heterogeneous collection of crystals is that if the lava chemical composition is plotted on a conventional diagram of CaO versus MgO (in wt.%), the variation appears as that due to perfect fractionation of olivine crystals indigenous to the magma (see **Figure 10**). Wright (1971) has shown that when these relations are considered in more detail for individual eruptions, the variations due to olivine control are even cleaner and tighter. Wright calls these trends olivine control lines. That is, all of the variation in MgO can be effected purely by the addition or loss of olivine tramp crystals. These exotic crystals have a strong effect on magma composition also through diffusional exchange.

As soon as a tramp crystal enters the ascending magma, it begins to chemically exchange Fe and Mg with the melt. The melt is much poorer in Mg and richer in Fe than typical tramp crystals. The time for these crystals to come to equilibrium with the melt can be estimated from eqn [2]: $t \sim a^2/D$, where a is crystal radius ($\sim$1 mm) and D is the chemical diffusivity controlling the exchange ($\sim 10^{-6}\,\mathrm{cm^2\,s^{-1}}$). It takes about a month or so to erase the original compositional identity of the tramp crystal and bring it into equilibrium with the melt. The melt has lost Fe to the crystal and gained Mg, which has made the apparent magma composition 'more primitive', exactly opposite to a normal (and commonly assumed) liquid line of descent. Conversely, these tramp crystals to have maintained their exotic compositional identity, have been entrained in the melt for a very short time, perhaps only days.

Given the eruptive compositional variability of the lavas, especially in terms of the entrained crystal compositions, the magma filling Kilauea Iki Lava Lake varied daily during the eruption. The initial conditions in the lava lake sheet of magma, in terms of the abundance of tramp crystals, is in striking contrast to Shonkin Sag. At Shonkin Sag, the magma ascended from depth and the crystals were

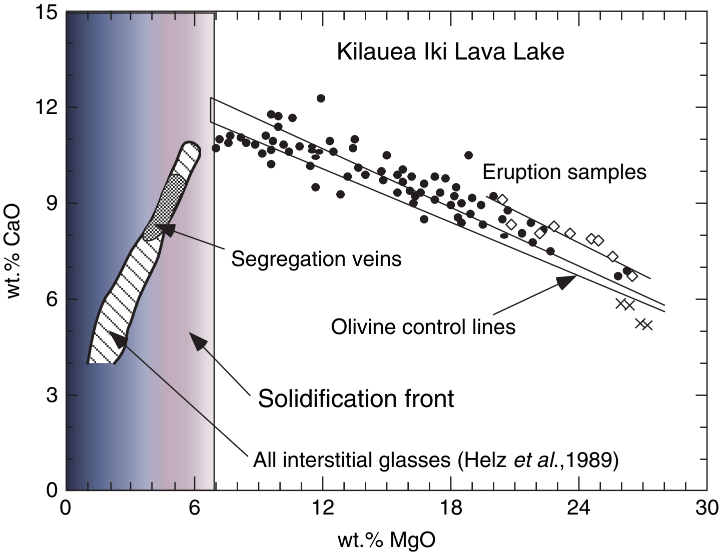

Figure 10 Variation of CaO and MgO in samples from Kilauea Iki Lava Lake. Note the olivine control lines, which show the effects of gains and losses in entrained olivine crystals. All compositions at MgO less than about 7 wt.% are from drilling of the upper solidification front. Individual symbols represent whole rock analyses of eruption samples (see, e.g., Helz *et al.*, 1989).

presumably flow sorted and mixed prior to emplacement and the sequence of crystal settling leading to the final S-shaped profile. But at Kilauea Iki the S-shaped profile will also reflect detailed variations due to the eruptive filling process (see Figure 11). Similar small-scale variations in intrusive complexes, as is seen in the Basement Sill of the Ferrar dolerites of the McMurdo Dry Valleys, thus reflect periodic filling and repose times and may be a critical link between the similarity of intrusive and volcanic processes of magma transport.

Once the tramp olivine crystals have settled to form a cumulative pile on the floor of the lava lake, they begin to diffusionally exchange with the interstitial melt left in the bed and in a matter of a few months they have lost their original compositional heritage. A later analysis of this series of rocks would be difficult to unravel the true magmatic history due to this late, post-emplacement, re-equilibration. The clearest record of the role of tramp crystals, and their compositional diversity, is best recorded in the rapidly chilled rocks at the upper margin.

The sequence of chemical differentiation is controlled by two key processes. First is the loss of the load of entrained tramp crystals once the magma came to rest. The magma in the center of the body after loss of the tramp crystals is a melt containing only tiny crystals that differentiated from ~20% MgO to ~7 wt.% MgO. It is essential to note that the change in composition took place, in essence, instantaneously as the tramp crystals settled out. This is ‘punctuated crystal fractionation and differentiation’. Second is the fact that after loss of the tramp crystals, the center of the lava lake contains only crystal-free melt, and the system now resembles a phenocryst-free system discussed earlier. The system continues to cool and solidify without further differentiation. And if by chance this magma were to be erupted, only the low-viscosity, crystal-free core melt would be eruptible. The ensuing lava would thus show extensive chemical signs of differentiation, but it would mainly be due to the role of the entrained tramp crystals.

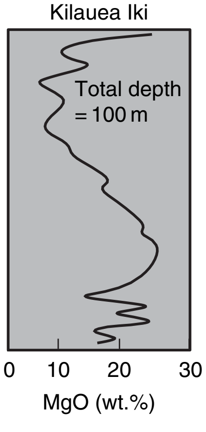

Figure 11 The S-shaped profile for Kilauea Iki where the detailed variations reflecting variations in eruption flux are clear.

The dramatic contrast in evolution of magma with and without initial concentrations of large crystals is central to understanding all magmas. Yet the importance of this distinction, and even the recognition of this feature itself, was not appreciated in the formative stages of magmatology. The essential concepts of differentiation and, especially, the evolution of magma in chambers were conceived and put into scientific play, in many ways, on faulty reasoning. The field relations were clearly recognized, but the physical processes giving rise to them were unknown. Through these considerations is where the concept came about of magma chambers, undoubtedly the most universal concept in magmatology.

6.07.3.3 Primitive versus Primary Magmas

When considering a magmatic complex or system, petrologists are literally obsessed with identifying the magmatic composition from which all other related compositions in the suite could have arisen by crystal fractionation processes. Norman Bowen himself, as we will see below, incited this obsession by discovering the crystallization reaction series whereby, starting with basalt, granite could be formed by growing and progressively settling out crystals with silica contents less than that of the adjacent magma. The natural tendency has thus been to automatically take the rock with the highest MgO content and assume it is the primary magma of the series. Magma MgO content has become synonymous with primitiveness. This reflects the direct connection between all basaltic magmas and mantle peridotitic rock. After all, there is no doubt whatsoever that basalts generally come from partial melting of the mantle and every other igneous rock, continents included, comes from basalt. It also reflects the observation that at Hawaii there is a clear succession from MgO-rich picrites right on through to tholeiitic basalts with 5–7 wt.% MgO. It is naturally assumed and inherently adhered to, without even having to defend the proposition, that any basaltic rock with low MgO must be a differentiate. It cannot be a primary composition.

The general fallacy of this line of reasoning comes from not recognizing the fundamental mechanical role of tramp crystals in deciding magma bulk composition. We shall see repeatedly below that virtually any basalt can be a primary magma regardless of its MgO content. Any such basalt traversing the lithosphere has the opportunity to entrain high concentrations of nonindigenous crystals of olivine or other mafic phases. The new bulk composition certainly appears primitive, but it is not primary, and to assume that it is short-circuits the reasoning process leading to understanding magmatic process. It is much more appropriate to consider magmatic processes as being characterized by a 'carrier magma' that is subjected to the mechanical gain and loss of crystals throughout its life. The carrier magma itself can be, within reason, of almost any composition. It certainly need not be inherently primitive, and it may be challenging to recognize the carrier magma, which, depending on the age and size of the system, may be of several different types. This concept is particularly important when considering the role of magma chambers in magmatic processes.

6.07.3.4 Historical Note on Solidification Front Fractionation

The possible role of solidification fronts in capturing phenocrysts was first noticed by Pirsson (1905) in studying Shonkin Sag. Two of his students (Osborne and Roberts, 1931) were the first to analytically model the growth of the solidification front and compare this with the rate of settling of crystals due to Stokes' law. They compared their results to observations at Shonkin Sag, but due to a misnumbered sample the calculated profile did not match that observed. Jaeger and Joplin (1955) made a substantial contribution when they realized that newly grown crystals falling from the advancing solidification front will dissolve as they sink into the hotter interior magma and will not contribute to fractionation. They were taken to task for this point of view by Walker (1956) and Hess (1956) who could not understand Jaeger's straightforward analysis. Walker and Hess firmly held the assumption that, in essence, "it is well known by petrologists that crystals grow in the interiors of magmas and commonly settle to fractionate the system." They did not realize that the effect they were thinking of came from systems injected with phenocrysts from the start. J. C. Jaeger was the author with H. S. Carslaw of the fundamental treatise on heat conduction in solids, and his analytical insight into cooling and solidification of magma was clear and considerable. The inability of leading petrologists of the day to recognize the truly original and valuable contributions by Jaeger set back the development of magma physics by several decades. The production of S-shaped profiles was analyzed again by Gray and Crain (1969) and Fuijii (1974).

6.07.4 Magma Chambers

Magma chambers are the conceptual cornerstones of every magmatic process. They are high-level staging areas that charge volcanoes for eruption. They are cavernous pools wherein complex patterns and cycles of crystallization take place to transform initially homogeneous melt into spatially differentiated sequences, which may or may not be erupted. They are enormously versatile in size, shape, and function, and can produce layered intrusions, a layered oceanic crust, and homogeneous diabase sills and granitic plutons. The central feature of this dynamic versatility is the pervasive nucleation and growth of crystals throughout the chamber that can be separated, sorted, or re-entrained in a vast array of processes (see **Figure 12**). This valuable and useful concept of magma chambers has been adhered to for over one hundred years. It is based on an exceedingly fundamental and misleading premise of how silicate melts solidify. Here we examine this concept in detail, to strengthen it fundamentally, and to show that all magmatic systems function by a common, basic, and simple set of processes.

6.07.4.1 The Problem: The Diversity of Igneous Rocks

The abundant variety of igneous rocks found on Earth's surface has long spawned an innate curiosity into the processes responsible for this variety and how these processes might have shaped the very structure of Earth itself. A strong burst of intellectual activity concerning the origin and evolution of magma was brought on by the advent of thin section-making, western exploration in the United States, and by the general intense activity in chemistry and physics taking place at the beginning of the twentieth century. The rapid discovery of new elements, radioactivity, blackbody radiation, and the development of chemical thermodynamics by

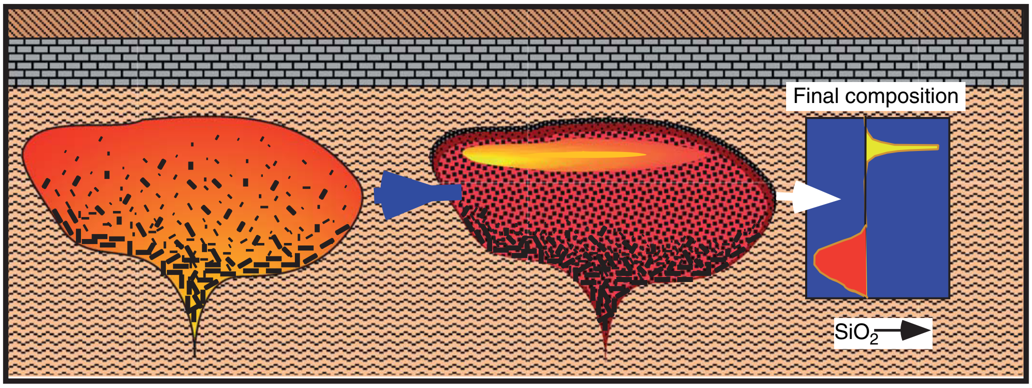

Figure 12 The historically imagined or classical magma chamber showing crystals settling from the center of the chamber leading to a pile of cumulates on the floor and a silica-rich sandwich horizon at the interface of the upper and lower crystallization zones.

J. Willard Gibbs, for example, set the stage for fundamental advances in understanding magma.

6.07.4.2 George Becker's Magma Chamber

In 1897, George Becker (1847–1919) set forth the basic concept of magma chamber differentiation that is still largely adhered to this day. Becker was mainly a chemist who worked for the US Geological Survey. He was impressed by how a cooled bottle of wine grows ice crystals around the edges and as crystallization proceeds the mother liquor or residual melt toward the center becomes increasingly rich in alcohol, the component with the lowest freezing temperature. If the temperature is progressively lowered, the container could become compositionally zoned to form, in effect, a differentiation sequence, which he said would be a perfect analog of a laccolith. Becker said: "A bottle of wine or a barrel of cider exposed to low temperature deposits nearly pure ice on the walls, while a stronger liquor may be tapped from the center. If still a lower temperature were applied the central and more fusible portion would also solidify. Such a mass would be, so far as I can see, a very perfect analogue to a laccolith." He had in mind the rock sequence displayed by Shonkin Sag laccolith, which had been discovered in north-central Montana during mapping of the 49th parallel. This style of fractional crystallization was well known from ancient times and was practiced by Native Americans in concentrating maple sap prior to boiling down to syrup. Charles Darwin noticed on his visit to the Galapagos during the *Beagle* voyage that large olivine crystals had clearly settled to the base of lobes of basalt. Fouque realized in 1879, in his chemical study of the eruptives of Santorini, that the separation of plagioclase enriched the lava in silica. Crystal fractionation was a common chemistry laboratory technique in the late nineteenth century. Madam Curie used it to isolate radium and Becker, having been trained as a chemist, certainly knew of the effectiveness of this process.

Becker's idea undoubtedly describes the most fundamental concept in magmatic processes. The fact that crystals in multicomponent, multiphase systems always have compositions different than the host liquids allows a systematic evolution in melt composition with crystallization. This feature of solutions is what makes metallurgy, ceramics, and igneous petrology the rich fields that they are. Although this feature of solutions was long known, Becker made the important realization that this process might also gives rise to a 'spatial' variation in final rock composition. Spatial variations in rock composition are fundamental to magmatic systems.

The downside to Becker's idea, which has been overlooked in deference to its conceptual usefulness, is that the process really only works with dendritic crystals, which are the rule in metals and aqueous solutions but not silicate magmas. The whole essence of magmatic processes, and rocks themselves in the broadest possible sense, rests on the fact that magmas and rocks consist of very small crystals or clusters of small crystals that grow in essentially parasitic chemical relationships (e.g., Marsh, 1998). This simple subtlety in crystal size and form, known so well by every petrologist, coupled with a spatially varying thermal regime is the basis of all magmatic processes. It simplifies and changes completely Becker's concept of magma chambers, and it exposes a robust continuum linking all magmatic events.

Louis Pirsson (1860–1919) picked up on Becker's idea and significantly extended it to explain the lithologic variations seen at Shonkin Sag laccolith. Pirsson, a petrologist at Yale, R. A. Daly, W. H. Weed, and others visited Shonkin Sag and found it to be a remarkably differentiated, small (70 m) sheet-like body. Although Shonkin Sag will be discussed in more detail later, Pirsson combined Becker's idea with his own insight on thermal convection in fluids to give a plausible explanation of how Shonkin Sag evolved. His detailed exposition (Pirsson, 1905; pp. 187–188) of this process is at the very root common beliefs of magmatic processes:

> It seems almost impossible to resist the view that in an enclosed mass of magma sufficiently mobile for local differentiation to take place convection currents due to unequal cooling would occur. On the upper surface and along the outer walls cooling would take place more rapidly; on the floor of the chamber, protected by the heated mass above and with heated rocks below, less rapidly. Thus there would be a tendency along the top and sides for the magma to grow heavier and to descend. Material from the more highly heated central part would tend to rise and replace this, and thus currents would be established in the magma, rising in the center, flowing off to the sides at the top, and descending along the cooler walls. . . . Such currents, once established, would continue as long as sufficient mobility remained in the magma to permit them.
>
> At some period crystallization would take place, and this most naturally would begin at the outer walls. It would not begin at the top because the material would arrive there from below at its highest temperature. Moving off toward the sides the material begins to cool and descend and becomes coolest as it nears the floor; here crystallization would commence. The first substance to crystallize is the solvent, which in this case would be the femic minerals, chiefly augite. Part of the material solidified would remain attached to the outer wall and form a gradually increasing crust, and part would be in the form of free crystals swimming in the liquid and carried on in the current. Probably at first, as the liquid moved inward over the floor of the laccolith and became reheated, these crystals would remelt, giving rise to numerous small spots of magma of a different composition, which would slowly diffuse. As time went on, however, there would be a constantly increasing tendency for the crystals to endure; they would be carried greater and greater distances. But as they are solid objects and of greater specific gravity than the liquid, there might be a tendency for the crystals to drag behind and accumulate on the floor of the chamber. Moreover, from the heat set free at the time of their crystallization and from the resulting concentration of the chemically combined water vapor in the magma, the residual liquid would tend to have its mobility kept undiminished, since these would be factors which would tend to counteract the increase in viscosity due to cooling. In this manner it may be possible to understand how there would form a femic marginal crust and a great thickness of the femic material at the bottom of the laccolith. As the cooling went on the edges of the outer crust would rise more and more toward the top, finally spreading over it, and as a result the crust should be thinner on the top than elsewhere, as in the Shonkin Sag laccolith, in which the upper crust of femic rock is still preserved.

Beginning with a crystal-free melt, Pirsson suggested that crystals nucleate and grow inward from the edges of the laccolith, convecting melt moves through the growing marginal band of crystals, chemically exchanging with them freely, and unattached crystals pile up on the floor. He suggested that crystallization will be most intense near the roof where cooling is strongest and that these crystals will be carried downward by convection along the walls and then outward over the floor and deposited as the melt itself keeps circulating and differentiating. The end result is a thick pile of crystals on the floor, a thin rind of crystals welded to the roof, and a layer of highly differentiated rock just below the roof in what later came to be called the sandwich horizon. This basic idea, which was given root by Louis Pirsson to explain Shonkin Sag, has pervaded all of igneous petrology, with only minor modification to this day. This is a powerful, well-reasoned, and clearly stated idea. It is based on seemingly straightforward, but faulty, reasoning, which inherently exists, without any clear enunciation or realization, in the reasoning behind almost every present-day petrologic scenario. The key features of this reasoning are an assumption of the knowledge of the 'initial conditions' of the system at the time of emplacement, the 'spatial style of crystallization' of magma and the 'size of crystals' that can be grown after emplacement. These concepts remain elusive to this day, and need to be examined in detail. Before dong this, however, in order to understand how this idea flourished, it is essential to appreciate the historical context and activity of the petrologists alive at this time.

6.07.5 Historical Setting

The propagation of ideas very often rests on the random happenstance of how people appear and disappear from science. And it is in the mix of expertise lost and gained with the loss and gain of these people that ideas become taken seriously, become modified, and inadvertently become fundamental principles of the science itself. A corollary to this is the remark often attributed to Max Planck that beliefs in science mainly change through the loss by death of the holders of the old, out-of-date ideas. But it also sometimes true that with the loss of these people a vast resource of experience in observation is also lost. And some of these lost observations may be those that present serious obstacles to the acceptance of the newer ideas. This is especially serious in petrology where a great deal of the fundamental observations reside in a life's experience in studying field relations and gaining impressions of processes that may be impossible to quantify or record in any permanent way. So the science may sometimes suddenly proceed not because of the establishment of a new fundamental principle, but by the inadvertent removal of an obstacle through the loss of understanding of a fundamental observation or of the loss of the observer him/herself. It was this nature of events that largely defined the research field of igneous petrology for all of the twentieth century. And the period of 1905–15, in particular, was perhaps the most critical of all in shaping the concepts of magmatic processes and, especially, magma chambers.

Prior to about 1905, arguably the greatest advance in understanding magma was in the development of thin sections and the establishment of the CIPW norm. Thin sections allowed a detailed inspection of the intimate relationships between minerals quenched in the act of crystallizing. Although discovered and developed by the Britons W. Nicol (1768–1851) and H. C. Sorby (1826–1908) (e.g., Dawson, 1992), it was principally the Germans K. H. F. Rosenbusch and F. Zirkel who quickly and systematically developed petrography into a science and trained a cadre of petrographers. The exceedingly fundamental realization that a rock composition could be expressed in any number of textures and crystal sizes spawned the need for some way to normalize texture, or remove its influence altogether, in order to put all rocks on the same basis for classification. The CIPW norm was the outgrowth of this need, whereby each composition could be represented by its equivalent plutonic texture. This removed the mystery of falsely classifying rocks due to overall crystallinity rather than simply due to chemical composition. The CIPW Norm was a monumental product of the penetrating petrologic insight of G. H. Williams (1856–1894) of Johns Hopkins, W. Cross (1854–1949) of the US Geological Survey, J. P. Iddings (1857–1920) of the University of Chicago, and L. V. Pirsson (1860–1919) of Yale, and the analytical chemistry insight of H. S. Washington (1867–1934) of the Carnegie Institute's Geophysical Laboratory. Williams died in 1894 before full development and publication of what became the CIPW norm in 1903. These men quantitatively combined rock chemistry with their intuitive understanding of observational phase equilibria to predict with uncanny accuracy the crystallization sequence of virtually every igneous rock. In light of the fact that no systematic experimental phase equilibria were yet known for igneous rocks, this was a monumental and sophisticated scientific achievement. Nowadays, we have the equivalent operation in the form of comprehensive thermodynamic models of crystallization, two of which are, among others, the MELTS program by Ghiorso and associates (Ghiorso *et al.*, 1983) and COMAGMAT by Ariskin and associates (Ariskin, 1999). This is a direct reflection of the rapid development of experimental petrology beginning at about 1910.

In 1900, the level of petrologic insight within single individuals from the perspectives of field and thin-section studies was very possibly more sophisticated than it is today. There were, however, three major undeveloped areas that critically impeded the understanding of magmatic processes. These were: (1) mechanics of viscous fluids, (2) experimental phase equilibria, and (3) kinetics of crystal nucleation and growth. First, although George Gabriel Stokes (1819–1903) and Claude-Louis-Marie-Henri Navier (1785–1836) beginning in about 1850 had developed the basic equations of motion of viscous fluids, which set forth a stream of analysis involving both viscous and inviscid fluids, including Stokes' famous result for the drag on a sphere, it was not until 1919 that J. W. Strutt (1842–1919) (Lord Rayleigh) solved the problem of simple thermal convection in a layer heated from below. Second, on phase equilibria, there were many bits and pieces of experimental information scattered about on natural systems starting with James Hall in 1798 through to F. A. Fouque in 1879 and Frederick Guthrie's (1884) experiments on melting of metal alloys who stated: "I submit that, according to analogy, we should regard compound rocks and minerals [i.e., multicomponent systems], other than sedimentary rocks, as representing various kinds of eutectic alloys." But there was no general understanding of the structure of phase diagrams for magmas. Many petrologists believed because of the apparent preponderance of granites and basalts that this reflected the presence of pole compositions in the solution chemistry of silicate magmas. That is, in a phase diagram of temperature versus solution silica content, there might exist two eutectic regions, one for basalt and the other for granitic or silicic residual compositions. Cooling and crystallizing magma inevitably ends up at one or the other compositional end point. Earth as a planet is essentially bimodal in granitic continents and basaltic ocean basins, observed R. A. Daly (1871–1957), which reflects this process. And third, there was no general appreciation of how the rate of solidification is related to the size and number of crystals in a rock. The distinction between crystals nucleated and grown in place over phenocrysts carried in with the magma was not appreciated. The role of rapid quenching at the contacts of sills and dikes producing chilled margins, laced with large numbers of small crystals, and slower cooling in the interior producing larger crystals, was clearly long recognized. But there was no realization that inordinately large crystals in small sills like Shonkin Sag could not have grown after emplacement. In fact, there was little understanding of the need to isolate and define the initial conditions of a newly emplaced magma. Although not explicitly discussed until much later, it was apparently assumed that all magmas arrived for emplacement essentially free of crystals. Today, these three areas are each becoming mature fields in and of themselves, but the complex interplay of these areas, considered as one dynamic continuum, still remains as the foremost frontier to understanding magmatic processes.

6.07.5.1 Life Time Lines

The life spans of the principal petrologists of this time are shown by **Figure 13**. Nearly all of those mentioned so far were born in the middle 1800s and by about 1915 they were either dying or retiring from the field. The new wave of petrologists (e.g., Bowen, Grout, Wager) were emerging from graduate school with a desire to apply new methods, mainly phase equilibria, to solve classical magmatic problems. Although Becker and Pirsson had clearly defined the dynamics of magma chambers, the usefulness of this concept was yet to be measured against the phase equilibria of real silicate systems, which hitherto was completely unknown in any quantitative sense. This entire area was ripe for development in the wake of the seminal experimental work by Arthur L. Day on the plagioclase binary. N. L. Bowen (1887–1955) rapidly became the leader in this area and in 1915 he published one of the most important papers of the century (Bowen, 1915).

Armed with a relative wealth of basic information on silicate phase equilibria, diffusion constants, and elementary thermodynamic constants (e.g., heats of fusion), which he had extracted from phase diagrams, Bowen systematically evaluated, one by one, all the various suggested mechanisms thought perhaps to effect the differentiation of magma. His logical, detailed, and quantitative approach of coupling experiment, theory, and field inferences swept away a host of processes as being ineffective. He established fractional crystallization by crystal settling as the primary means of differentiation. That is, prior to knowing silicate phase equilibria, nearly every mechanism known to chemistry had been argued to be important in explaining the diversity of igneous rocks. Diffusional exchange with wall rock, Soret effect, wall rock assimilation, gas fluxing, among many other processes, had been suggested to be important. They were all equal competitors. Bowen evaluated each of these in a fashion that is remarkably similar to the modern method of scaling analysis in applied mathematics. He was forceful and thorough in his conclusions and he left no room for argument. He demolished all competing theories on differentiation. He even attacked the Becker–Pirsson model where the residual convecting melt continually reacts through diffusion with dendritic crystals growing on the walls. Instead, he said that only by crystal growth and settling could significant differentiation proceed. He overlooked the fact that this is exactly what Pirsson himself had said in applying Becker's wine bottle model to Shonkin Sag.

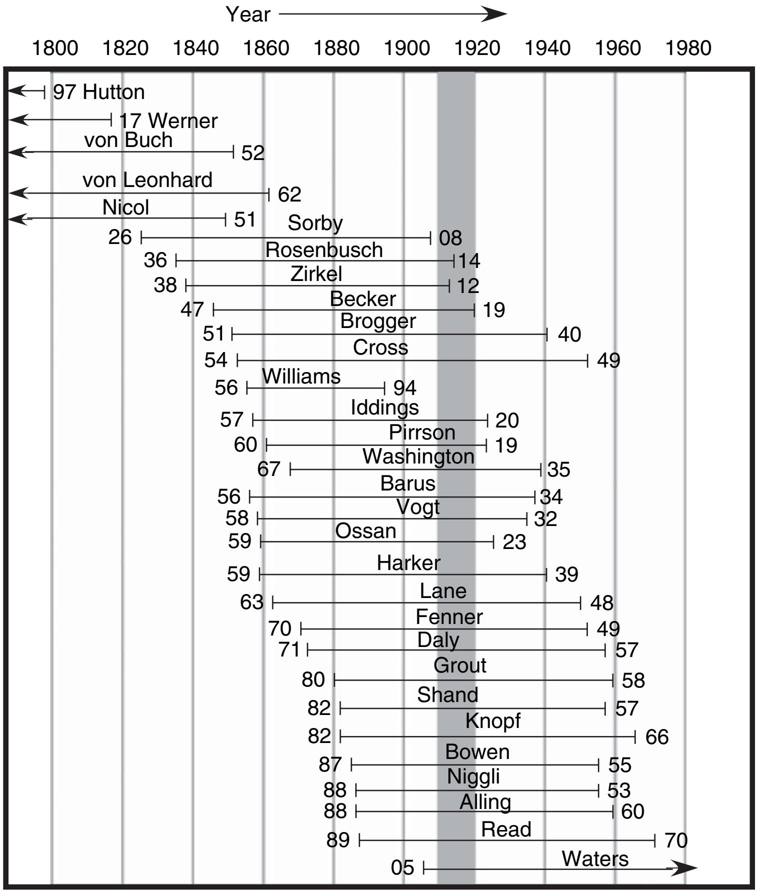

Figure 13 The names and dates of existence of prominent geologists and petrologists of the late nineteenth and early twentieth centuries.

In this 90-page treatise, Bowen showed (see Figure 14) that it is principally the phase relations of solid solutions and not eutectics that control igneous systems, and that there is therefore no practical end to how far differentiation can proceed as long as crystals can settle or be otherwise physically separated from the melt. There were, however, many petrologists who did not believe that crystals could settle in viscous magma. Bowen not only showed experimentally in a large experimental charge that olivine in picritic magma did clearly settle, but he also deduced the viscosity of melts and used Stokes' law to calculate settling velocities (Bowen, 1947). He performed novel experiments and produced data crucial to answering the central question posed by the earlier generation. The amount of printed material he turned out was enormous and a great deal of it is still pertinent.

The bottom line is that Bowen pushed and promoted his model thoroughly and hard. He said crystals grow in the middle of a charge or a magma chamber. They settle to the bottom and the residual liquid compositionally evolves from basalt to granite. It is simply an unavoidable fact of silicate phase equilibria. In its simplest dynamic sense, petrologists have stuck with this to the present. No one today would refute that the separation of crystals from melt causes chemical differentiation, but what is still unclear is how this actually takes place in a physical sense. For if all significant nucleation and growth of crystals is in marginal fronts and there are no crystals in the interior, how does crystal–liquid separation take place? To his credit, Bowen did worry about this and he proposed that melt buried in high-crystallinity mushes might be kneaded out by tectonic processes. But later he realized that this would probably be ineffective because the timescale of deformation is generally much longer than that for solidification.

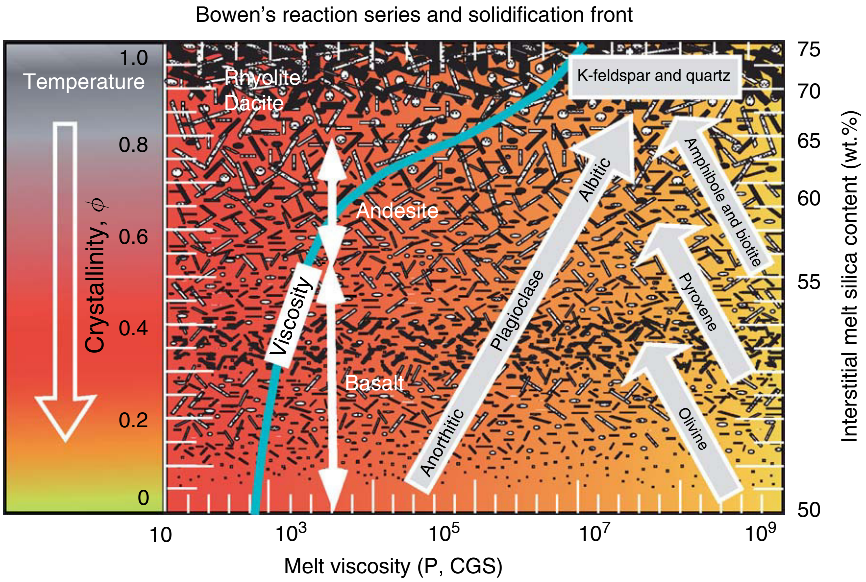

Figure 14 Bowen's reaction series superimposed on an active basalt solidification front at the roof of a sheet of magma. Variations of composition and viscosity as a result crystallization are also shown.

6.07.6 Initial Conditions of Magmatic Systems

All natural processes involve time. And the most critical part of analyzing and understanding magmatic processes involves a clear and concise knowledge of the nature of the system at the outset when it all began. The ensuing process itself, especially including the eventual final outcome, reflects in every detail the initial state of the magma. The final product, more than anything else, simply reflects the initial conditions. The importance of these conditions has been routinely overlooked, and the process conjured up to explain rock sequences, especially complicated ones, are often unrealistic and overly complicated. They are complicated mainly because the assumed initial conditions are so far from the final state of the system and are hence impossibly difficult to sensibly connect in any logical construct. These initial conditions, as mentioned earlier, are:

1. the spatial pattern of cooling and crystallization;
2. the composition and initial state of crystallinity of the magma;
3. the sequence of emplacement of the magma; and
4. the final distribution of crystal sizes throughout the body.

These are, in and of themselves, often exceedingly difficult conditions to ascertain without first knowing what evidence in the rocks clearly reflects these conditions. In early studies, the critical importance of these conditions to the final outcome was unknown and the simplest possible conditions were assumed. In their classic study of the chemical evolution and layering of the Skaergaard Intrusion, for example, Wager and Deer (1939) and Wager and Brown (1968) stated at the outset that crystal-free magma was instantaneously injected, perhaps in a violent fashion. For the initial composition of the magma, they took that composition of the chilled against the wall rock, gabbro. Skaergaard contains about 600 km^3 of magma in a body with an aspect ration of about 2:1. This is not a large body of magma – many large dolerite sills are this large. But why does it exhibit such well-formed layering? Is it the form of the container holding the magma? The style of cooling? Or is it the chemical composition of the magma? Given the initial conditions assumed for the formation and condition of the initial magma, a host of processes involving sorting of crystals existing in the initial magma are excluded, as are also processes associated with the emplacement sequence itself.

Given the assumptions, Wager and Deer explained Skaergaard, with no (or very few) initial crystals, as crystal growth starting somewhere in the middle of the body in response to strong cooling from the roof. The melt mingles with any crystals that are around the edges and keeps reacting like the bottle of wine so that the middle of the body chemically evolves with time. Cumulous crystals, like snowfalls, build up on the floor and form sequences of modally layered rocks in response to periodic loading and unloading of the system with crystals due to roofward cooling. The geometric form of the body encourages cascades of crystal-laden currents down the sloping walls. Within the piles of cumulate crystals on the floor, compaction, continued crystal growth, and melt migration physically modify the textures and chemically evolve the rock to fit the final product. Additional liquid may leak out, but eventually we end up with some liquid left at the roof with some rind on the top. This perspective is heavily influenced by Pirsson's treatise on Shonkin Sag. Wager and Deer got this perspective from Harry Hess who was working on the massive, heavily layered Stillwater Intrusion. (Although Hess's memoir was published much later in 1960, his incidental reports on his Stillwater work are cited by Wager and Deer.) Faced with similar sequences of modally layered rocks, Hess went back to the early work of Becker, Pirsson, and Grout, and incorporated the overall process spelled out by Pirsson. The important point here is that the Pirsson model is the fundamental idea from which all explanations for the evolution of layered intrusions have emanated. It is thus important to understand this model in more detail in light of discerning the importance of magmatic initial conditions.

6.07.6.1 Cooling from the Roof

When an opening is made in the crust for emplacement of a magmatic body, the upper and lower contacts of country rock initially had exactly the same temperature. The magma is generally much hotter than the country rock and the difference in temperature between magma and country rock is large and virtually identical at upper and lower contacts, regardless of the thickness of the body. The rate of cooling of the magma by conduction through the upper and lower wall rock is also virtually identical. The body thus cools at the same rate from top and bottom. This is shown by considering the central temperature in identical hot sheets emplaced far from, near, and on Earth's surface. There is no difference, especially in early times, in the rate of cooling for deeply buried and shallow intrusions, and only a sight difference for a body (e.g., lava or lava lake) on the surface. The sheets of magma are so much hotter than their surroundings that it is essentially immaterial what they are surrounded by. This also holds for all the other margins of the body, that is, sidewalls. Other processes of cooling, such as hydrothermal convection, will influence differently the upper and lower contacts, but mainly only in the later stages of cooling when solidification is no longer important (e.g., Marsh, 1989). The conclusion is, thus, that magmas in general do not cool more strongly from the roof and crystallization is no more intense along the roof than it is elsewhere along the margins of the body. Cooling is characterized by heat flow from all outer margins of the magma at 'approximately' similar rates, and this cooling is characterized everywhere by crystallization. For every unit of thermal energy flowing from the magma, a specific mass of crystals is produced in a specific spatial pattern.

6.07.6.2 Style of Crystal Nucleation and Growth

In Becker's original model of magma chamber crystallization, for example, liquid moves freely in and out of the mass of growing crystals, carrying, in effect, nutrients to the crystals. The residual melt becomes increasingly depleted in time in crystalline components, thereby becoming enriched in unwanted or residual components. The center of a crystallizing bottle of wine becomes increasingly rich in alcohol. This is essentially what happens in any system where dendritic crystal growth prevails as in metallic alloys and aqueous solutions. These solutions are also commonly of low viscosity melt and low Prandtl number. Compared to silicates dendritic crystals are unusually large and can span a significant distance within a solidification front. If these dendritic systems were scaled up to the size of typical bodies of magma, dendritic crystals might reach sizes of tens of meters or hundreds of meters long. Large compositional boundary layers develop on the large crystals and are buoyant, highly mobile, and highly effective in carrying 'used up' fluid from the crystals. This is very much unlike what we see in silicate magmas.

One of the curious things about magma is that the size of crystals in most igneous rocks is on the order of tenths of a millimeter to a centimeter. That reflects the multisaturated, multicomponent nature of silicate magmas where chemical diffusion is slow and the melts are highly viscous (e.g., large Prandtl number). Within thickening solidification fronts, crystals nucleate and grow at the leading edge near the liquidus. Nucleation certainly does not start here, for magmas are essentially dirty systems, laced with nuclei. Only in some very rare systems are magmas ever free of nuclei as an initial condition. This reflects the fact that endogenous magmas are never found to be superheated. Nuclei are thus always present and serve as seeds for crystallization regardless of the exact phase involved. Once the cooling front arrives, existing nuclei increase in size outward through the solidification front. The tiny growing crystals are in a parasitic relationship where what chemical components one crystal does not want, another one will nucleate and grow to use. Diffusion is so slow in silicate liquids that if an olivine crystal is growing on the liquidus of tholeiitic basalt, for example, unwanted components like CaO, Al_2O_3, Na_2O, Fe_2O_3, SiO_2, and K_2O build up in the surrounding melt. This increases the chemical potentials of clinopyroxene and plagioclase, spawning nucleation and crystal growth. This reflects the common state near multiple saturation in many basaltic magmas, a slight enhancement in concentration of rejected components will saturate the melt in another solid phase. Continual growth of these crystals will enhance nucleation and growth of the other phases and vice versa. This creates local intense clusters of crystals of several phases and, eventually, from these clusters appears single large, well-formed crystals (see Figure 15). The small crystals combine through aggregation and grain boundary migration into large, optically continuous crystals. The process is part of the phenomenon of Ostwald ripening, where touching grains combine in response to lowering the net surface free energy. This is, in effect, a form of high-temperature annealing, and it happens so rapidly that it is difficult to observe except in samples quenched from lava lakes. The long-believed perception of crystals nucleating and growing at widely separate locations and only eventually impinging on one another at the close of solidification is a reflection of an assumption of homogeneous nucleation, which rarely occurs in magma. Heterogeneous nucleation is the rule in magma.

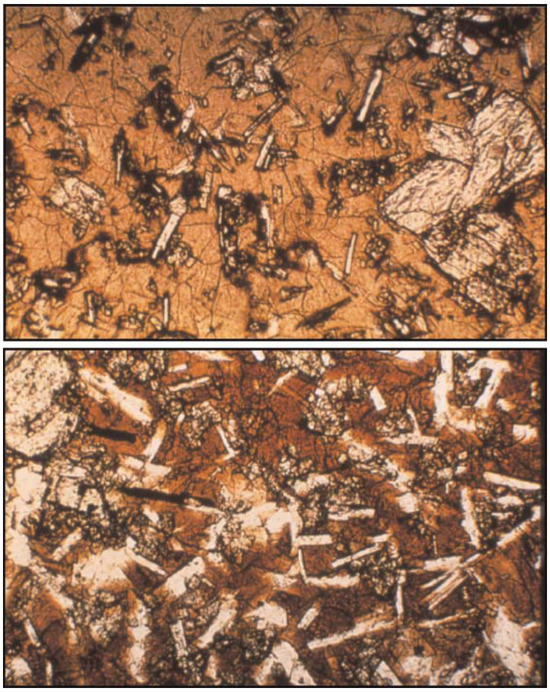

Figure 15 Thin sections (~5 × 2 cm^2) from Makaopuhi Lava Lake (courtesy of Dr. T. L. Wright) at crystallinities of *c*. 20 and 40 vol.% (upper to lower) showing the tendency for crystallization to occur in dense clusters.

6.07.6.3 The Critical Connection between Space and Composition

The variations in melt silica content and viscosity with distance or crystallinity within a typical tholeiitic basalt solidification front are shown by Figure 16. Both silica content and viscosity increase dramatically with the degree of crystallinity or distance outward in the solidification front. It is especially notable that silica enrichment increases gradually for the first 50 vol.% of crystallization, increasing by only about 5 wt.%. It is only outward of this point, at much higher crystallinities, that strong enrichment occurs. But once the level of crystallinity reaches 50 vol.%, the point of critical crystallinity has been reached where the magma is a rigid network of crystals laced with melt. The melt and crystals cannot

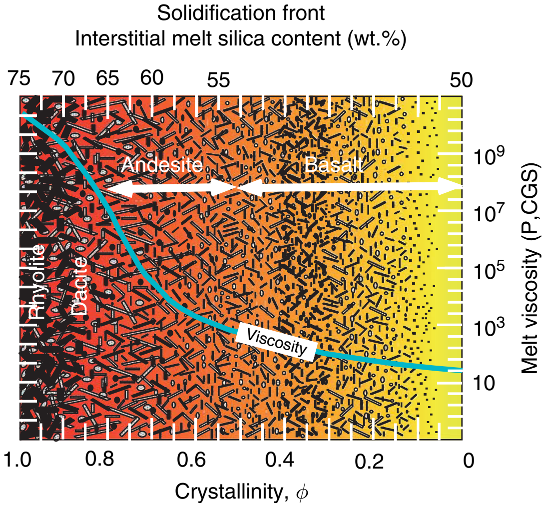

Figure 16 A solidification front on the sidewall of a basaltic magma showing the variations in composition, viscosity, and crystal mass as a function of position.

be easily separated, and the crystals surely cannot be separated by conventional crystal settling. Andesitic, dacitic, and rhyolitic melts occur at increasingly higher states of crystallinity, where the separation of melt and solids in increasingly difficult. The key to chemical differentiation of the magma is to isolate the enriched melt at a separate body of magma. How does this occur?

Out in the center of the body nothing is happening. As seen earlier, crystals will not begin growing there until the inward propagating solidification front arrives. Even small crystals escaping from the suspension zone of the solidification front will have no effect on the overall magma composition. Tiny crystals falling from the suspension zone are resorbed in the inner hotter magma and do nothing to change melt composition. Even a big plume of crystals and slightly cooler melt dropping from the suspension zone, which might survive transit of the hot inner magma, simply enters the suspension zone of the lower solidification front with no net spatial change in the composition of the system. It just goes from one part of the system to another. Low-density melt might escape from the lower solidification front, but the viscous chemical boundary layers on the tiny crystals have little buoyancy and are stabilized by the cluster style of nucleation and growth and the advancement of the solidification front itself. Chemically, nothing is going on out in the center of the body. It is within the solidification fronts that any differentiation will take place.

The most critical relationship to appreciate in understanding magmatic processes is the relationship between moving across a conventional phase diagram and moving in space in a magmatic system. Because the temperature field of a magma is closely tied to space, phase diagrams are also tied to space. Moving on a phase diagram, thus, always involves moving in space (i.e., x, y, z) in a magma, and these moves are almost always within solidification fronts because that is where temperature varies the strongest with spatial coordinates.

This critical relationship can be readily appreciated by considering a David Walker-style normative ternary phase diagram with the normative components olivine, diopside, and silica at the apices and the systems is saturated everywhere with plagioclase (see Figure 17). These phase relations fit a wide range of basaltic magmas from tholeiites to high-alumina basalts (HABs). There is a single major cotectic boundary separating the two major phase fields of olivine, or alternatively orthopyroxene at higher silica contents, and diopside or clinopyroxene. Because of the mapping between temperature and space, any movement on this phase diagram, along the cotectic or anywhere else, involves a move in magma space. Beginning in the middle of the magmatic system, the corresponding point on the phase diagram is the beginning bulk magma composition on the cotectic boundary (see the large block dot). Moving in space from the center outward into the upper solidification front no move occurs on the phase diagram because there are no temperature or composition changes. Once the solidification front is entered there is a choice whether to follow the bulk composition on the phase diagram or only the interstitial melt composition. If the local bulk composition is followed, all points map onto the same initial starting bulk composition (i.e., the same starting black dot). This is because there has been no separation of crystals and melt. If, on the other hand, the local residual melt composition is monitored, then the compositions migrate, with increasing crystallization or depth outward in the solidification front, along the cotectic toward the silica corner of the ternary. The silica corner will, in fact, be closely approached as the very last bit of melt

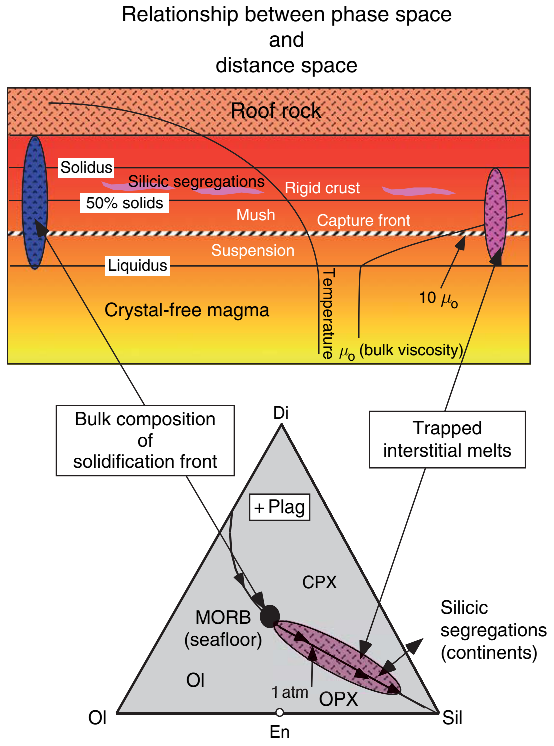

Figure 17 The fundamental relationship between spatial position (upper) in a solidification front and phase position in the normative basalt ternary system.

crystallizes near the solidus at the back end of the advancing solidification front. It is important to realize that these late-stage, highly fractionated melt compositions do not exist separately, in and of themselves, as an actual physical entity that could be erupted as lava or re-emplaced as a pluton. These melts are locked within the crystalline framework of the solidification front and cannot be separated by any simple means; more on these processes later.

An understanding of this critical relationship between spatial variations in magma and moves on a phase diagram makes solving, or at least understanding, many fundamental petrologic occurrences straightforward. Magmatism at ocean ridges the world over is predominantly tholeiitic with subtle variations of many kinds. No silicic differentiates are ever seen as lava. The volumetrically overwhelming composition rests on the cotectic and does not move toward the silica corner as might be expected from a viewpoint of classical crystal fractionation theory. No continent-like rocks are produced. As will be seen later, the ocean ridge magmatic system is essentially a sill or series of sills, called the axial ridge magma chamber, perched at the top of a vertically extensive magmatic mush column. When the plates move apart, aliquots of essentially crystal-free magma are withdrawn or pulled from the subjacent sill by disrupting the roofward solidification front. No magma comes from within the solidification fronts, so the lavas are generally always just basalts. Once the system is activated in this way, more magma arrives from below, which may contain 'tramp' or dynamically entrained crystals from the underlying mush column. Upon entering the axial sill, these crystals will settle from the magma, which is an example of 'punctuated differentiation' discussed earlier, and the magma will sit there surrounded by solidification fronts.

This process also explains why Hawaiian and similar large-volume basaltic centers in oceanic settings produce such a paucity of silicic differentiates. The summit lavas from Kilauea, for example, are never more fractionated than about 51.5 wt.% SiO_2 and 7 wt.% MgO (see Figure 18). If this composition is traced from the chemical variation diagram to a solidification front, it is seen that this composition defines the inner, leading edge of the suspension zone of the solidification front. The more fractionated, more

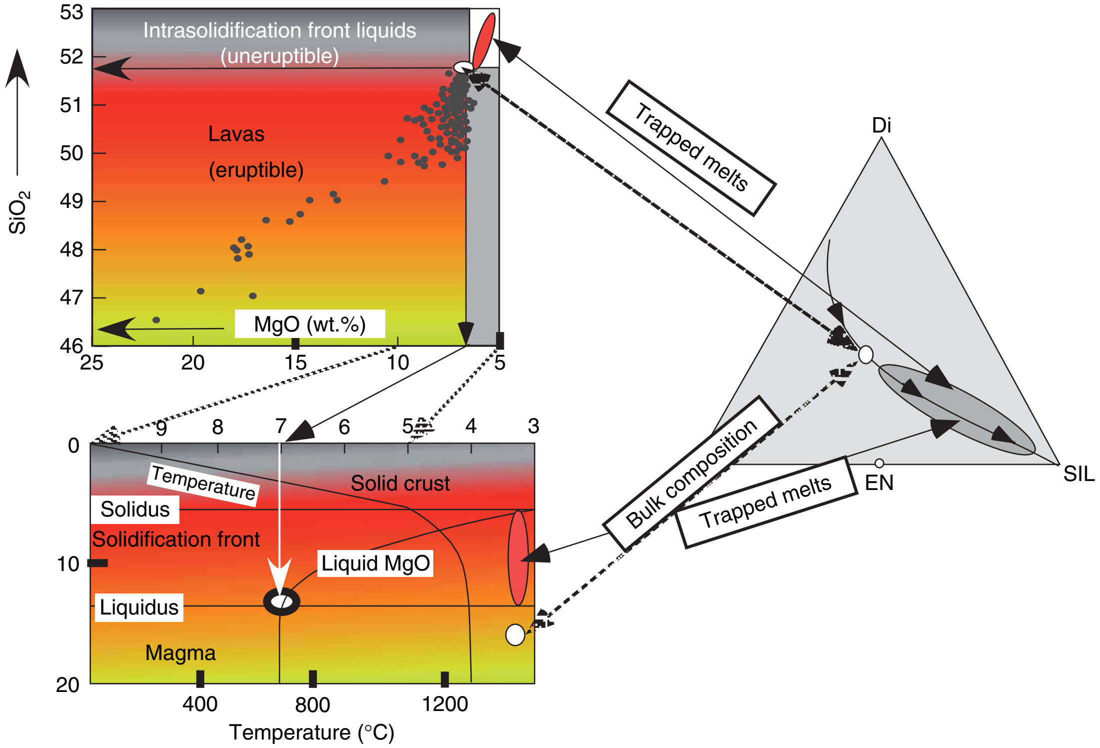

Figure 18 The explanation for the absence of lavas erupted from Kilauea summit with silica greater than about 51.5 wt.% is found in tracing the magma composition to the spatial position at the leading edge of the solidification front.

siliceous compositions are, again, locked within the front and are not available by simple means for withdrawal and eruption. It should also be noticed that there are many more primitive, high MgO compositions, which represent, by and large, magmas carrying an abundance of entrained forsterite-rich olivine xenocrysts or tramp crystals. Once the magma comes to rest, these crystals fall from the magma as in punctuated differentiation and the usual magma type of ~51.5 wt.% SiO_2 and 7 wt.% MgO is produced. There are sometimes mildly differentiated lavas erupted from the Kilauea rift system, silicic pods are also found in the crusts of the Hawaiian lava lakes, and on Iceland about 18% of the surface lavas are true rhyolites and process leading to these effects is examined later. We will see bimodal differentiation comes from solidification fronts that tear open and form lenses of silicic liquids or silicic segregations. These even show up in the lava lakes in Hawaii, but the key for recognizing the role of this material as eruptable magma on Earth's surface is recognizing a means to collecting individual segregations into large, eruptable masses of magma.

6.07.6.4 The Sequence of Emplacement or Delivery of the Magma

The fundamental question always lurking about but rarely answered in analyzing exhumed magmatic systems is: How was the system built? What was the overall nature of the event in time span and volumes of individual deliveries of batches of magma that made the system? How did the system operate on a year-to-year basis? These are difficult questions and the postmortem evidence in exhumed magmatic systems is rarely conclusive. Rather, the most direct evidence of the time scales and volumes of individual batches of magma comes from volcanic systems. Volcanic systems, on the other hand, lack all information on the details of the internal arrangement and local physical environments of the system in which the volcanic products formed. It is no wonder, then, that volcanologists and plutonists have widely divergent views on the basic structure and workings of magmatic systems. Yet it is the coupling of this evidence that gives critical insight into the real-time dynamics of the establishment and sustaining of magmatic systems. The quantitative connection between volcanism and plutonism is the product of observed erupted flux and the volume of individual plutonic complexes. This product measures the 'filling time' or time to establish a magmatic complex. To estimate this product, something of the form and volumes of plutonic systems must be appreciated along with the temporal pulse of volcanic systems.

6.07.6.4.1 Forms of magmatic bodies

Magmatic systems come in all shapes and sizes, but the most common shape is sheet-like for plutons, sills, and certainly lavas. This reflects the common vertical orientation of the least principal stress in the upper crust. Magma ascends as fluid-filled cracks (dikes) or viscous blobs (diapirs) or as a combination of each. Dike and fissure propagation is common in young or developing systems, where the country rock is cool and brittle, or in systems where the crust is in tension as in continuous rifting as at ocean ridges. Magma ascends due to its low density relative to the wall rock and the influence of gravity. Ascension is a gravitational instability. Ascension is impeded by loss of hydrostatic head (e.g., Ryan, 1994). The leading mass of magma reaches a level of neutral buoyancy, which may be due more to the vertically integrated buoyancy than to merely the local density contrast, and is forced to spread laterally by the continual rise of magma deeper in the rising column, thus forming sheet-like bodies, which in the upper crust are known as sills. Sheet-like forms are fundamental to all magma, regardless of level of emplacement in Earth. Magmatic systems are, to first order, a series of sheets connected by circular conduits and dike-like fissures.

Diapirism is more the rule in stationary, well-developed magmatic systems, as perhaps beneath older volcanic centers in island arcs where the system has had ample time to develop, and the underlying lithosphere has had ample time to heat up from the long-term passage of many magmatic bodies. But here, too, stalling diapirs mushroom out and go to form sheet-like bodies.

6.07.6.4.2 Internal transport style

Once the system is established and has formed a magmatic mush column of some type (**Figure 1**), the form of magma transport is probably more a combination of many processes driven by density variations reflecting basic differences in chemical composition due to melt composition and the abundance and type of crystals carried by the melt. At every level in a magmatic mush column the process of local transport, although broadly similar overall, may vary over time from diapiric on many length scales to slurry flow as in a pipe to dike flow. The style of the process itself and time series of repetition is certainly chaotic. But since the material is a viscous fluid of a relatively narrow range of composition and crystallinity, the outcome, almost regardless of the details of transport, is distinct to the tectonic setting and to a large extent predictable.

Because of the strong effect of annealing during solidification, it is almost impossible to gauge the importance of repetitive reinjection during building of a plutonic complex. Internal chilled margins as indicators of the sudden juxtaposition of magma batches of contrasting temperature do not survive solidification, and the strong textural changes that do survive are almost universally interpreted as reflecting internal solidification dynamics. There are few if any true indicators in intrusive complexes of the nature of the time series of deliveries of the batches of magma that collected to make the final magma. As noted above, this is where the fluxes and eruptive timescales are absolutely critical to understanding magmatic systems.

6.07.6.4.3 Eruptive timescales and fluxes

The observed durations of volcanic eruptions have been summarized by Simkin. By far the most common eruption lasts from about a month to a year, with the overall spectrum of times spanning about 100 years.

Measures of eruption flux come from mass balances on both large and small scales. The flux of magma from global ocean ridge systems can be estimated from the product of the average rate of spreading (double sided, $\sim 5\,\mathrm{cm\,yr^{-1}}$), the thickness of the oceanic crust ($\sim 8\,\mathrm{km}$), and the length of the ridge system ($\sim 40\,000\,\mathrm{km}$), which amounts to about $15\,\mathrm{km^3\,yr^{-1}}$. This is clearly a minimum estimate, for the actual amount of magma existing in the system at any time, because a significant amount of magma probably gets trapped in the deeper parts of the system and is recycled back into the mantle source rock. The flux that established the island of Hawaii must have been, on average, about $1\,\mathrm{km^3\,yr^{-1}}$. The age of the island is about 1 My and it has a volume of about $10^6\,\mathrm{km^3}$. The apparent fluxes that established large igneous provinces fall in this range of ~ 1–$15\,\mathrm{km^3\,yr^{-1}}$. For examples, consider the Columbia River flood basalts ($\sim 1\,\mathrm{km^3\,yr^{-1}}$), the Deccan traps ($\sim 3\,\mathrm{km^3\,yr^{-1}}$), and Ontong Java ($\sim 15\,\mathrm{km^3\,yr^{-1}}$) (see Coffin and Eldholm, 1992). The volumes of these lava sequences are generally much larger (~ 1–$50 \times 10^6\,\mathrm{km^3}$) than any known magmatic intrusions, the largest of which are Bushveld (S. Africa), and Dufek (Antarctica), each at about $500\,000\,\mathrm{km^3}$. The Sudbury impact melt sheet may originally have had a volume of about $35\,000\,\mathrm{km^3}$, and Skaergaard is on the order of $650\,\mathrm{km^3}$. By far the largest single 'day' eruptions are those of silicic pyroclastic ash flows. The Fish Canyon ash flow is about $3000\,\mathrm{km^3}$, the Toba Tuff is about $2000\,\mathrm{km^3}$, and the two Timber Mountain Tuffs are 1200 and $900\,\mathrm{km^3}$ (e.g., Smith and Roobol, 1982). The huge flux of these silicic events undoubtedly reflects the mode of transport of uncapping an overpressured, near-surface system containing large amount so dissolved volatiles. It would be difficult imagining an intrusive even of this magnitude.

6.07.6.4.4 Filling times

Given the final volume of a pluton or sill, the filling time is a multiple of the input flux. For a body of the size of Skaergaard ($\sim 650\,\mathrm{km^3}$), for example, the filling time is ~ 45 years if all the magma produced at the ocean ridges ($15\,\mathrm{km^3\,yr^{-1}}$) were directed to this location. For a Hawaiian rate ($1\,\mathrm{km^3\,yr^{-1}}$), the filling time is longer, 650 years. There is no simple way to decide the actual filling time (U–Th and Po–Pb–Ra isotopic disequilibrium may offer some information) – the only physical constraint comes from rate of solidification. The rate of filling must be significantly greater than the rate of solidification. For these sheet-like systems, it is straightforward to show by scaling the heat equation (see eqn [1]) and including the effect of latent heat (e.g., Jaeger, 1968) that the solidification time (t)is well approximated by the simple formula

$$t = 0.694\frac{(L/2)^2}{K} \qquad [17]$$

where L is the half-thickness of the sheet and K is the thermal diffusivity (e.g., $\sim 10^{-2}\,\mathrm{cm^2\,s^{-1}}$). The half-thickness of a sill or pluton can be estimated by noting that the aspect ratio (n) of sills is 100 or more whereas that of plutons is about 10; there are of course large variances in these values, especially for plutons. Nevertheless, for a given volume (V), of magma the half-thickness of the equivalent rectangular sheet of dimensions $n2L \times n2L \times 2L$ is given by $L = (V/8n^2)^{1/3}$. Under this approximation, for a given volume of magma, sills will be thinner than plutons and the solidification time of sills will be significantly smaller than for plutons. The competition in filling time and solidification time for a range of fluxes operating over the characteristic eruptive times found by Simkin is shown by **Figure 19**. In light of the earlier discussion of the controls of crystallinity on magma fluidity, the calculated time for solidification has been lessened by a factor of 10 to ensure that the body is sufficiently fluid to ensure reinjection without creating an internal chilled margin, or also to

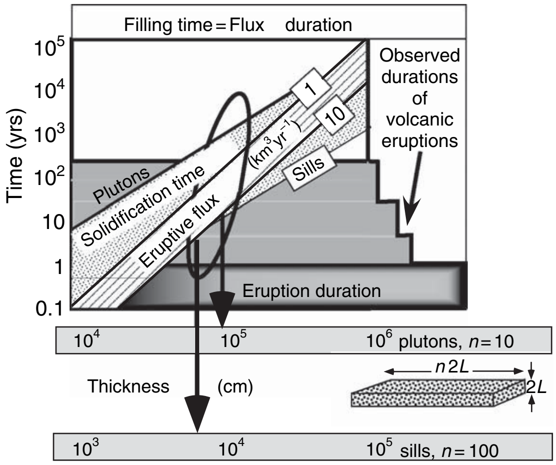

Figure 19 The time to fill sheet-like plutons and sills of a given aspect ratio (lower axis area) found using observed durations of eruptions and the estimated fluxes from large igneous outpourings. The time of solidification as a function of body size (half-thickness) is also shown as a constraint on the time of filling.

ensure that the sequence of arrivals of magmatic parcels can mix to make a single body. From this constraint, the characteristic thickness of a sill is ~100 and ~1000 m for a pluton, and the filling times are, respectively, about 10 and 300 years. These are geologically reasonable results, but the actual filling times may be much less. This sequence of events for sills will be revisited below when discussing the Ferrar dolerites.

6.07.6.4.5 Magmatic deliveries, episodes, periods, and repose times

At a more detailed level, it is also clear that the full volume of the body is probably not delivered in a single event, but, in keeping with the typical style of volcanic eruptions, individual batches of magma may arrive serially perhaps every few weeks or months as in a volcanic episode. The accumulated volume from the full series of deliveries amounts to a volcanic episode, which gives rise to the final body of magma. This is an important distinction as a series of episodes may also be strung together to make up a much longer magmatic period giving rise to a sequence of sills or a compound pluton consisting of multiple lobes each associated with one another but having separate cooling times. The episodes themselves reflect volcanic repose times, which for many active volcanoes may occur for tens to hundreds or perhaps thousands of years. Moreover, the longer the series of deliveries, the more chance there is for variations in phenocryst content in the batch of arriving magma, which, as been discussed for Hawaii, is highly dependent on the magnitude of the eruptive flux. Thus, the larger the final body of magma, the larger is the probable variance in the concentration of large crystals, both phenocryts and tramp crystals, contained in the ensemble of the individual delivered batches of magma. The more variance in the deliveries, the more variance to be expected in the final sequence of the rock within the pluton or sill. It is very likely exactly these variances that give rise to exotic sequences of layering from modal sorting during deposition of crystal-laden deliveries of magma in the building of large igneous bodies. Nevertheless, in this context, what is perhaps also surprising is the abundance in volume flood basalt provinces of extensive lavas containing low concentrations of phenocrysts.

6.07.6.5 Thermal Ascent Characteristics and The Role of Thermal Convection

From the earliest models of magma chambers, as in Pirsson's discussion of Shonkin Sag, convection has always played a role in establishing the final product. The exact nature of this convection, whether it was driven by thermal, compositional, or sedimentation effects, has never been clear. Convection has been a necessary convenience in magmatic histories and it has taken on a multifaceted physical nature, most often without explicitly defining its specific form. The process of ascent, transport, and emplacement of magma is certainly a form of convection or advection. Fluid motions accompanying the deposition of phenocrysts, however complicated this might be due to the dynamics of slurries (e.g., Marsh, 2004), are also certainly a form of convection. But most often, perhaps in response to the concentrated attention on mantle convection in driving plate tectonics, magmatic convection has been assumed to be primarily thermal. The physics of conventional thermal convection in a crystallizing solution is not entirely straightforward as has been summarized by Zieg and Marsh (2005), from which the following summary comes.

The importance of thermal buoyancy relative to viscous drag and heat transfer by conduction is a measure of the tendency for thermal convection to occur in a layer of fluid. These effects are collectively measured by the dimensionless Rayleigh number (*Ra*). The physics of thermal convection in many types of fluids with various forms of heat sources, geometries, and boundary conditions is well known (e.g., Turner, 1973). Relatively little is known, however, about thermal convection in fluids undergoing crystallization in marginal solidification fronts, especially in fluids as diverse as silicate magmas (Marsh, 1989). This uncertainty has spurred debate over the occurrence of thermal convection in common magmas (e.g., Marsh, 1991). With no direct experimental observations of magmatic thermal convection, experimental attention has been focused on analog fluids that might be similar to magma. These systems are molten paraffin (Viskanta and Gau, 1982; Brandeis and Marsh, 1989, 1990) and solutions of isopropanol and water (Kerr *et al.*, 1989; Hort *et al.*, 1999). This work shows that in an initially superheated melt convection sets in rapidly and persists only until all the superheat has been dissipated. Thermal convection steadily wanes with approach to the liquidus and ceases at the liquidus. All further cooling is by conduction, which may be the behavior of many crystallizing fluids. The strong contrast with nonsolidifying systems is marked by the kinetics of crystallization (Hort *et al.*, 1999; Marsh, 1996; Hort, 1997). There is indirect evidence that it is also the case in magma in comparing the cooling of Hawaiian lava lakes with lava flows. The growth of the crust of the lava lakes, measured through direct drilling (e.g., Wright and Okamura, 1977), shows the same pattern of growth for lavas as measured by Hon *et al.* (1994). This is fundamentally significant, as will be seen below, for the magnitude of the Rayleigh number (*Ra*) depends on the characteristic length scale to the third power, and *Ra* must be much larger than about 10^3 for convection to be possible. Since most lavas are quite thin (~5 m), *Ra* is small, certainly subcritical, which suggests the same for the much thicker (~100 m) lava lakes.

6.07.6.5.1 Superheat

This apparent lack of thermal convection may also be a reflection of the lack of superheat in terrestrial magma, which may erupt at or below the liquidus temperatures. This is because undersaturated magma adiabats are steeper than liquidi, which promotes superheating. The appearance of any superheat leads to an enormous Rayleigh number, which brings on vigorous thermal convection, dissipating the superheat to the wall rock and bringing the temperature strongly back to the liquidus (see **Figure 3**). With the loss of superheat, thermal convection ceases, and the process repeats itself on a timescale governed by the rate of ascent. The thermal ascent trajectory is an oscillation about the liquidus. For sufficiently rapid ascent rates, magma temperature is, in effect, buffered at the liquidus. When ascent is sufficiently slow, heat loss by conduction sustains magma temperature at subliquidus values, but here the magma flirts with stagnation through critical increases in viscosity due to crystallization (note shading in figure). ‘Dry’ magmas, like at Hawaii, erupt at near-liquidus temperatures. No magma is ever bone-dry, and Hawaiian MgO-rich lavas contain significant amounts of ‘phenocrysts’, which are a combination of so-called ‘tramp’ crystals entrained from earlier crystallization cumulates and even wall rock materials (e.g., Wright and Fiske, 1971; Garcia *et al.*, 1989; Marsh, 2006). The relatively low volatile content makes the ensuing eruption of low explosivity, but the lavas are highly mobile. This is just the reverse for ‘wet’ magmas. Here ‘wet’ means magma containing significant amounts of dissolved volatiles, especially water, which for alkali basalts may mount to 2–3 wt.%.

Wet magmas similarly follow the liquidus, but only as long as they remain undersaturated. At the depth of volatile saturation, the liquidus and adiabat cross. At this point, the liquidus, depending on the exact water content, may be at or below the 1 atm solidus. Further adiabatic ascent is, at best, isothermal (allowing for some crystallization; see details below), and the magma undergoes progressive devolatilization, bubble nucleation, bubble coalescence, fragmentation, and extensive ash and tephra formation. The eruption is highly explosive, but the ensuing lavas are highly immobile. By analogy with siliceous systems (e.g., Jaupart, 1998; Dobran, 2001; Melnik *et al.*, 2005), the magma degasses and slowly squeezes out as a viscous sludge.

The pervasive lack of superheat in endogenetic magma bodies may thus reflect the efficiency of convection in eliminating superheat as it occurs during ascent (Marsh, 1989). Magmas formed by impacts, however, can become instantly superheated *in situ*. This results in vigorous magmatic convection that lasts until all the magma has cooled to its liquidus temperature. The initial temperature of the Sudbury impact melt sheet, as will be considered below, was approximately 1700°C, well above the liquidus temperatures. In this context, and also perhaps for the lavas on Io, it is useful to consider the role of thermal convection in superheated magma.

The magnitude of the governing *Ra* at the onset of convection determines the time scales for convection to become fully developed and also for the superheat to be removed from the system. *Ra* can be estimated directly from the definition

$$Ra = \frac{\alpha g \Delta T L^3}{\nu \kappa} \qquad [18]$$

where g is gravity, ΔT is the initial amount of superheat (~500°C for Sudbury), α is the coefficient of thermal expansion ($\sim 5\times 10^{-5}\,{}^{\circ}\mathrm{C}^{-1}$), L is the thickness of an individual layer (norite ~1 km, granophyre ~1.5 km for Sudbury), v is the kinematic viscosity of the melt layers (norite $\sim 10\,\mathrm{cm^2\,s^{-1}}$, granophyre $\sim 100\,\mathrm{cm^2\,s^{-1}}$), and κ is the thermal diffusivity ($\sim 10^{-2}\,\mathrm{cm^2\,s^{-1}}$). With these values,

$$Ra = 10^{15} - 10^{17} \tag{19}$$

For reference, the Ra governing convection in Earth's mantle is $\sim 10^5$, and convection commences in a layer of fluid contained between two solid boundaries heated from below and cooled from above when $Ra = 1708$. For one solid boundary and one fluid boundary, $Ra = 1100$, which is appropriate for Sudbury. This implies that convection in the Sudbury melt sheet was initially in the regime of vigorous turbulence (e.g., Khurana, 1988). This means that the thermal regime was chaotic and the layers would have been rapidly mixed and homogenized. It is important to emphasize that, during convection, all the main dynamic features of the system (e.g., convective velocity, rate of heat transfer, etc.) depend intimately on Ra. It is also important to realize that even for a magma with a very small amount of superheat (~1°C), Ra could be large if L is sufficiently large. In the above estimate of Ra for Sudbury, reducing ΔT to this level only brings Ra down to about 10^{12}–10^{13}. This suggests that any amount of superheat whatsoever will bring on vigorous convection and rapidly bring the temperature back to the liquidus. Thermal convection cannot be expected as a common process in magma chambers. For completeness, especially in considering ascending magmas, extraterrestrial magmas, and impact melt sheets, it is essential to consider the startup time and rate of cooling in convecting magma.

The time (t) for convection in each layer to start and become fully established, for example, is given by (e.g., Jhaveri and Homsy, 1980)

$$t = \frac{L^2}{\kappa}\left[\frac{B}{Ra}\right]^{2/3} \tag{20}$$

where B (~350) is a constant and the other symbols are as above. Using Ra as found earlier, thermal convection in the Sudbury melt sheet would have fully developed within about an hour. This reflects the potential strength of convection due to the presence of such a large degree of superheat. The rate of cooling also reflects this extreme vigor of thermal convection.

There are two extremes for the emplacement and cooling environment of magma. The first is magma cooled rapidly at the margins due perhaps to hydrothermal transfer in the roof and footwall, and the second is magma deeply embedded in a purely conductive medium.

6.07.6.5.1.(i) Rapid convective cooling The average temperature (T) in a rapidly convecting layer, strongly cooled from its margins, especially from above, is given by

$$T = T_\mathrm{L} + \Delta T_\mathrm{o}\left[1 + \frac{t}{\tau}\right]^{-1/b} \tag{21}$$

where T_L is the liquidus temperature, ΔT_o is the amount of superheat, t is time, and τ is a group of parameters that characterizes the overall cooling time. The value of τ is given by

$$\tau = \frac{L^2}{2Cb\kappa'}Ra^{-b} \tag{22}$$

The symbols used here are as defined above, except for C and b, which come from the parametric relationship ($Nu = CRa^b$) between the rate of heat transfer, as measured by the dimensionless Nusselt number (Nu), and Ra. (Nu measures the magnitude of heat transfer by convection relative to that by conduction.) For high Ra convection, typical values of these constants are $b = 1/3$ and $C = 0.4$ (e.g., Turner, 1973; Marsh, 1989). The thermal diffusivity ($\kappa' = K_\mathrm{c}/\rho C_p$) derived here contains mixed properties; the thermal conductivity (K_c) is of the wall rock and the density (ρ) and specific heat (C_p) are of the magma, but a representative value of about $10^{-2}\,\mathrm{cm^2\,s^{-1}}$ is still appropriate.

The drop in temperature, as calculated using eqn [20], is shown in **Figure 20**. Even in a body as large as the Sudbury impact melt sheet, which may have contained ~35 000 km of magma, albeit in a thin sheet (~3 km × 200 km), the superheat could have dissipated in ~10 years. This reflects the great efficiency of thermal convection in removing heat from a layer when there is little resistance to heat flow at the margins. For a body buried deeply in a conductive environment, as in continental crust, cooling is significantly slower.

6.07.6.5.1.(ii) Slower convective cooling in a conductive medium For this extreme, consider a melt sheet sandwiched between upper and lower rock units that transfer heat only by conduction. To assure that this is the slowest possible rate of convective cooling and to simplify the problem, assume

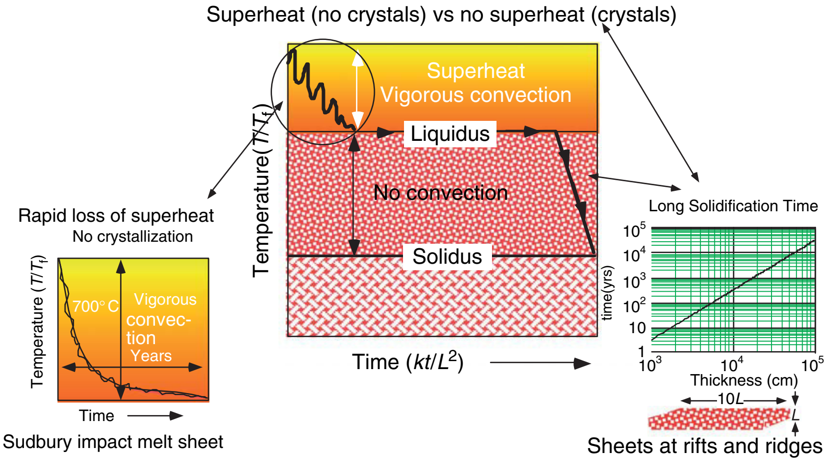

Figure 20 Modes of magmatic cooling for superheated magmas, like impact melt sheets (thermal convection), and for all other magmatic bodies (conduction). The scales are in nondimensional temperature vs nondimensional time, where T_f is the final temperature, t is time, L is body half-thickness, and K is thermal diffusivity.

that the upper and lower layers of country rock are infinitely thick. The temperature of the magma as a function of time is given by (Carslaw and Jaeger, 1959; see also Marsh (1989))

$$\frac{T-T_w}{T_m-T_w} = \exp\left(hx+h^2\kappa t\right)\mathrm{erfc}\left(\frac{x}{\sqrt{4\kappa t}}+h\sqrt{\kappa t}\right) \qquad [23]$$

where exp and erfc are, respectively, the exponential and complementary error functions, T_m is the initial magma temperature, T_w is the initial wall rock temperature, x is the vertical spatial coordinate, and $h=\rho C_p/MC_p'$, where p is wall rock density, C_p and C_p' are the specific heats of, respectively, the wall rock and magma, and M is the mass of magma (of density ρ') in contact with a unit area of wall rock. For a melt sheet of thickness L cooling from above and below where $C_p \sim C_p'$, $M=\rho' L/2$, and $\rho \sim \rho'$, whence $h=2/L$, the temperature of the magma over time is found by setting $x=0$:

$$\frac{T-T_w}{T_m-T_w} = \exp(4F)\,\mathrm{erfc}\left(\sqrt{4F}\right) \qquad [24]$$

where $F=\kappa t/L^2$. Since the magma is always well mixed and of uniform temperature, the contact temperature is also the overall magma temperature. In this example, the magma reaches its liquidus temperature in about 10 000 years; this variation in temperature is shown by **Figure 20**.

From these two bounding examples, it is clear that highly vigorous convection in magma lasts a relatively short period of time, probably between a few tens of years and a few hundred years. Once convection ceases, the magma continues to cool solely by conduction of heat.

Early petrologists thought magmas were commonly intruded in a superheated state, or at least there was confusion on this issue. And, as mentioned already, even though crystal-laden volcanic eruptions are the rule, the meaning of this feature relative to magma chamber evolution was not appreciated. Coupled with the inaccuracy appreciated of assuming the importance of cooling mainly from the roof, these misconstrued initial conditions set the stage for a century of research on magma chamber processes.

6.07.6.6 Summary of Magmatic Initial Conditions

Like most Earth processes, including the formation of Earth itself, the initial conditions are well nigh impossible to ascertain. This is especially true for magmatic systems. And because the initial conditions, regarding timing and mode of delivery of volumetric inputs and, especially, the concentration of phenocrysts, are only rarely known, it is critically important not to assume initial conditions that are unrealistic. For in any physical process, identifying the correct or reasonably correct initial conditions is absolutely critical to the outcome. The assumption by early petrologists of large magmatic bodies being ‘instantaneously emplaced free of crystals’ is not only incorrect and untenable, but it is an impossibly difficult starting point from which to reach the observed end result of an exotically layered body. The most obvious cause of layering in intrusive bodies is the periodic influx of crystal-laden magma (e.g., Marsh, 2006), and not due to some form of periodic overturning related to thermal convection during crystallization. In fact, from all experimental evidence on analog systems and circumstantial field evidence, magmas only thermally convect if they are superheated, which is a state never observed for any endogenetic magma. Convection in response to the density contrasts of periodic injections of deliveries of magma, some containing heavy concentrations of crystals, leading to establishment of a large body, must certainly occur. This convection would clearly be periodic and related to crystal deposition and layer formation. In this fashion, the larger the body, the higher the probability of acquiring textural diversity.

6.07.7 End-Member Magmatic Systems

Perhaps the most revealing and insightful means of understanding magmatic processes is to examine unusually complete, well-exposed systems where the initial conditions are especially clear. Here we will examine two such systems that in a strong sense define the end members of magmatic system establishment and evolution. The two examined below are the Sudbury impact melt sheet and the Ferrar dolerite system of the McMurdo Dry Valleys, Antarctica. When deciphering these and any other magmatic system, it is critically important to keep in mind the role of solidification fronts in forming the final product and also the major controls that the initial conditions have on deciding the final outcome. In trying to recognize the initial conditions two features must be sought. One is the concentration of large crystals in the initial magma forming the body, and the other is the number of possible injections that gave rise to the body.

6.07.7.1 The Sudbury Igneous Complex (SIC)

The Sudbury impact melt sheet is the closest example on Earth of a massive magmatic laboratory bench experiment. This is a body that was emplaced instantaneously free of crystals. These are the exact initial conditions postulated by early petrologists. In this context alone, it is enormously valuable to examine the end product. The SIC was produced 1.85 Ga in a matter of minutes (~5) by impact of 10–12 km bolide (e.g., Grieve *et al.*, 1991). Perhaps originally containing as much as 35 000 km^3 of magma ~3 km deep and spread across a crater ~200 km in diameter, the melt sheet had the aspect ratio of a compact disk. Moreover, the initial temperature, which can be ascertained by several methods, was ~1700°C, well beyond the liquidus (~1200°C) of the magma (Zieg and Marsh, 2005). The melt was intensely superheated, destroying all existing crystals. For all intents and purposes, this is an infinite sheet of magma. The body today (see **Figure 21**) has been deformed by continent-to-continent collision during Grenville time, which has folded it from south to north much as one would fold a sandwich. This folding, along with glaciation, has made the stratigraphy particularly accessible as has extensive drilling associated with mining (~1.5 billion metric tons) of massive deposits of Ni–Cu sulfide ores along the crater floor.

The final section of igneous rock is an upper layer of ~2 km of granophyre (~70 wt.% SiO_2) and a lower ~1 km layer of norite (~57 wt.% SiO_2) separated by a transition zone of quartz gabbro of several hundred meters, which is the densest rock in the entire section (**Figure 21**). The most surprising aspect of this body is the degree of homogeneity of the norite and granophyre. The same stratigraphy is laterally continuous across the entire body. There is no modal layering anywhere. Trace element and isotopic ratios are much too similar to ascribe to pure chance or a protracted igneous process. For example, isotopic ratios, such as $^{87}Sr/^{86}Sr$ (Dicken *et al.*, 1999) and La/Sm, Gd/Yb, and Th/Nb, are nearly identical in the two main units (Lightfoot *et al.*, 1997). Although sill-like in form, which is similar to other large bodies, like Bushveld, Dufek, and Stillwater, it has none of the features of major sills. The average composition is ~64% SiO_2 but this material is not found as extensive chilled margins at the top and bottom, and there is no systematic chemical progression inward to suggest any form of differentiation by crystal fractionation. These features, among many others (see Zieg and Marsh, 2005), along with unusually uniform textural homogeneity, suggests that, once formed, the body did not evolve at all along the lines long assumed for magmatic bodies. In fact, to a close first approximation, once formed, the main units did not evolve at all. They simply crystallized in place. All of these features are likely natural consequences of the impact process.

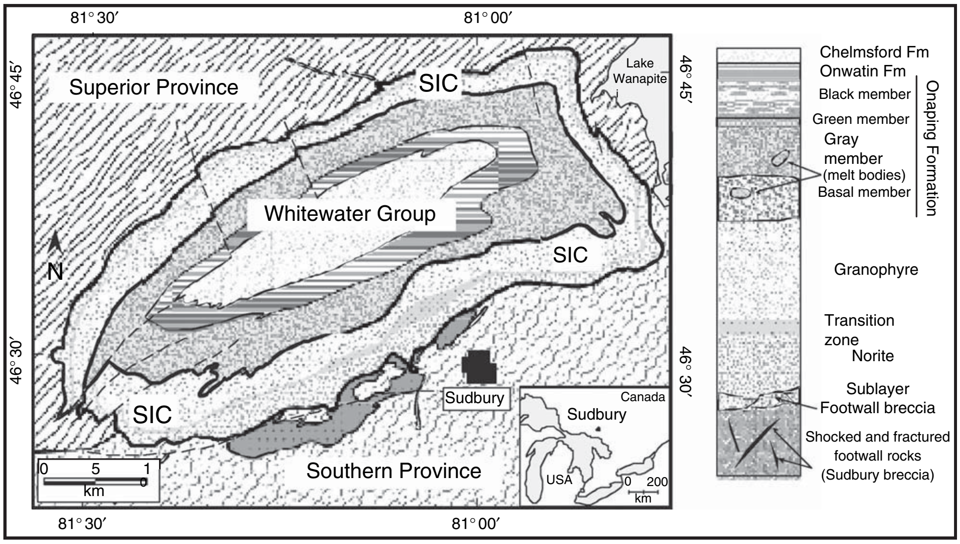

Figure 21 Geologic map of the Sudbury Igneous Complex, ON, Canada. At right is the general stratigraphy of the crater. After Zieg MJ and Marsh BD (2005) The Sudbury Igneous Complex: Viscous Emulsion Differentiation of a Superheated Impact Melt Sheet. *Bulletin of Geological Society of America* 117: 1427–1450.

Impacts of this size generate an outward moving shock wave of ~500 GPa (5 Mb), which is equivalent to the pressure at Earth's center. Temperatures reached about 4000°C at the center of the impact, vaporizing the impactor and adjacent silicate crust. Beyond the vaporization zone an extensive melting front existed and beyond this a fracture front. The production of breccia of all sizes (tens of meters to nanometers), in states of vapor, liquid, and solid, characterizes all aspects of the cratering event. As the impactor penetrated downward, it produced within a few minutes a transient cavity ~30 km deep and ~90 km in diameter. The target materials from which the breccias were made consisted of highly evolved continental crust. The crust was granitic overall, but in detail it consisted of granitic plutons, gneisses, swarms of diabase dikes and sills, gabbroic plutons, quartzose sediments, and untold other lithologic varieties. These materials form an extensive 3-km-thick sequence of 'fallback' breccia (Onaping Formation) that cascaded in from the crater rim and atmosphere as the crater relaxed over a few minutes into the final shallow impact melt sheet (~6 × 200 km). The magmatic part of the sheet is the molten breccia (Zieg and Marsh, 2005). This molten breccia is more properly described as a magmatic viscous emulsion. That is, it consisted of blobs of silicate melt of a wide spectrum of chemical composition and thus density and viscosity. Although certainly not chemically immiscible, small density and compositional differences gave rise to an exceedingly heterogeneous melt where each blob had the freedom to sink or rise. Large volumes of near-identical composition rapidly coalesced into an extensive 'continuous phase' within which were other smaller chemically and physically distinct blobs, which formed a 'dispersed phase'. Because of the inherent granitic nature of the crust here, the continuous phase was granitic and the dispersed phase basaltic. Once the sheet formed, this superheated magmatic emulsion immediately began to separate and coalesce into an upper granitic layer and a lower basaltic layer. The separation and coalescence process was rapid, taking place within a few years. Although a rapid process, this process also allowed extensive intimate chemical exchange between the dispersed and continuous phases.

Melt parcels smaller than a certain critical size (~1 cm) rose or fell so slowly that they were chemically resorbed by diffusion into the surrounding melt. Moreover, the vast surface area available to chemical exchange allowed the entire melt sheet to chemically interact by diffusion during coalescence of the emulsion. And once the two layers had separated, each superheated layer went into vigorous thermal convection, which thoroughly homogenized each layer. Prior to this time, the strong upward and downward flow of melt parcels had suppressed thermal convection. This convective phase of cooling lasted at most a few tens of years (Zieg and Marsh, 2005). The net result is two layers of strongly contrasting chemical composition that have intimately and thoroughly exchanged trace chemical components to a high degree and, then, each has been thoroughly homogenized internally by exceedingly vigorous convection. The high temperature and the vigorous convection stripped the entire body of volatiles, making it unusually dry for magmas of these compositions.

Once the superheat had been dissipated from each layer through thermal convection, convection ceased and crystallization commenced in the form of inward propagating solidification fronts from the top and bottom. These fronts were unusual in that the contact temperatures at the base and roof were each near the solidus temperature of the respective magmas, granophyre and norite. This pinned the solidus at or near the boundaries while the liquidus, defining the leading edge of the front, freely propagated inward to meet, perhaps coincidentally, at the juncture of the two layers. This allowed for unusually thick solidification fronts to form. This made thick crystal mushes at the top and bottom that acted to retard the descent and rising of solid breccia debris from, respectively, the roof and floor. Rafts of Onaping breccia foundering from the roof fall in the less dense granitic magma and descend until reaching the lower layer of basaltic magma. At the same time, rafts of breccia and individual large blocks from granitic plutons forming the crater floor rose until encountering the upper granitic magma. The net result of the movement of all this debris is a zone of collection at the interface between the two layers. This debris, some of which further disaggregated and dissolved in surrounding magma, and mafic melt squeezed from slight compaction of the lower solidification combined in the end to make the transition zone. The collection of all this debris formed an unusual environment in terms of chemical compositions and also oxidation state and collection of volatiles. This debris carried hydrous minerals that dehydrated upon heating, further shattering the breccias into smaller fragments and freeing volatiles to collect and form miarolitic cavities. This all produced an oxidized environment of heterogeneous composition of strong density contrasts that may have allowed internal gravity waves to propagate along this interface. The culmination of this collection process occurred as the lower solidification front reached the interface, structurally supporting this unit, which is the densest horizon in the entire body. This strong density gradient and overall structure of the transition zone is remarkably consistent everywhere it has been measured (see **Figure 22**).

The net result of generating a large body of magma instantaneously and free of all crystals is to produce two essentially homogeneous layers with no internal modal sorting or layering. This is a dramatic confirmation of the null hypothesis, which states that given a sheet-like magma free of crystals it will crystallize to homogeneous rock with only slight internal variations (Zieg and Marsh, 2005). Magmas do not become exotically layered and show strong

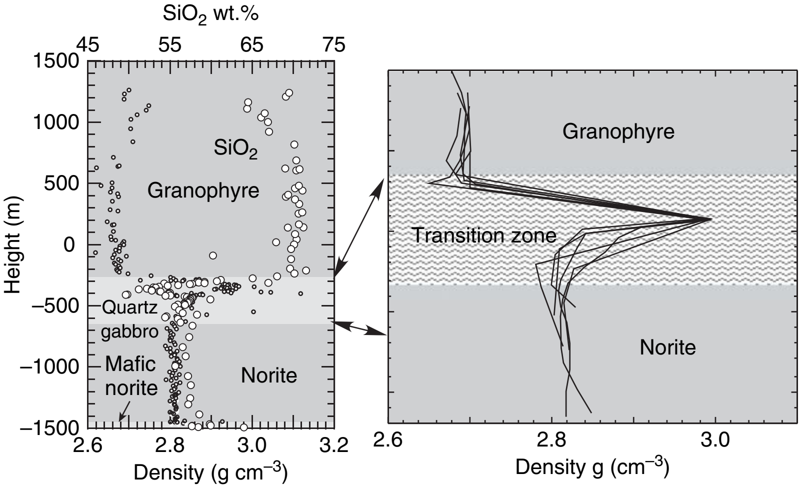

Figure 22 The variations (left) in density and bulk rock silica content through the Sudbury impact melt sheet, showing the granophyre and norite units, and a detailed view (right) of the density structure in the transition zone where the profiles have been normalized for position to the maximum density at each drill hole location. The remarkable similarity throughout the body suggests a delicate mechanical equilibrium.

differentiation trends from basaltic to granitic by crystal fractionation within such bodies. Then, how does it happen? It happens by injections of magma laden with large crystals. The extent and degree of layering is a direct indication of the extent of injection of crystal-laden magma.

The Sudbury record is also valuable in showing what happens to true granite target rock once it is heated beyond its liquidus and then allowed to crystallize as a dry high silica magma. The surprising result is that the final texture is not a coarse-grained typical granite. It is a fine grained granophyre. This is likely due to the loss of its textural template due to superheating and higher viscosity, and thus slower diffusion rates, under anhydrous conditions.

Sudbury is also a prime example of how the continental crust became organized early in Earth history. Ongoing impacts extensively melted the fledgling crust, allowing it to continually reorganize through emulsion sorting and coalescence.

As mentioned above, Sudbury is critically important in clearly showing what happens to magma when the initial conditions are explicitly known. In this regard, it is an end-member example. Many thinner diabase sills the world over are examples of this type of magmatic body.

6.07.7.2 Ferrar Dolerites, Antarctica

Another end member is represented by systems that are multiply or serially injected, partly with magma literally choked with large crystals. An excellent example of such a system that is unusually well exposed is the Ferrar dolerites of the McMurdo Dry Valleys, Antarctica.

The Ferrar dolerites, like similar systems worldwide, were emplaced with the breakup of Gondwana ~180 Ma. Instead of the magma occupying the central rift and being eventually lost with widening of the rift, these magmas were emplaced in the stable west continental shoulder of the rift. The magmas were mainly injected into a thick section of Mesozoic sediments called the Beacon Supergroup, consisting of sandstones and associated sediments including coal deposits. The overall package dips slightly (~5°) to the west and is remarkably unfaulted, intact, and exceedingly well exposed. The McMurdo Dry Valleys are Earth's most ancient landscapes and have remained since the Early Tertiary essentially unchanged (e.g., Wilch *et al.*, 1993). Deep and long east–west river-cut valleys expose ~4 km vertical sections over and area of ~10 000 km^2 revealing four major mafic sills each ~300 m thick. Sill composition is broadly similar to dolerite/diabase sills of this age and type emplaced with the Gondwana breakup worldwide. And with ~55 wt.% SiO_2, they are similar compositionally to the norites of the lower part of the Sudbury melt sheet, but the overall result could not have been more different. The fundamental reason for this difference is the presence of a rich abundance of large orthopyroxene (Opx) crystals and the piecemeal injection of the system as sills rather than as a single large body (Marsh, 2004).

A general geologic map of the Dry Valleys showing the distribution of the dolerite sills is given by **Figure 23** (Marsh and Zieg, unpublished). The four-sill system is capped by extensive flood basalts called the Kirkpatrick Basalt (e.g., Fleming *et al.*, 1992), which are directly connected in age, composition, and field relations to the underlying sills. The general stratigraphic layout is shown by **Figure 24**. Besides the unusually clean exposures, the singularly valuable feature of this system is the presence of an extensive distribution of large Opx crystals in the lowermost sill, the Basement Sill, which can be used as tracers to follow sill emplacement and solidification. These Opx crystals in every way play the same role here as do the olivine tramp crystals in Hawaiian lavas and lava lakes. They are crystals from earlier magmatic events deeper in the underlying magmatic mush column, and also possibly from subcontinental mantle wall rock, that have been entrained by the rising magma. Sills and dikes containing similar concentrations of phenocrysts have been long recognized (e.g., Drever and Johnston, 1967; Gibb and Henderson, 1996), and Simkin (1967), building on an idea by Baragar (1960), generalized the concept of flow differentiation to suggest a sequence of ascent and emplacement as sills of crystal-laden magma. This Simkin sequence is also shown in **Figure 24**.

A fundamental property of particles in ascending fluid is the tendency to sort themselves by buoyancy and drag (i.e., size, shape, and density contrast) relative to the walls containing the flow. Heavy particles move away from walls and fall, relatively speaking, in the ascending fluid establishing a central high concentration or tongue of particles. The mechanics of this process is not entirely clear, but is associated with small inertial effects in an otherwise essentially inertia-free flow. Because the crystal tongue falls progressively behind the leading tip of the ascending column of magma, the leading magma and the magma on the margins is the most refined, having been stripped of crystals, and is positioned to cool

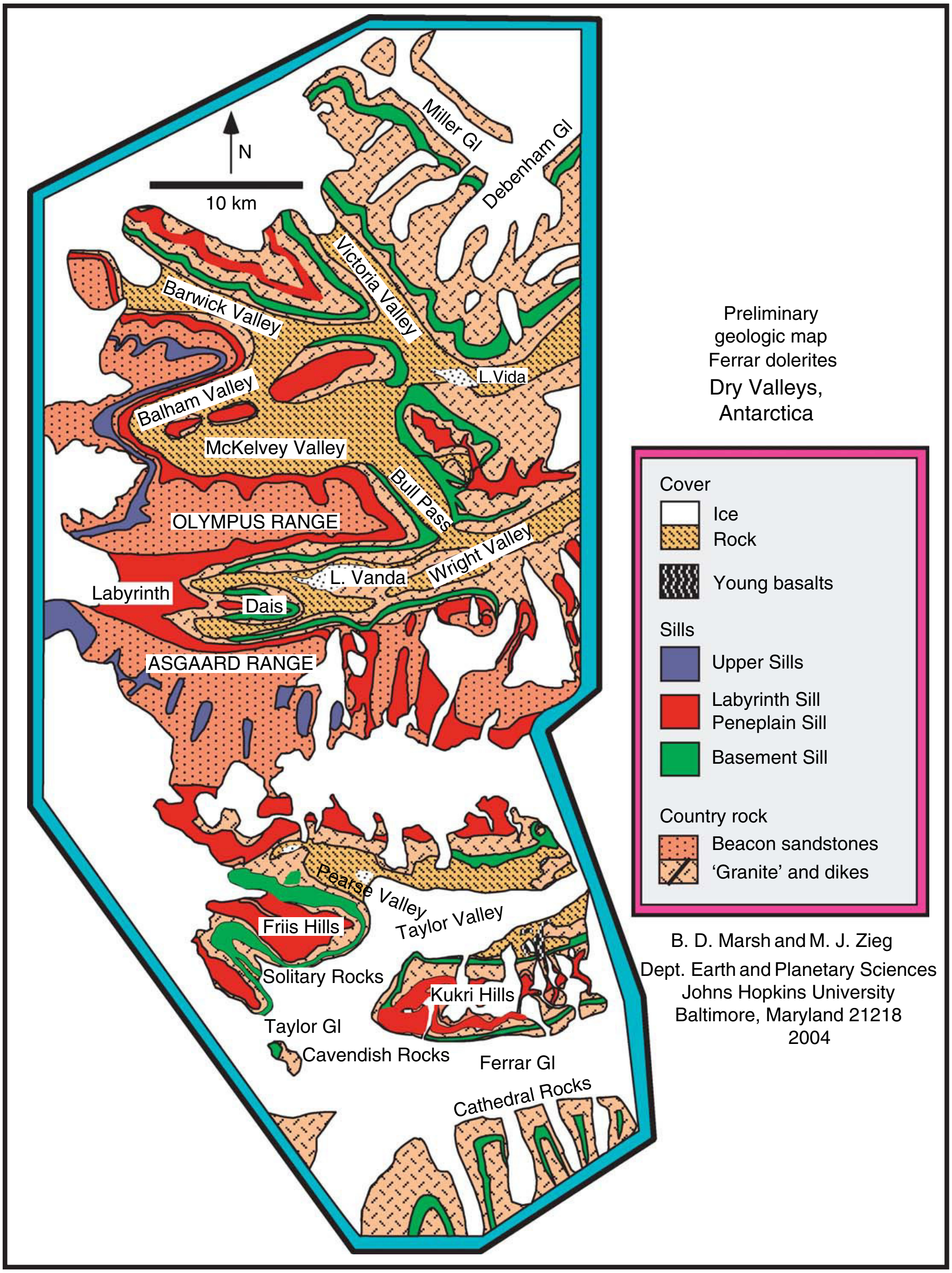

Figure 23 The distribution of dolerite sills (Ferrar dolerites) throughout the McMurdo Dry Valleys of Antarctica (Zieg and Marsh, unpublished).

and solidify first after emplacement. That is, once ascent stalls and the magma begins to spread laterally, the leading crystal-free magma coats and essentially cauterizes the wall rock as the sill wall rock is progressively opened. All the crystal-free magma about the sill margins is quickly chilled into fine-grained rock. The tongue of crystals is uniformly deposited along the lower solidification front,

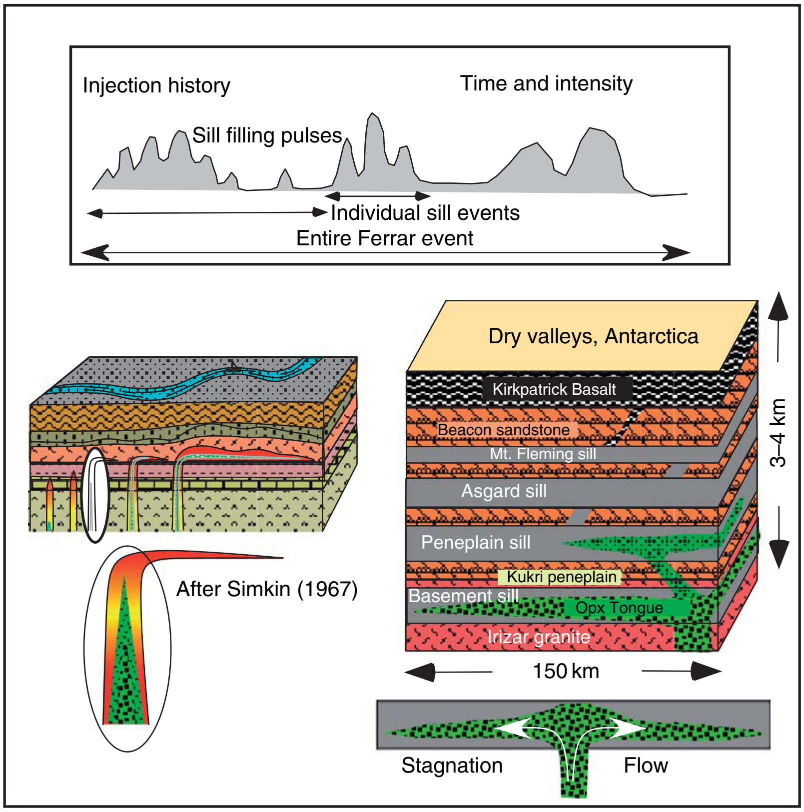

Figure 24 The stratigraphy of the dolerite sills of the McMurdo Dry Valleys, showing (left) the process of filling a sill by magma laden with entrained crystals, as envisioned by Simkin (1967). The inferred time sequence of filling of individual sills as a series of pulses leading to a prolonged periodic episode of sill formation is depicted at the top.

forming a classic S-shaped profile after solidification. Seminal fluid mechanical experiments realistically depicting this process have been performed by Bhattacharji in 1963.

This Simkin sequence of emplacement is found in the Basement Sill, where an extensive Opx tongue is found throughout the Dry Valleys. Although the locus of emplacement of sills is rarely found, the distribution of the Opx tongue gives direct insight into this point. The Opx tongue diminishes in thickness in all directions outward from the general area of Bull Pass, a pass in the Olympus Range forming the north wall of Wright Valley. From this area, a series of petal-like lobes propagated outward from a central funnel-like magmatic feeder zone to establish the Basement Sill. Profiles of MgO concentration through the Basement Sill and the upper sills are shown by Figure 25. The chilled margins and the leading tip of the Basement Sill all have low MgO contents of ~7 wt.%, similar to Hawaiian basalts free of large crystals, but the composition at the sill center reaches about 20 wt.% MgO, reflecting the high concentration (~40 vol.%) of entrained Opx crystals. The shape of the MgO concentration profile is parabolic and the sizes and abundance of Opx crystals are also of this form, which is due to the emplacement flow field.

Upward in the sequence of sills, the maximum MgO content decreases systematically (**Figure 25**), with less and less indication of Opx involvement. The compositional progression blends into the composition of the overlying Kirkpartick flood basalts. Coupled with the field relations, the overall system appears to have developed from the top down with the flood basalts first arriving from a plexus of regional dikes. Thickening of the basalts progressively capped the dikes forcing later arriving magma into sills that intruded increasing deeper in concert with the magma density. The Basement Sill intruded last in a slow sluggish fashion due to its high crystal content. This slow ascent and lateral emplacement was aided by heating of the country rock by earlier magma. That the emplacement process was very likely pulsatile is indicated by internal irregularities in the MgO profiles.

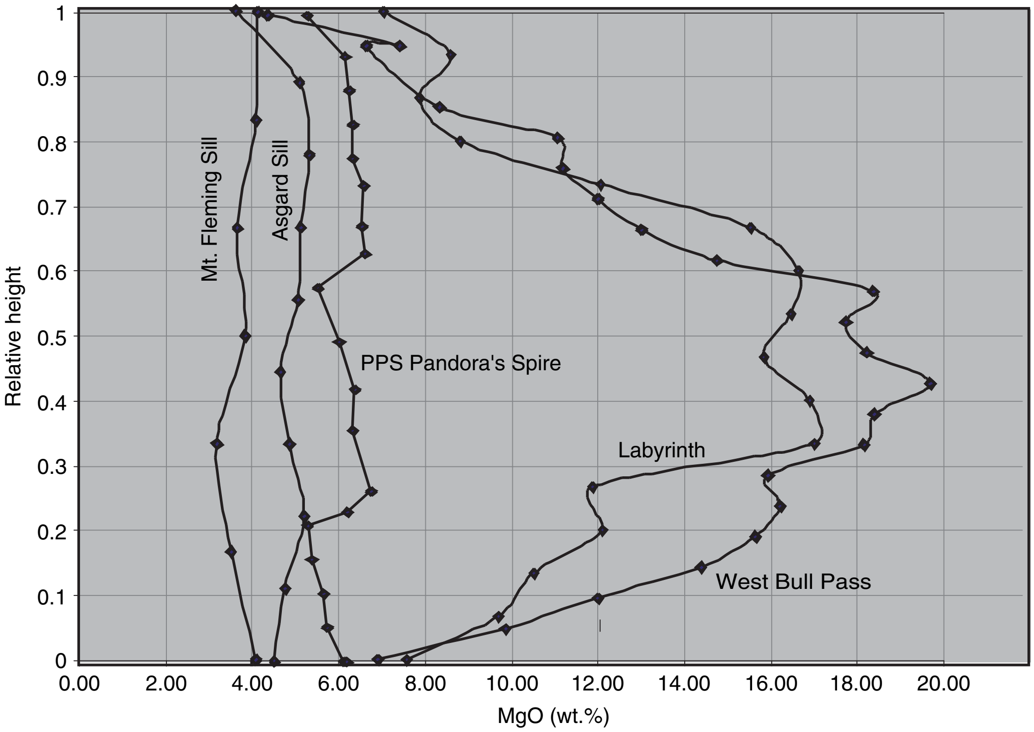

Figure 25 Variations of bulk rock MgO (wt.%) through the McMurdo Dry Valleys sills showing the large concentrations in the Basement Sill, reflecting the high concentration of entrained orthopyroxene, and the monotonically decreasing average composition in each higher in the sequence.

Stopping and restarting the emplacement process, as in volcanic reposes, cause resorting due to the steady advance of the upper and lower solidification fronts.

Everywhere within the Opx tongue are clear signs of further detailed crystal sorting between Opx and plagioclase. Plagioclase is the other major mineral phase in the Opx tongue, but it differs greatly in size as it nucleated and grew mainly during ascent and emplacement. It is generally ~10 times smaller in grain size than the Opx (~2–5 mm). This large contrast in size allows plagioclase, given the chance, to sieve through the Opx and collect in pockets and layers. In most places, this sorting reflects the shearing nature of the magmatic flow and plagioclase forms thin undulating horizontal stringers or schlieren. That is, in shearing of dense particle-laden slurries, the flow dilates as the larger particles attempt to move past one another. The dilation allows the smaller particles to sieve into the shear zones and form deposits or schlieren. There are many processes of this nature that occur in granular materials and all of them lead to sorting or layering of the final assemblage (e.g., Savage and Lun, 1988; Makse *et al.*, 1997). Signs of these processes are everywhere in the Basement Sill and they culminate in the Dais section in central Wright Valley. Here the Basement Sill literally cascades downward and ponds at the deepest part of the body to form an intricately layered complex called the Dais Intrusion (Marsh, 2004). The layering ranges between Opx-rich zones, called orthopyroxenite or websterite, to almost pure anorthosite layers up to 0.5 m thick and laterally continuous for hundreds of meters. This general style of layering between Opx and plagioclase is common in many large layered intrusions like Bushveld, Stillwater, and Ddufek, but here it has been preserved in an unusually pristine form due to the relatively rapid cooling of a body of this size. Cooling and solidification here took place overall in about 2000 years, but much quicker locally. In the noted large-layered bodies, cooling and solidification, like at Sudbury, took hundreds of thousands of years, during which time the initial textures annealed, destroying detailed indications of how the layers were formed. In most cases, the cause of the layering has been ascribed to internal nucleation and growth of crystals that have been resorted due to magma flow, but not as an obvious result of injection of a crystal-laden slurry.

Considered overall, this magmatic system is chemically similar to Hawaii. Plots of CaO versus MgO for Hawaii and the Dry Valleys Ferrar system are shown by **Figure 26**. Each system shows strong MgO control at high concentrations of MgO due to the mechanical addition or loss of olivine (Hawaii) and orthpyroxene (Ferrar). The other major difference in these two systems is in the context of the samples. All of the Hawaiian samples are of erupted lava, and only magmas with less than about 50 vol.% crystals can be erupted. Where exactly they came from in the underlying magmatic column and how they achieved their final chemical state is unknown, although it can be conjectured through geochemical methods. In the Ferrar case, the context of each sample is known exactly. In short, all of the rocks richer than 7 wt.% MgO come from the Opx tongue, with the richest in MgO coming from the central part of the Opx tongue, and all rocks with less than 7 wt.% MgO come from either the chilled margins or the upper sills that are free of entrained Opx. The mechanical and chemical processes by which these compositional states were reached can be traced by the spatial context of the rocks themselves within the overall system. In this sense, it is revealing that none of the upper sills, nor the Kirkpatrick Basalt, carry any Opx phenocrysts and there is no other physical indication of the role of Opx in their evolution. It is clearly evident in their chemical compositions, being so similar to the fractionated compositions of the Basement Sill, that these magmas are the product of an underlying magmatic mush column dominated by Opx.

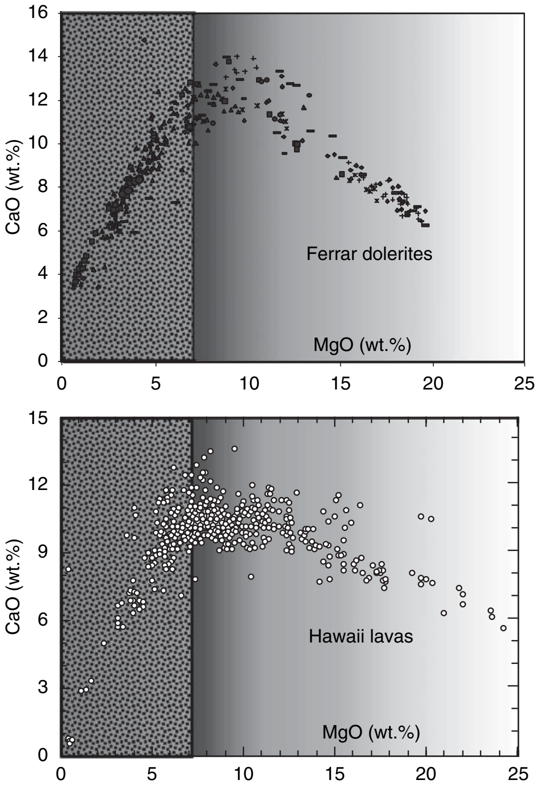

Figure 26 A comparison of the field of compositions (CaO versus MgO in wt.%) of the Ferrar dolerites and the lavas from the island of Hawaii.

An additional fortunate characteristic of the Ferrar system is the occurrence of four separate interconnected massive sills and a contiguous overlying sheet of flood basalts. The overall structure of the system is a stack of sills forming a fir tree-like magmatic system. This has allowed substantial volumes of magma, each perhaps representing a volcanic episode, to be serially emplaced as separate aliquots that cooled relatively rapidly to preserve an accurate magmatic record. If, on the other hand, all of this magma had gone to fill a single reservoir, with the time between each episode being short relative to the full solidification time, a massive layered intrusion would have resulted and all the revealing textures would have been lost to annealing (see **Figure 27**).

6.07.8 Lessons Learned from Sudbury and the Ferrar Dolerites

Magmatic systems are made of individual batches of magma delivered in amounts and over time as expected from volcanic processes. If the accumulated body is made of crystal-free contributions and is roughly sheet like, it will crystallize to an essentially uniform mass of rock, regardless of size. In the strictest sense, there will be many local chemical and textural aberrations due to untold local hydrothermal and solidification front processes, but these are second-order features. Strong textural and chemical variants come from variations in the nature of the injected magma. The bigger the body the more injections necessary to build it, and the more chance there is for strong variations in the crystal content of the incoming magma. Pervasive and exotic layering, clearly, reflects the deposition, sorting, and subsequent chemical annealing, including refinement of the incipient texture (e.g., Boudreau, 1994), of large crystals carried into the body by incoming magma. The old adage that only large bodies cool slowly enough to grow crystals large enough to become layered is untenable. Shonkin Sag at 70 m and the Basement Sill at 330 m negate this

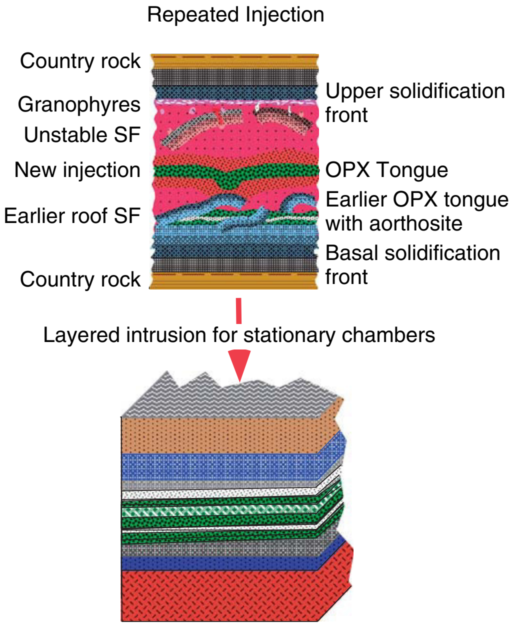

Figure 27 A schematic depiction of the repeated injection of basaltic magmas into a single reservoir where the crystal content can vary strongly from one injection to the next. In the end, this leads to an intricately layered pluton.

premise, whereas the many featureless sills and plutons throughout the world are like this because of the phenocryst-free magma from which they were built. The common occurrences of featureless granitic intrusions achieve this state because of the inefficiency of crystal sorting in highly viscous magma. In essence, the final state of most magmas is not too far different than their state.

With this basic understanding of magmatic systems gained from systems well exposed and relatively straightforward to understand, it is useful to extend this insight to other magmatic systems. The two most common and extensive systems of Earth are those represented by Ocean Ridge and Island Arc magmatism. These systems are mainly studied from a purely chemical point of view that, in and of itself, can be misleading as to the physical basis behind the outcome, and the following will emphasize more the physical workings of these systems.

6.07.9 Ocean Ridge Magmatism

In concert with the classical concept of magma chambers as giant vats of magma undergoing slow progressive cooling, crystallization, thermal convection, and crystal deposition into systematic layers reflecting the history of the system, vast reservoirs of magma were expected at the level of the oceanic crust beneath ocean ridges. When these features were sought using seismic methods, they were not found. Instead, thin (50–100 m), wide (2–3 km) ribbons of magma, or sills, were found (Sinton and Detrick, 1992). This spawned a general model of ridge magmatism more consistent with what is found for systems like the Ferrar and even Sudbury, albeit on a smaller scale, and the structure of the oceanic crust is an intimate reflection of the combined process of magmatism in response to plate tectonics.

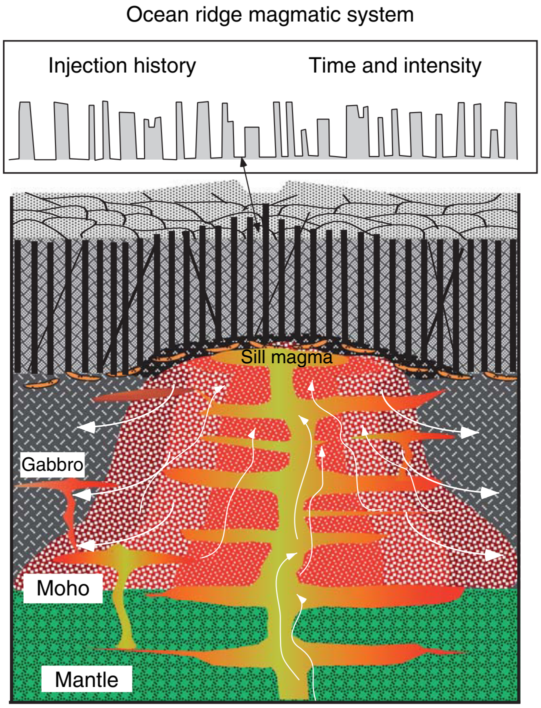

Figure 28 The mush column magmatic system at ocean ridges. The system is characterized by a thin sill (axial magma chamber, AMC) capping a vertically extensive system of thin sills and conduits within a massive column of mush. The sheeted dike complex at the top records the history of extraction of magma from the AMC as the plates suddenly pull apart over time periods depicted at the top. Note the small plagiogranite lenses within the upper gabbros formed by solidification front instability.

This general system is shown schematically by Figure 28. This depiction stems from the general form of magmatic sill complexes found in the Ferrar system, in old continental crust, in ophiolites (e.g., Nicolas, 1995), and in three-dimensional multichannel seismic studies in the North Atlantic (e.g., Cartwright and Hansen, 2006), and it is also consistent with what should be expected on a mechanical basis in this tectonic region. This is a magmatic mush column under steady-state operation in response to mantle upwelling associated with large-scale mantle convection. The mush column stands in partially molten mantle ultramafic rock modally dominated by olivine with subordinate orthopyroxene, clinopyroxene, and plagioclase, with spinel and pyrope-rich garnet at successive higher pressures. At the deeper levels (~50–100 km), significant partial melting due to adiabatic decompression (McKenzie, 1984) forms an anastomosing complex of melt veins and channels concentrating upward into a main mush column stalk with periodic sills. The mush column is capped by the axial magma chamber beneath the ridge axis.

The system works through hydrostatic head produced in response to, in effect, suction at the top associated with the abrupt splitting and spreading of the lithospheric plates. From an initial state of near-hydrostatic equilibrium, this abrupt motion withdraws magma from the underlying axial magma chamber, some of which erupts as pillow lavas and that in the feeder solidifies as a dike. The loss of hydrostatic equilibrium at the head of the system propagates downward throughout the system, perhaps partly as solitons, drawing magma upward in the mush column and reestablishing stability. Because all parts of the contiguous ridge plates do not move at exactly the same time and to the same degree, the process of melt motion at depth is certain to be complicated. Magma at some depths may at various times be pulled laterally as it ascends, making its overall trajectory significantly nonvertical. The intimate history of this process is recorded in the vast sheeted dike complex, which is a characteristic byproduct of ridge magmatism and is known so well from ophiolites. Because they are random samples of the axial magma chamber, they give an excellent inventory of the general state of this magma, both in terms of composition and crystallinity. These dikes are typically fine grained and of low phenocryst content; the phenocrysts are also mostly plagioclase. This information strongly suggests that the axial sill is a passive body of magma that experiences bursts of withdrawals followed by recharging from below.

The basalts erupting at the ocean ridges are tholeiitic basalts, with low K_2O (~0.2 wt.%), modest TiO_2 (~1.5 wt.%), and low and unfractionated rare earth elements (REEs), and are commonly called mid-ocean ridge basalts (MORBs). To first order, these basalts are chemically among the most globally uniform of any class of magmas. These are called N-MORBs for normal MORBS. But at a more detailed level of inspection, they show significant variations in many facets, the most common of which is enrichments in K_2O and TiO_2 and sometimes iron. These are called E-MORBs or enriched MORBs and also sometimes Fe–Ti MORBS.

The first-order bulk composition of these basalts reflects the underlying magmatic process of prolonged intimate contact with a vast solid assemblage in the magmatic mush column. In effect, the chemical composition is buffered by the mechanics of the overall process, much as in a water purification system. This uniformity is also a result of the uniformity of mantle composition itself, which has probably not changed drastically over Earth history. That is, at the present rate of ridge magmatism (~20 $km^3 yr^{-1}$), the mantle will be recycled about once every 50 Gy, which, even allowing for the role of contamination by subduction, suggests the mantle composition has been, to first order, fairly constant. But as a result of initial inhomogeneities, subduction, and other styles of magma generation, there are certainly subtle and significant chemical variations in the mantle source rock. In addition to these variations, there are also regional variations in the thermal regime as a result of the form of mantle convection. These effects cause the depth of the principal melting region to vary in extent and depth, which altogether causes distinct fluctuations in the bulk composition of the magmatic product. Another major factor is the rate of spreading, which may strongly affect strength of the melting anomaly and thus the overall mass and activity of the mush column.

It is interesting to consider ridge magmatism from the past point of view of classical magma chambers, where, once emplaced in a large vat, the magma differentiates by crystal growth and settling. This strong uniformity of composition of MORBs is explained by starting with MgO-rich magma produced by partial melting of peridotitic mantle to a degree necessary to produce a large mass of mobile magma. This process would produce a series of magmas ranging from picrites to olivine basalts and tholeiites. Yet picrites (olivine-rich basalt) are not found at ridges, and arguments always persisted that if picrites are parental to MORB then why are they never seen? Why don't they erupt more often, or at all? This is not an uncommon situation in petrologic studies where critically important parts of the hypothesized dynamic puzzle are not seen, but are postulated to be in a hidden zone, or uneruptible due to density difficulties, or other factors. On the other hand, to others, the fact that critically important magmatic parts of the system are never seen means simply that they do not exist. In the present understanding of ridge magmatism, the magmas are chemically fractionated by contact with olivine, and other phases, but it comes through intimate, diffusional, contact within the mush column. The lack of presence of an actual powerful magma chamber, as found on chemical grounds, is replaced by a virtual magma chamber, which is an integrated chemical process taking place over the full extent of the mush column.

6.07.10 Island Arc Magmatism

6.07.10.1 Introductory

Arc magmatism contrasts fundamentally with ocean ridge magmatism. The points of volcanism, the volcanic centers and surrounding crust, can remain fixed for long periods of time ($\sim$1–10 My, depending on location), and the flux of magma is much lower ($\sim 10^{-2}$ km^3 yr^{-1}). Also, there is a universal relationship between the rate of subduction and volcanism. Where there is no subduction there is no volcanism. There are also some close similarities and these are in the spatial trace of volcanism on the surface; both are long, sharp narrow welts, and the compositions of the most voluminous magmas are to first order similar, tholeiitic basalt and HAB. But unlike at the ridges, where there is no choice in the ultimate source of the magma, in arcs a wedge of asthenosphere sandwiched between the arc lithosphere and the subducting oceanic crust provides almost any number of end members and combinations, with and without continental crust, from which to get magma. As at ridges, the main approach to understanding arc magmatism has been, and is, mainly through geochemistry, but here the focus will be more on the fundamental geophysical controls. Moreover, petrologists have long assumed, as based on early thermal models, that the subducting plate is too cold to melt and that the source of arc magma must be from the mantle above the plate, forming in response to fluxing by volatile rising from the dehydrating plate.

A perusal of the principal volcanic arcs of the world (**Figure 29**) shows a diverse range of geologic

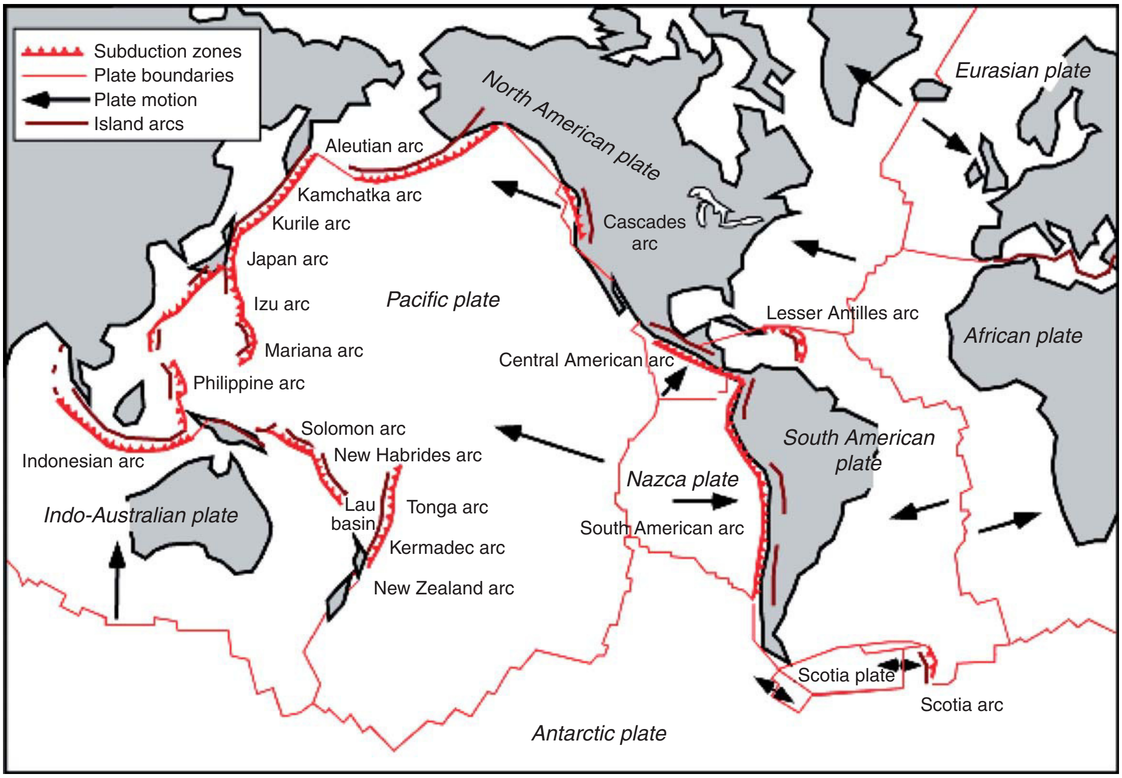

Figure 29 Islands arcs of the world.

environments. There are arcs built on thick continental crust in South America, arcs built on oceanic crust in the Scotia arc southeast off South America, arcs traversing from continental to oceanic crust as in the Aleutian Islands, and arcs on young mixed crust in Kamchatka and Japan. The ages of the arcs also vary a great deal from those like the Aleutians that may be as old as 40 My to those as a young as the Scotia arc at ~3 My. This is not to say that the arc has been in continual operation for long periods of time. In fact, from the evidence of ashes deposited on the sea floors around arcs, there is an apparent periodicity of eruptive activity, especially around the Pacific, of about 2 My (e.g., Hein *et al.*, 1978; Scheidegger *et al.*, 1980). Coupled with a record of continuous subduction over much longer periods of time, this may indicate that the arc systems periodically load with magma and then discharge over and over again.

The force of the volcanism, even within a single arc, can also vary significantly as can the nature of the dominant lavas. In South America, there are major gaps along the strike of the arc where there is no volcanism. These correlate closely with shallowness in the angle of subduction. If the plate subducts too shallow, essentially adhering to the keel of the continental lithosphere, there is no wedge of asthenosphere and no volcanism. The depth of the top of the subducting plate is most commonly ~125 km, but it can be as large as ~150–160 km. And the detailed structure of the volcanic front of any arc often intimately reflects the structural morphology of the subducting plate. Arc volcanic fronts are not simple continuous arcs, but are almost always segmented into a collection of individual short segments forming a piecewise continuous arc. And the arc segments are usually bounded by major fracture zones or structural irregularities in the subducting plate.

6.07.10.2 Arc Form

There are two spatial characteristics of island arc volcanism that set it aside from all other forms of volcanism. These are the regular spacing of the arc volcanic centers and the segmentation of the volcanic front. Although when built on continental crust, the form of island arcs are can appear cluttered and unclear, it is always there and clearest in young and tectonically uncomplicated regions.

6.07.10.2.1 *Spacing of the volcanic centers*

The basic structure of island arcs in terms of the positions and form of the volcanic centers is exceptionally clear. The arc begins with a single sharp line of volcanoes. This is the volcanic front, as named by A. Sugimura (1968), which is, by far, the principal locus of volcanism. The front fills in to a series of unusually regularly spaced volcanic centers separated by 50–65 km. The relatively young Scotia arc shows this basic developmental form rather clearly (see **Figure 30**). After existing for about 3 My, secondary volcanic centers may appear behind the front, forming a weak secondary front. These are always smaller and spaced closer to the front than the principal spacing (d) of centers along the front. There is some sign that this secondary spacing (d') follows the relation $d' = d\cos(\theta)$, where θ is the angle of dip of the subducting plate (Marsh, 1979a, b). Leskov Is. in the Scotia arc and Amak and Bogoslof islands in the Aleutians are prime examples of these secondary centers. Every arc seems to have them, although

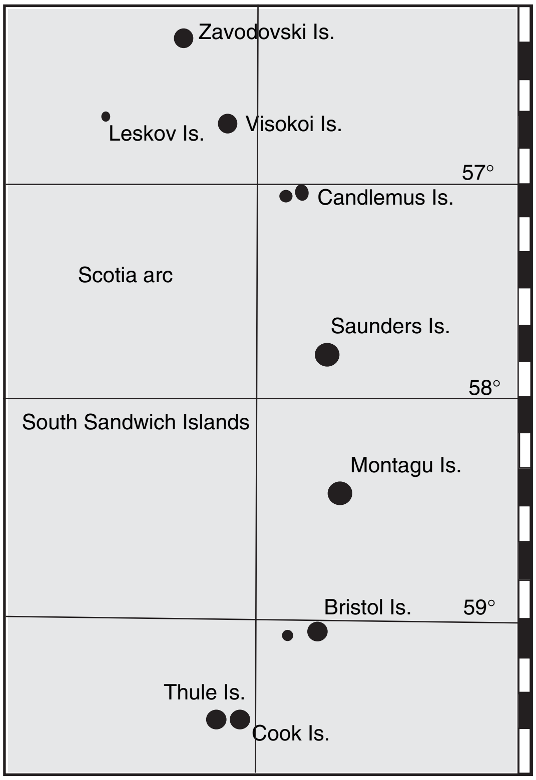

Figure 30 Detailed view of the Scotia Arc or South Sandwich Islands. Note the prominent volcanic front, the even spacing of volcanic centers, and the location of the secondary volcanic center, Leskov.

other forms of volcanism especially on continents sometimes complicates identification. On a similar timescale, young centers also appear within the main front at points approximately midway between the older initial and well-developed centers. These centers never reach the strength of the main centers. Bobrof Is. and the doublet Koniuji–Kasatochi islands in the central Aleutians are such late centers.

6.07.10.2.2 Arc segmentation

That the arc volcanic front can be broken up into piecewise continuous segments that may reflect a similar structure in the underlying subducting plate was noticed and developed by Richard Stoiber and Michael Carr (e.g., 1971). Every arc shows this basic form and it is especially clear for the Aleutian arc (see Figure 31). To be clear, these are alignments between only the 'active vents' of the front and not simply the volcanic centers, which often contain a series of waning and waxing vents. Although some segments contain only two or three vents, most segments contain many vents, and this is much more than simply the correlation of large dots on a map. The alignments are particularly striking and delicate if viewed from the exact summit of an active vent. Stepping away ~10 m from a vent within a segment will lose the alignment, which can often be seen for 200 km or more in each direction. Considering that the principal active vent within any center usually migrates slowly (~10 km My^{-1}) in time away from the original front, that the alignment exists at any time is suggestive of a deep-seated fundamental cause.

6.07.10.3 Character of the Volcanic Centers

The general pattern of development of individual volcanic centers often shows a similar progression from initiation to final size and this progression can be arrested at any stage. These stages can be called young, mature, and supercenters. The final form, which is reflected by strength or volume of the center, depends critically on the position of the center within the front and within the arc itself. The

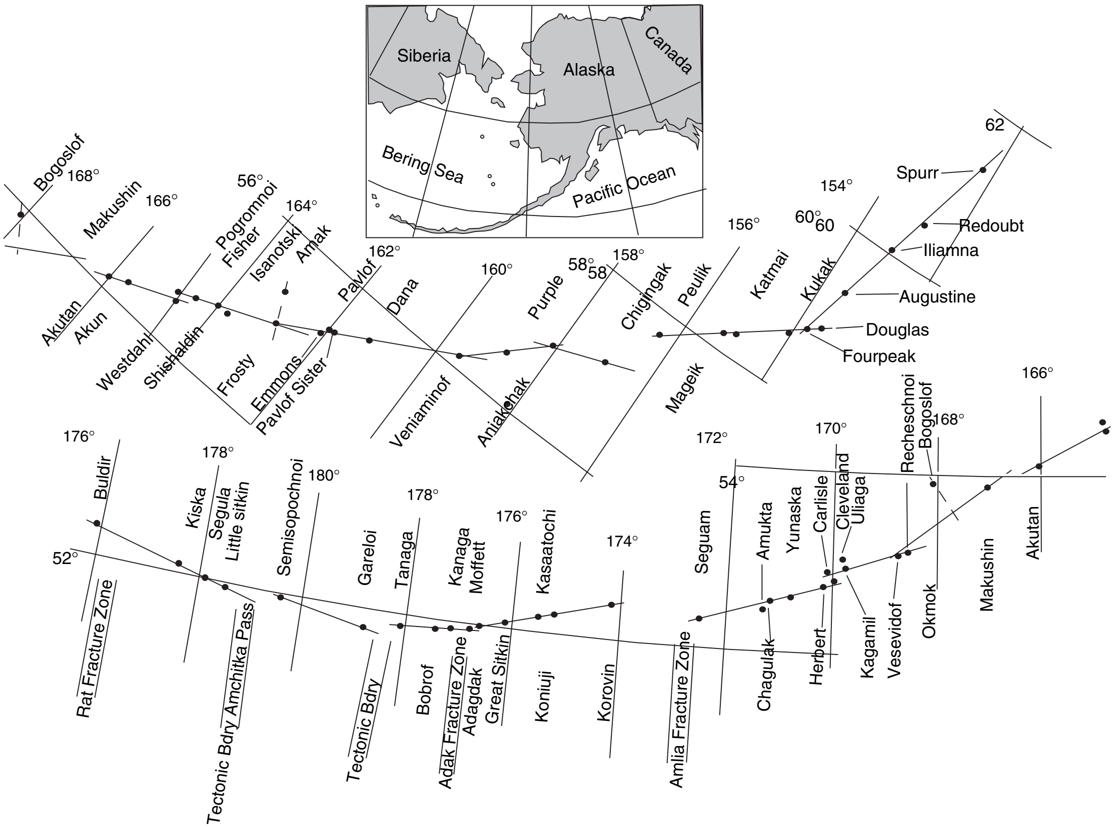

Figure 31 Segmentation of the Aleutian Island arc volcanic front.

stronger the rate of subduction, the larger the centers. Centers deeply within a segment are generally larger than those at the ends of segments. Centers begin, as can be seen from the appearance of secondary centers, as essentially large multiple domes; the magma is of low volume, highly crystalline, and sluggish. Others begin with the eruption of a series of highly mobile basaltic lavas interbedded with thin deposits of tephra to form a low-profile shield. Continued growth adds more to the shield and then sharply transitions into a steeper-sided cone of primarily (50–70 vol.%) volcaniclastic debris trussed together with occasional lavas. Low-crystallinity basaltic flows may be thin (~1 m, especially near the vent) and of limited extent (hundreds of meters), whereas high-crystallinity andesitic flows may be thick (~100 m), massive, and extensive (kilometers). This basic transition from shield to steep cone forms the classic composite cone of island arc, consisting of a stratocone built on the foundation of a shield cone. Many volcanoes go no further in development. Reposes in activity allow erosion to deeply incise the cone; summit craters of tall stratocones commonly become glacial cirques that breach the crater and dig deep U-shaped valleys. In the next phase of activity, the cone reconstructs itself with the lavas and debris filling the topographic voids, making the field relations challenging. This is a mature volcanic center. Further development often results in a series of domes and fumaroles ringing the cone at an elevation of about 50–70 % of the cone relief. This is commonly encouraged by deep erosion that may weaken the cone near the main vent, allowing stagnant, high-crystallinity magma to sluggishly extrude laterally. This signals the solfateric stage of development. These locations also sometimes develop into a series of satellite cones, evicting a series of flows that may mimic development of the central cone.

Supercenters develop when activity is particularly strong and the stratocone phase outstrips erosion, forming volcanoes of unusually large relief like Mt. Fuji, Mt. Rainer, and Shishaldin (~3000 m) in the Aleutians. Beyond this point, the cone can become structurally unstable due to size and subsurface magma ponding and catastrophic caldera collapse often occurs (e.g., Williams, 1941; Smith and Bailey, 1968). The majority of the cone relief is destroyed through collapse and violent ejection, leaving a low-relief, distinctive crater as at Crater Lake, Oregon. Further activity builds domes and new cones within the caldera, generally not of a size commensurate to the original cone, but sometimes even larger. This cycle of growth and collapse may repeat itself many times until the locus of volcanism migrates to a new nearby location.

The style of eruption for arc volcanoes, unlike for Hawaiian and Icelandic volcanoes where fissure eruptions are common, is most often from the central vent. These central vents are highly concentrated and cylindrical that may fill and empty repeatedly during a eruptive episode. This ~500 m wide vent at Korovin in the central Aleutians has been observed empty to a depth of ~1.5 km and later brimming with magma and then spilling over into lavas (see Figure 32). Acoustic echoing due to explosions at the base of the vent when evacuated can be heard for hundreds of kilometers. The highly explosive nature of stratocone eruptions may more reflect this concentrated plumbing system coupled with high-crystallinity magmas, making them unusually viscous, than an undue effect of high concentrations of volatiles (as is more often assumed). Large regional dikes are uncommon, although they do sometimes accompany inflation and the precursory events of attending caldera collapse. Small local dikes are common near vents and deeply eroded cones sometimes show dikes radiating from the central vent that have trussed together the volcaniclastics of the stratocone and sometimes served as conduits for flank domes and lavas.

Ash flows or ignimbrite deposits, so common to continental volcanism and caldera collapse eruptions, are also common to arc volcanism. But because of their high mobility and erosiveness, evidence of these events are often difficult to find and trace, especially in oceanic environments.

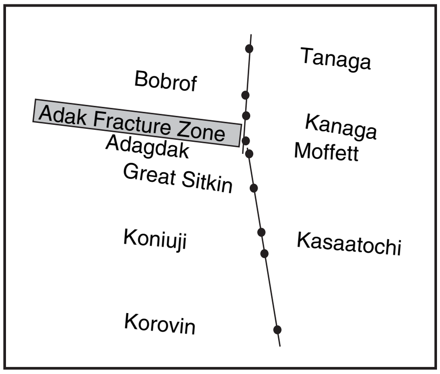

Figure 32 View of the detailed relations between two segments of the Aleutian volcanic front at the island of Adak and the position of the prominent fracture zone in the subducting plate.

6.07.10.4 Magma Transport

The strong centralization of arc volcanoes and the lack of dispersion on the surface of vents over periods of millions of years suggest deep magma transfer by diapirism rather than by dike propagation. Deeply eroded terrains also show bulbous plutons and a paucity of dikes. When built on continental crust, expansive welts of plutons form vast linear batholiths, like the Sierra Nevada, formed in the subsurface from foundered magma and from reprocessing of crustal wall rock. The dominant type of magma emitted is also affected by the density of the underlying crust. Arcs on continental terrains are dominantly andesitic (i.e., $\sim$60 wt.% SiO_2), whereas arcs on oceanic crust are dominated by HAB ($\sim$50 wt.% SiO_2). This sensitivity to density contrast is locally critical in diapiric transport and much less so in dike transport. That is, standing dikes in elastic cracks operate more on an integrated, columnwide, density and the strength of the walls rather than on the local buoyancy at each horizon. The extreme paucity of mantle-like ulramafic xenoliths may also reflect the slow diapiric mode of transfer where the same conduit is used over and over, making the column traveled thermally and chemically insulated from access to primitive lithospheric rock.

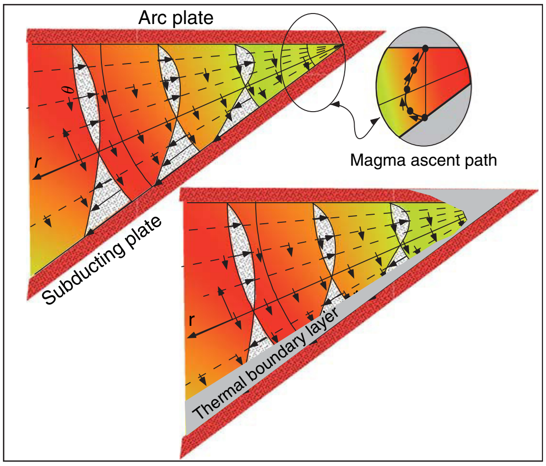

Figure 33 (upper) The flow of mantle material within the asthenospheric wedge induced by subduction, with the streams lines shown. (lower) The position and development of the cold thermal boundary layer at the slab–wedge interface; also shown is the strong thinning in the boundary layer near the corner and directly beneath the volcanic front. The inset diagram shows the trajectory of ascent of a diapir of mush from the slab as it traverses the wedge flow and repeatedly enters the same spot within the overlying arc lithosphere.

6.07.10.5 Subduction Regime

Perhaps the most unusual aspect of arc magmatism is the deep presence of the wedge flow of asthenospheric mantle driven by the subducting plate (Figure 33). At shallow depths, the subducting lithosphere is in fault contact with the adjacent arc lithosphere. The depth extent of this contact is commonly 70–100 km, but may be much longer in continental terrains where the lithosphere or tectosphere can be very old and thicker as in some places along the subduction zone of South America. The nature of the arc lithosphere is also not well known in many areas. Below this depth of fault contact, the subducting plate is in contact with the mantle wedge or asthenosphere, a high-viscosity fluid ($\sim 10^{17}$ Pa s). In most regions, this is the so-called seismic ‘low-velocity zone’, reflecting incipient melting at the solidus of the regional mantle country rock. The asthenosphere in this wedge-shaped region adheres to the upper boundary with the arc lithosphere and at the same time is dragged downward by the motion of subduction. The streamlines, depicting the mass transfer, due to this dragging tilt upward in direct response to the angle of subduction. This flow field is found by solving the biharmonic equation for viscous flow, which comes from the Navier–Stokes equation. A key feature of this flow is that the associated stress field creates a traction or coupling between the two plates that, in effect, welds them together along the lithosphere-to-lithosphere fault contact. This junction is locked in place, and the volcanic front, as we have already seen, reflects this intimate connection.

This is an unusual flow in several regards. First, the flow is the same at all distances from the corner. The upper part is essentially a parabolic flow between parallel plates and the lower half is a shear flow. For conservation of mass, all the fluid in the top half must turn and flow through the lower half of the flow field. Along the plane of symmetry fluid moves from one side of the flow to the other. This flow is directed normal to the face of the subducting plate. Although normally at great distance from the plate interface, with approach to the corner this flow becomes arbitrary close to the plate. It is in exactly above this corner region where the volcanic front is found. Second, since the downgoing plate is cold and the flow above it is mostly a shear flow, with streamlines parallel to the plate, a cold thermal boundary layer develops near the corner and thickens down the plate. This thickness δ_T can be estimated from eqn [2] as a function of distance (x) from the corner, which is measured by $x = t/V$, where t is time and V is the subduction velocity. Then,

$$\delta_T = C\sqrt{K}\left[\frac{x}{V}\right]^{1/2} \qquad [25]$$

where C is a constant of order 1 and K is thermal diffusivity. The boundary layer thickens downward (see **Figure 33**) along the plate as $x^{1/2}$, and it thins or thickens inversely with $V^{1/2}$. At a common distance from the corner, slow plates have much thicker boundary layers than fast-moving plates. This behavior is very much akin to the growth of the lithosphere itself as it moves away from ocean ridges. In this respect, is also critical to recognize that any diffusive process associated with the plate, including chemical diffusion involving volatiles, will have a similar boundary layer development. The third unusual feature of this environment is the corner region where the motion goes from a fault interface controlled by friction to a fluid–solid interface dominated by a shear flow; friction is also involved but to a lesser extent. In a shear flow like this, heat flow is produced according to $q = V\tau$, where τ is the local shear stress ($\tau = \mu(\mathrm{d}V/\mathrm{d}y)$, where μ is viscosity and y is the coordinate normal to the plate). But within the arc plate, with approach to the surface, the effective thermal boundary thickness becomes very large.

There are thus two key features in this regime that fundamentally affect the production of magma. One is that the corner flow continually brings into the wedge region hotter mantle material from greater depths, and this material is continually brought in contact with the subducting plate. It continually coats the plate and the cold thermal boundary layer is never allowed to become unusually large, as it would if the corner were stagnant. Second, the thermal boundary layer becomes pinched near the corner as the corner flow turns and becomes a shear flow. This thermal pinch is exactly below the volcanic front, and it, in effect, intimately ties the spatial position of the front to the position of the plate. The thermal regime inside the subducting plate is also central to understanding how magma might be produced.

6.07.10.6 Subducting Plate Internal State

Two key processes within the downgoing plate affecting the production of magma are the thermal regime and the transport of hydrothermal fluids. The oceanic crust at the surface of the plate has a strong chemical affinity to arc basalts and is clearly a prime potential location for magma production. But as mentioned already, it is commonly considered too cold to undergo melting. This impression stems from early thermal models (e.g., Toksoz and Bird, 1977) and also from the fact that the slab interface was once on the seafloor, the coldest part of the lithosphere.

6.07.10.6.1 *Thermal regime*

This latter impression can be appreciated by recalling that if two solids at contrasting temperatures T_1 and T_2 are abruptly brought into contact, the temperature of the interface (T_i) immediately becomes the average of the two initial temperatures, $T_i = 0.5(T_1 + T_2)$ (e.g., Turcotte and Schubert, 1982). For seafloor rock at 0°C brought up against mantle wedge at, say, 1300°C, the crust interface would thus achieve a temperature of about 650°C, which is well below the solidus. The problem with this result is that the thermal path that the slab takes between leaving the seafloor and reaching a depth of ~125 km must be considered. The section where the two plates are in fault contact is especially critical as the frictional interaction produces heat and there is strong evidence that at shallow depths (0–50 km) the preponderance of earthquakes is along this interface, and at great depths the strong band of earthquakes migrates slightly deeper into the plate to perhaps a depth of 10–20 km below the interface. So, the temperature calculated here is an absolute minimum; frictional heating will preheat the oceanic crust such that when it enters the asthenosphere it will attain a significantly higher temperature. And the inclusion of the flow in the wedge is essential to achieve for any realistic estimate of the prevailing temperature along the slab interface. The full problem is quite involved and of the many studies that of Kincaid and Sacks (1997) is notable for its thoroughness (they also give an extensive review of associated seismic and tectonic studies). They find that near the corner, in the location indicated by the flow in **Figure 33**, there is positive temperature anomaly of about 80–100°C at the slab–asthenosphere interface; over a thin (maybe only tens of meters), the oceanic crust may be brought to a temperature of about 1350°C. This is enough to initiate melting, and that this spot is exactly below the volcanic front is important. This spot is also tied to the plate-to-plate junction and may well determine the position of the volcanic front.

6.07.10.6.2 Hydrothermal flows

Being a solid, the thermal regime internal to the subducting plate is usually considered as solely due to heat conduction and this is certainly true to first order. But there is also hydrothermal circulation in response to dehydration. This reflects extensive hydrothermal circulation starting at the ridge and extensive alteration and exchange between the seawater and the oceanic crust. This exchange takes place over tens of millions of years. The principal effect is to alter the original minerals to hydrothermal equivalents, thus partially hydrating the oceanic crust. For example, olivine is partly altered to serpentine, plagioclase feldspar to forms of sericite, and clinopyroxene to hornblende. Although this alteration can be extensive in local areas, overall these effects probably do not affect more than about 15–20 vol.% of the crust. What is much more pervasive is exchange at the isotopic level involving, for example, oxygen ($^{18}O/^{16}O$) and strontium ($^{87}Sr/^{86}Sr$), which can take place at high temperature and leave little to no visual trace. Fresh glassy MORBs erupted at the ridges commonly have, for example, initial $^{87}Sr/^{86}Sr$ near 0.702 5 and, with ocean water at 0.709 0, after about 30–40 My the oceanic crust, which has migrated to significant distances from the ridge crest, now has an $^{87}Sr/^{86}Sr$ closer to 0.704 0. These variations in depth are found in ophiolites (e.g., Gregory and Taylor, 1981) where a net increase is found in $^{87}Sr/^{86}Sr$, but $\delta^{18}O$ is increased at the crust top ($\sim$+12 per mil) due to low temperature exchange and decreased at the crust base due to high temperature exchange such that the integrated effect is $\sim$5.8 mil^{-1}, which is the normal value of fresh MORB. Thus there is no net exchange in $\delta^{18}O$.

As the plate subducts and becomes heated, a new hydrothermal circulation system sets up due to phase transformations associated with dehydration. Because of the large horizontal temperature gradient across the oceanic crust the form of this flow is horizontal and upward, which, in effect, makes it helical. This flow is confined only to parts of the plate where there is sufficient permeability to allow flow. Similar hydrothermal flows have been studied over extensive regions about solidifying plutons and the patterns and basic mechanics of these flows are well known. Permeability is directly tied to the temperature and brittleness of rocks, and from these studies it is abundantly clear that rocks are sealed beyond temperatures of about 700°C. For this reason, this hydrothermal flow is confined wholly within the oceanic crust, which is the coldest, most brittle part of the subducting slab. Moreover, the region has been (and is being) subjected to extreme fracturing in response to earthquakes; each cubic kilometer experiences about 10 000 events during subduction. This makes a strong permeability guide within the oceanic crust. At the same time, for these same reasons, the overlying asthenosphere in the wedge is tightly sealed; it is hot and weak and has nil permeability. Hydrothermal fluids released from the plate do not enter the overlying mantle wedge – they travel upward and repeatedly cycle across the oceanic crust (see **Figure 34**). This flow has a critical effect on the chemical nature of the subducting plate.

This intense, internally confined flow redistributes the initial variations in $\delta^{18}O$ and $^{87}Sr/^{86}Sr$. Because from the interaction with seawater there has been no net gain in $\delta^{18}O$, it is reset to its normal value of $\sim$5.8. But because the crust has gained ^{87}Sr from seawater, there is a net increase throughout the crust in $^{87}Sr/^{86}Sr$ to a value of $\sim$0.704 0. The low solubility of isotopes like $^{143}Nd/^{144}Nd$ in seawater hence does not produce a corresponding effect on the oceanic crust. But perhaps the most remarkable and underappreciated effect of this flow is to produce an unusual skarn as it comes in contact with the slab–mantle interface. The flow cannot penetrate the mantle, but this interface, due to all the ongoing faulting and shear, is certainly a mechanical breccia of both rock types, namely, high-pressure MORB (i.e., quartz eclogite) and garnet peridotite. The hydrothermal flow is in approximate chemical equilibrium with the MORB crust, but far from equilibrium with the peridotite. As soon as it touches this hot heterogeneous rock, it precipitates out phases to bring it closer to equilibrium. Although the nature of this 'slab-skarn' assemblage is not as yet known with any exactness, it will be rich in trace elements like Ba, Rb, and elements with similar geochemical affinities. Thus the most likely area of magma production has a MORB-like bulk composition with an enrichment of some trace elements.

6.07.10.7 The Source of Arc Magma

Although the more popular source of arc magmas is from melting of peridotitic material within the asthenospheric wedge due to fluxing from volatiles escaping from the subducting plate, this is unlikely for several fundamental reasons. First, because of its high temperature the wedge is sealed to hydrothermal flows. Second, the composition of the predominant basalt found in island arcs has an exceedingly close chemical affinity to subducted

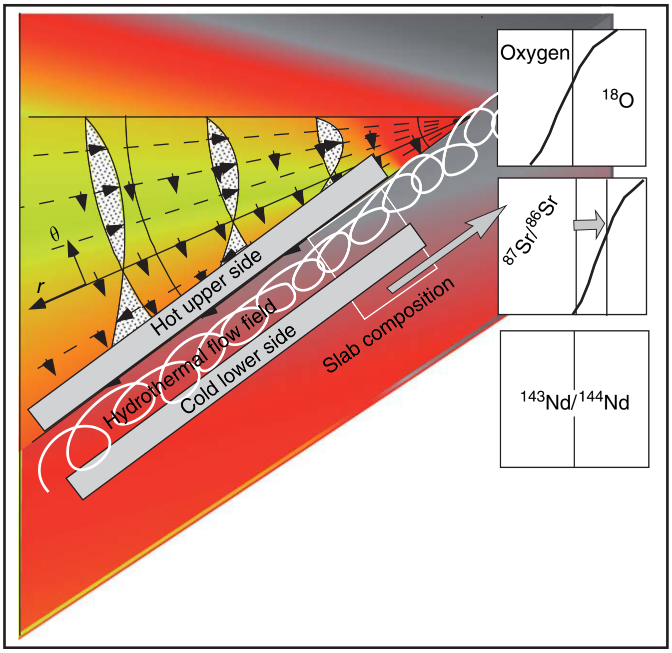

Figure 34 The flow of helical hydrothermal flow up the coldest, most brittle, and most permeable part of the subducting plate. This flow redistributes the concentrations of certain isotopes and trace elements within the slab. No fluid penetrates the overlying asthenospheric wedge.

MORB and virtually none to the wedge peridotite. Third, the strong focusing of arc volcanic centers at the surface, with very little dispersion, over millions of years, links it to a magmatic source that is virtually static with respect to the plate–plate subduction configuration. This cannot be achieved through magma production within the wedge flow regime.

The major elements of magma dominate the mass of the magma, take the most energy to change, and are therefore the most diagnostic deciding source characteristics. The close chemical affinity of melts from the plate to HAB, the arc parental magma, can be seen by comparing HAB melts with melts from both the plate and the wedge. This is shown by Figure 35, where melt composition is shown as a function of degree of melting at 30–40 kb (3–4 GPa). Across each panel are horizontal lines representing HAB composition and intersections or matches with melt from either of the two source rocks is indicated. No matches are found for melt from the peridotitic wedge material, but matches are almost complete for each of the major elements for slab melting. It is particularly notable that slab melts are low in MgO content. This reflects a fundamental chemical property of this source rock in that the MgO content cannot exceed about 7.5 wt.%. This is also a fundamental property of HAB. That is, arc basalts are characteristically low in MgO. For HAB from mature volcanic centers at SiO_2 ~50 wt.%, MgO content is typically about 4–5 wt.%. Some arc basalts are also found with significantly higher MgO, but these can almost universally be demonstrated to have suffered contamination with tramp olivine debris from lithospheric wall rock. Moreover, these basalts are also almost always from arc supercenters where there has been an unusually large eruptive flux. Large eruptive fluxes, like at Kilauea, lead to strong heating of the lithosphere wall rock, which causes structural weakening and collapse, furnishing peridotitic debris for entrainments by ascending arc HAB. Careful petrographic inspection of basalts with elevated MgO and/or Ni commonly reveals fragments of unzoned, often slightly strained, highly forsteritic (~Fo_{92}) olivine from the lithosphere. Because of the inherent assumption that magmas of high MgO contents are primitive and thus parental to the lower MgO suite, these contaminated basalts are often mistakenly assumed to be fundamental to the arc magmatic system. A second distinctive chemical feature of arc HAB is the elevated Al_2O_3 content (16–20 wt.%), which is reflected by high modal contents of plagioclase in the plutons and lavas. These high plagioclase contents give arc basalts their characteristic gray appearance.

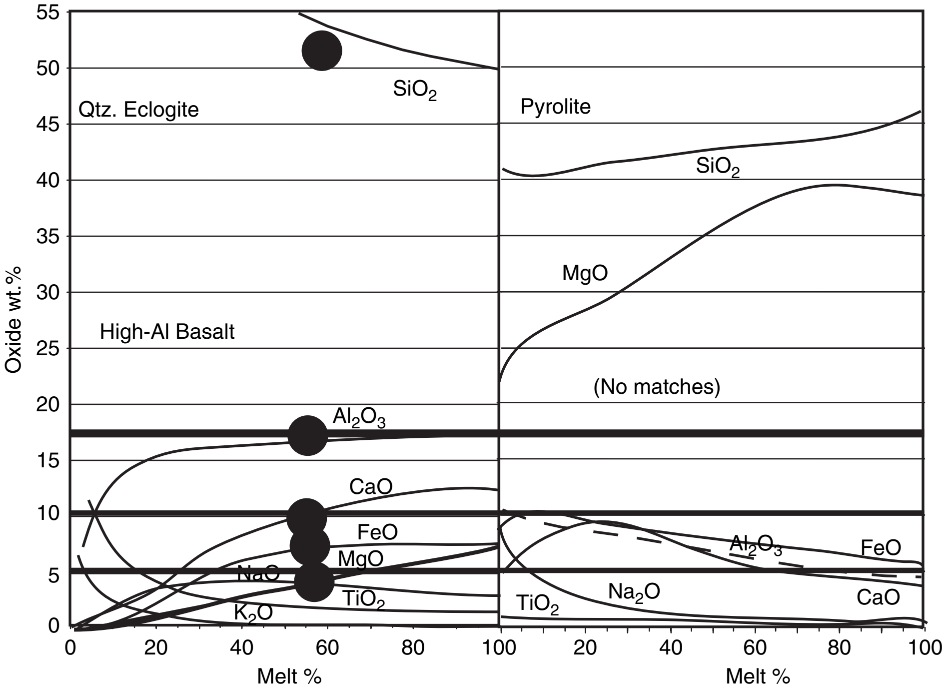

Figure 35 The compositions (oxides and curves) of melts as a function of degree of melting produced from quartz-eclogite subducted oceanic crust and pyrolite of the asthenospheric wedge. The straight horizontal lines show the composition of typical HAB of island arcs (Aleutians) and the large dots show matching points between the observed HAB and the calculated melts. There is almost perfect agreement with the slab source and no agreement whatsoever with the mantle wedge.

6.07.10.7.1 Slab quartz-eclogite

These chemical features also reflect the basic high-pressure mineralogy of the subducted oceanic crust. At pressures of 2–3 GPa, the MORB mineral assemblage of plagioclase, olivine, clinopyroxene, and Fe–Ti oxides transforms to quartz, garnet, jadeitic pyroxene, rutile, sanadine, and possibly kyanite, which is a quartz-eclogite. In comparison to the pervasive peridotitic country rock of the mantle at these depths, this quartz-bearing source rock is highly unusual. Melting of this assemblage produces the characteristic arc HAB bulk composition. A notable feature of this assemblage is the high modal content of garnet, which will strongly fractionate the concentration of REEs in the ensuing melt. That this is not observed in arc HAB has long been taken to be evidence that garnet, and hence also the slab itself, is not a reasonable source rock. But this conclusion assumes melt extraction takes place at a sufficiently high pressure to assure that garnet is still a dominant phase, which may be dynamically unlikely. That is, magma ascends because it is buoyant relative to its surroundings. And to become buoyant, or gravitationally unstable, only enough melting to make the mushy assemblage less dense than the surroundings is necessary. Further extensive melting will take place during ascension. The requisite amount of melting necessary to extract a melt free of solids will be, as in solidification fronts, ~50 vol.%. Melt extraction is also possible at lower degrees of melting due to compaction (e.g., Mckenzie, 1984), but in the slab this is probably inoperative because of the highly limited thickness of material involved, which makes compaction weak. Gravitational instability may take place after only about 10–15 vol.% melting, and the mushy assemblage may rise 20–30 km before enough additional melting takes place to enable the solids to repack and free a nearly crystal-free melt. By this point (i.e., ~2–2.5 GPa), garnet, although still present, is a relatively minor phase, and the REE pattern fits that observed in the arc HAB. A critically important physical aspect of this process is the unusually narrow liquidus–solidus relation of quartz-eclogite, which may be as small as 50–70°C. This means that once the temperature reaches this point, partial melting, melt production, and instability take place rapidly with relatively little rise in temperature. The process, in effect, has a trigger point that may spontaneously generate magma and diapers once the melting point is reached. This is in striking contrast to peridotitic mantle rock where the melting

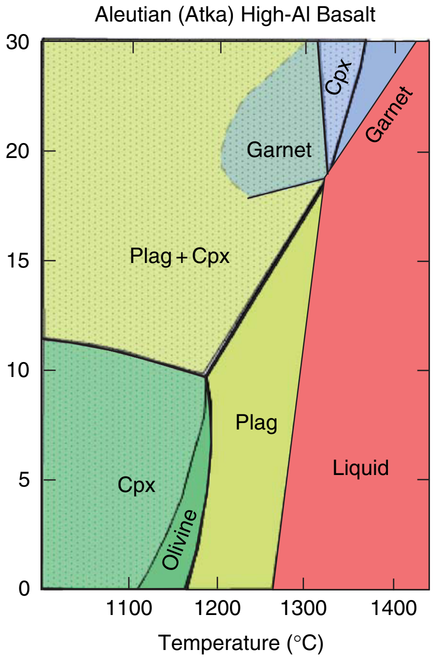

Figure 36 Phase diagram for typical Aleutian HAB. Note the rosette phase relations near 20 kb.

range is about 500–600°C (where melting takes place gradually).

The corollary of this deep-phase equilibria is the phase equilibria of arc HAB itself, which is shown for an Aleutian basalt by Figure 36 as determined by Baker and Eggler. A striking feature of this phase diagram is the phase rosette near 2 GPa defined by plagioclase, garnet, and clinopyroxene. These are phases also common to quartz-eclogite, which suggests that at this point these two rocks (i.e., HAB and quartz-eclogite) would be in equilibrium. This also suggests, alternatively, that this arc HAB may have been extracted from a mush of quartz-eclogite that rose buoyantly to this level. Similar rosette features were long looked for (to no avail) in MORB phase equilibria to identify the point of extraction from peridotitic mantle, and here in arc HAB this feature seems to have been overlooked.

6.07.10.8 Diapirism, Rayleigh–Taylor Instability, and Volcano Spacing

In this process of magmatism triggered by the temperature of the slab surface reaching a critical point, a thin band or ribbon of buoyant mush is produced everywhere beneath the arc on the surface of the subducting plate. A layer of lower-density material beneath higher-density material initiates a collective gravitational instability that leads to the formation of a family of (ideally) evenly spaced plumes or diapirs of the buoyant material (see Figure 37). The distance between the diapirs is given by

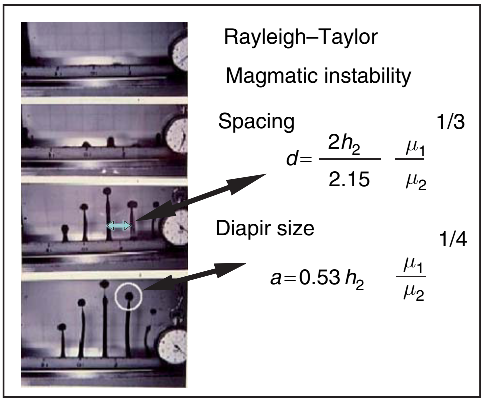

Figure 37 The process of Rayleigh-Taylor gravitational instability when a less dense fluid (black) lies beneath a more dense fluid (clear). Plumes automatically form as the most efficient form of fluid transfer. The equations at right shown the relationship between plume spacing and plume radius and the fluid viscosities and source thickness (h_2).

$$d = \frac{2\pi h_2}{2.15}\left(\frac{\mu_1}{\mu_2}\right)^{1/3} \qquad [26]$$

where h_2 is the buoyant layer thickness and μ_1 and μ_2 are, respectively, the viscosity of the overlying mantle and the mush. The radius of the diapir is given by

$$a = 0.53 h_2\left(\frac{\mu_1}{\mu_2}\right)^{1/4} \qquad [27]$$

If these equations are used in concert along with conservation of mass and the observed spacing of arc volcanic centers, an estimate can be made of the nature of the source region. The source region is thin (50–100 m), highly viscous ($\sim 10^{10}$ Pa s), and the diapirs have a radius of ~3 km. Not only do these estimates seem reasonable, but there are dynamic features of this process that fit or correlate well with the general observed style of magmatism.

The overall magmatic process is driven by the production of buoyant mush, loading the system to the point of systematic instability, which relatively rapidly unloads the system over and over. This is triggered by simply the temperature at the slab interface reaching above the solidus of the quartz-eclogite. Evenly spaced diapirs of mush rise into the convecting mantle wedge, traverse it, and essentially burn a hole upward through the overlying lithosphere. The hot diapirs soften the wall rock allowing it to flow around the diapir. Early diapirs undoubtedly stagnate before reaching the surface, but continued use by later diapirs eventually makes a path to the surface. This process chemically and thermally insulates the pathway, allowing later magmas to travel to the surface without suffering undue thermal and chemical contamination. Extraction of standard arc HAB takes place during ascent. Diapirs can traverse the mantle wedge and repeatedly enter exactly the same pathway point at the base of the arc lithosphere because the flow through the wedge, across any vertical section, obeys conservation of mass. Any diapir ascending at constant velocity entering this flow on one margin will exit the flow at exactly the same vertical point on the opposite margin. This will not be so for a magma generated ‘within’ the wedge region. The ribbon of melting on the slab surface will spread down-dip at the rate of subduction. Once the melt ribbon reaches a distance d down-dip, a new instability will commence. For typical subduction rates, this will occur about 3 My after the first instability, which is the time of appearance of the sporadic volcanoes of the secondary arcs, like Leskov in the Scotia arc and Amak in the Aleutians. Because of the angle of dip (θ) of the unstable layer, the spacing of these centers will be $d\cos(\theta)$, which is also observed.

6.07.10.9 Alkali Basalts Posterior to Arcs

Scattered behind many island arcs are contemporary alkali basalt volcanoes. These are very much unlike arc magmas in composition and spatial distribution. They are scattered over a vast region, are silica poor, alkali rich, commonly contain ultramafic nodules, and have an isotopic identity closely linking them to peridotitic source rock. Unlike arc HAB, everything about them suggests a mantle, not a slab, identity. These are exactly the characteristic magmas expected to be generated within the flowing mantle wedge. The stream lines of flow in the wedge are inclined upward as the flow moves into the corner region above the subducting plate. Already at the point of melting, this convective rise initiates further melting resulting in sporadic, disorganized volcanism on the surface.

6.07.10.10 The Arc Magmatic System

Arc magmatism is a mechanical system controlled by subduction of a MORB-like crust that is intimately coupled, physically and thermally, to the flow induced in the wedge region above the plate. Melting is initiated by this flow, which triggers a collective gravitational instability bringing magma periodically to the surface at prescribed locations over long periods of time. The entire process is buttressed by chemical processes that reflect, but do not control, the physical processes. The detailed chemical processes, at all levels, are best understood through an appreciation of the overall physical dynamics of the full system.

6.07.11 Solidification Front Differentiation Processes

6.07.11.1 Introduction

Magmatic systems, regardless of setting, are all broadly similar in the basic nature of the physical and chemical processes that shape the final product. The gain and loss of crystals, both indigenous and exotic or xenocrystic, their type, size, concentration, and length of time in contact with the melt are fundamental to the chemical evolution of the magma. But it is the dynamic role of solidification fronts that sets at any time the prevailing magmatic processes that go to determine the spatial pattern of rocks seen in the field and the temporal eruptive sequence of lavas. Crystal fractionation from the interiors of magma chambers, the classical approach to chemical differentiation, is not a realistic process. We have seen that the fundamental difficulty in achieving high degrees of chemical fractionation is that the silica-rich residual melt resides deep within solidification fronts where it is inaccessible to extraction accumulation, transport, and eruption. Given the observed diversity of igneous rocks on Earth and even at some small volcanoes, there are, clearly, other processes operating within solidification fronts that produce strong, bimodal chemical fractionation effects. The tearing open of solidification fronts under gravitational instability, flushing of residual melt from the front, and the sidewall upflow of residual melt are three key differentiation processes. These are processes that operate on relatively small spatial scales (1–10 m) but lead to planetary-scale differentiation effects.

6.07.11.2 Solidification Front Instability

A detailed examination of almost any thick basaltic sill reveals in the upper parts the presence of interdigitating lenses of silicic material (see **Figure 38**).

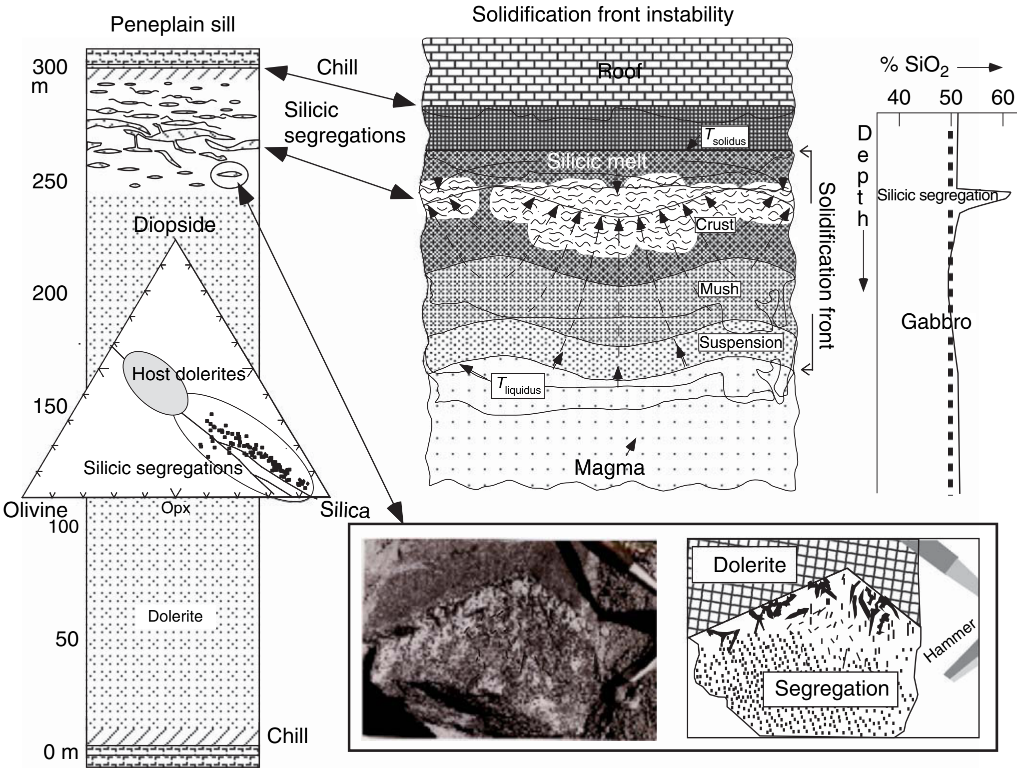

Figure 38 The process of solidification front instability (SFI) in the Peneplain Sill at Solitary Rocks. The left section shows the location and nature of the silicic segregations along with a normative ternary showing the range of segregation compositions relative to the dolerite sill compositions. The SFI process is shown schematically (upper center) and the nature of an actual segregation is also shown (lower right). Reproduced from Marsh BD (2002) On Bimodal Differentiation by Solidification Front Instability in Basaltic Magmas, I: Basic Mechanics. *Geochimica et Cosmochimica Acta* v66: 2211–2229, with permission from Elsevier.

The lenses often begin thin and small near the sill roof and increase in thickness and length up to, respectively, ~1 m and 20–30 m at a depth of about 25% full sill thickness. These bodies have been called by many names from pegmatitic segregations to silicic segregations to silicic schlieren to granophyres (e.g., Walker, 1956). As these names suggest, silicic segregations are significantly enriched in silica over the bulk composition of the sill, commonly ~60–65 wt.% SiO_2 versus ~55 wt.% SiO_2. They are also coarser grained and their physical form often suggests that they fill tears and fractures in the sill. A likely mechanism of formation is by internal failure or tearing of the solidification front (Marsh, 2002).

Roof solidification fronts are generally denser than the underlying uncrystallized magma, and as they thicken they will eventually fail under the action of gravity, producing internal gashes that fill with local residual melt. The process is similar to hanging an old rug from the ceiling and fastening weights along the lower edge. As more and more weight is added, the rug will eventually tear horizontally at the weakest spots. Solidification fronts tear where there is enough strength to fracture, which is within the rigid crust (see **Figures 4 and 5**). The internal distribution of both weight and strength within the solidification front are determined by the spatial increase in crystallinity with decreasing temperature. To avoid tearing, the local strength of the solidification front must increase proportionally with weight, and strength comes from increasing crystallinity. But crystallinity changes are dictated by phase equilibria and not by strength constraints. The noncovariant variation of strength and crystallinity sets the physical conditions for solidification front instability. With initiation of tearing, local interstitial melt is drawn into the tears. Due to conservation of mass, the infilling melt must come from below the tear, and the texture of the segregation reflects the filling process.

Prior to the tearing, from phase equilibria considerations, the interstitial melt is contained in the solidification front at a crystallinity of about 60–65 vol.%. The melt is multiply saturated with solid phases, and with tearing the local melt can now grow large (~1–10 cm) pegmatitic crystals of clinopyroxene, often in symplectic intergrowths with plagioclase. The melt arriving from lower in the solidification front is slightly hotter and as it cools it forms progressively smaller crystals downward in the segregation. The texture of the segregation is, thus, coarse at the top and finer downward, reflecting the filling process. This is just the opposite of expected if the segregations were blobs of residual melt from the lower solidification front that escaped and entered the upper solidification front.

Once generated, the silicic differentiates are almost impossible to remove or assimilate back into the basaltic magma. If the whole system became molten they will maintain their physical and chemical identity due to their contrast in viscosity, and being at near-chemical equilibrium they will not be assimilated by diffusion. Due to their density contrast they will, however, given the chance, tend to collect at the top of the system and undergo compaction into large silicic masses. Some large dolerite sills have large bulbous masses of such rock at the upper contacts. The inordinately large volume of these masses relative to the associated sill, the thin chilled margins of dolerite separating the mass from the country rock, and the often sharp contacts between the dolerite and the granophyre all suggest that these bodies have formed from reprocessing of basaltic bodies containing silicic segregations. This may be a process operating on many scales that contributes to building continental crust. It may today be operating at the ocean ridges in the formation of plagiogranite lenses and also in the crust of Iceland to form large bodies of rhyolite.

6.07.11.3 Silicic Segregations and Crust Reprocessing in Iceland

Silicic segregations are essentially unavoidable to form within any basaltic solidification front, yet they are spatially distributed and can only be collected if they are freed from the rock through wholesale melting. Large-scale systematic melting as in rifting provides a setting where this process can operate efficiently. The ideal locality for repeated rifting of basaltic terranes is at immobile oceanic volcanic centers where the crust can be reprocessed over and over. This promotes a strong bimodality of crustal composition. About 18% of the surface rocks of Iceland are highly silicic rhyolites. This is in striking contrast to Hawaii, where there are no rhyolitic rocks at all. Deep drilling in Iceland shows the crust laden with lenses and pockets of silicic segregations and coupled with a local ocean ridge that has periodically relocated into older crust, allowing for widespread remelting and conditions ideal for accumulating large amounts of silicic material. Detailed petrologic studies of the 200 km^3 rhyolite mass at Torfajokull Caldera shows that this body was formed by this process (Gunnarsson *et al.*, 1998). Fissures propagating into older crust bring hot basaltic magma into thin warm crust, which promote progressive wholesale melting via melting fronts propagating outward into the country rock. Because of heterogeneous melting the wall rock undergoes large-scale failure, freeing silicic segregations that collect into large masses of rhyolitic magma and sometimes erupt from the same craters as the basalts. This process is depicted by **Figure 39**. This overall process of collecting silicic segregations is very much akin to the emulsion coalescence that occurred in the Sudbury impact melt sheet. The net result of magmatic processes of this type is a bimodal suite of compositions characterized at each end by a basaltic and a silicic member.

6.07.11.4 Sidewall Upflow

Another means for escape of residual silicic melt from deep within solidification fronts is by upward flow along steep lateral walls. Since all magmas are contained within solidification fronts, some bodies will have tall steep lateral margins where low density residual melt can flow upward under Darcian dynamics and collect at higher levels (see **Figure 40**). This can only happen if the advance of the solidification front is slow enough to allow upward flow through the porous solidification front. In the upper crust solidification fronts move rapidly in response to high cooling rates, but with increasing depths in the crust cooling becomes increasing slow. This retards the inward advance of the solidus, marking the rear of the solidification front, allowing ample time for upward flow of viscous melt. Unlike the idealized flows that are depicted in **Figure 2**, these realistic flows occur deep within the solidification front and not along hard walls where residual fluid can essentially stream upward and collect rapidly at

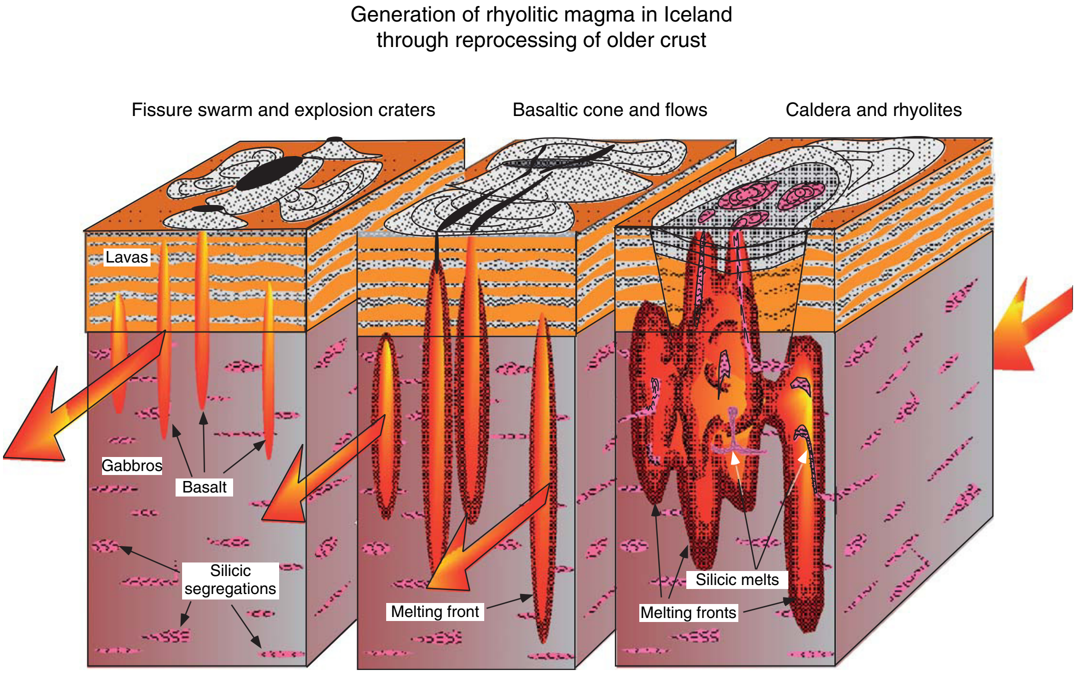

Figure 39 Reprocessing of the Icelandic crust due to propagation of basaltic fissures into older crust containing silicic segregations and the formation of large bodies of silicic material from the freeing and collection of these individual silicic segregations.

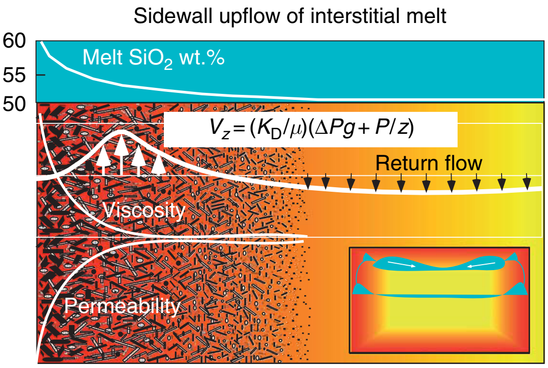

Figure 40 The flow up a vertical wall of interstitial residual, silica-rich melt deep with a solidification front. The variations in permeability and melt viscosity are indicated as is the form of Darcy's equation governing the flow.

the roof of the system. The flow is governed by Darcy's equation,

$$V_m = \frac{K_D}{\mu}\left[\frac{\partial P}{\partial Z} + \Delta\rho g\right] \qquad [28]$$

where V_m is the Darcy velocity, which is a measure of the melt flux per unit area, K_D is permeability, μ is melt viscosity, P is pressure, z is the spatial coordinate, $\Delta\rho$ is density contrast, and g is gravity. It is critical to note here that both m and K_D change strongly with distance outward in the solidification front; μ increases and K_D decreases such that the quantity K_D/μ decreases strongly with approach to the solidus. This regulates the flow and there is an optimum position within the rear of the solidification front where melt is most efficient at flowing upward. The slower the solidification front moves the more silicic is the optimum melt. In the upper crust, the dominant melt has a composition of about 55 wt.% SiO$_2$, and in the lower crust it approaches 65 wt.%. The buildup of volatiles in the residual melt helps the overall process.

6.07.11.5 Fissure Flushing

A broadly similar process to melt flow through the rear of a steep solidification front is the flushing of residual melt from an aging solidification front spanning a fissure or other sheet-like body. The process is depicted by Figure 41. During times of repose in magmatic systems, the driving pressure relaxes, conduit walls press in on the remaining magma, and solidification fronts move in from the lateral walls. The fronts eventually meet and form a bridge of

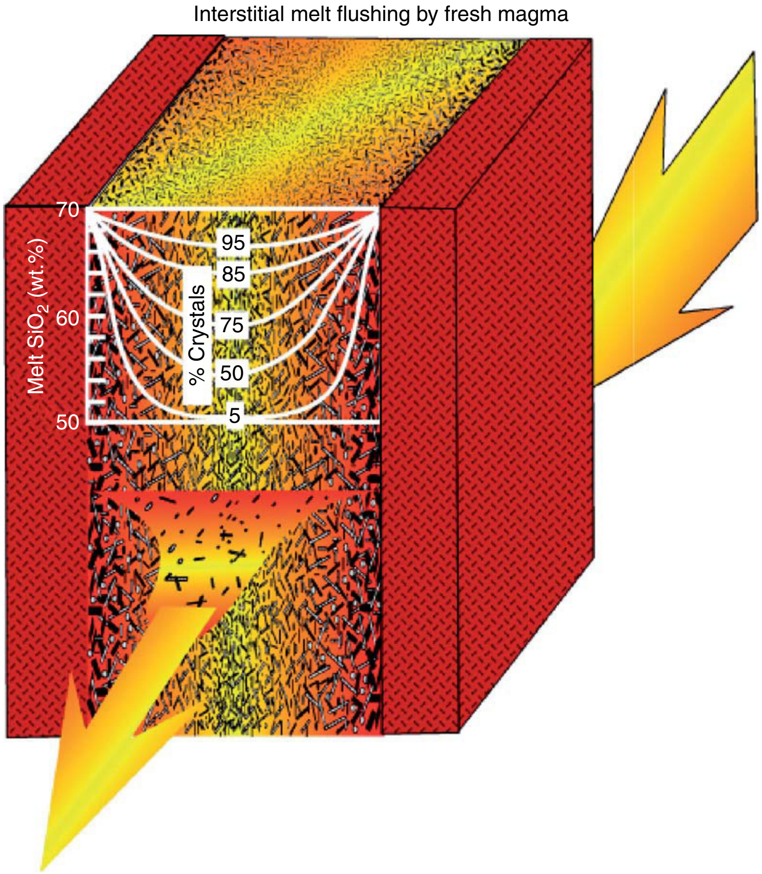

Figure 41 The process of flushing residual melt from a partially solidified fissure by reactivation of magma flow after a repose period. The curves show the variation in residual melt silica content as a function of position and degree of crystallinity within the fissure.

crystals across the conduit. As solidification proceeds, the interstitial melt becomes progressively enriched in silica as a function of position within the conduit. When the repose period ends and magma flow resumes, magma coursing this conduit will flush the residual melt from the crystalline matrix of solids. This melt will be distinctive in its differentiated chemical composition, which will appear chemically indistinguishable to crystal fractionation, and also in the telltale clots of crystals torn from the solidification front during eviction. It is processes like this that undoubtedly give rise to mildly differentiated magmas at many locations in large, long-lived magmatic systems like Hawaii. Another characteristic of these events is their optimum near-surface location on flanks of the volcano where magma transport in fissures is common. The 1955 Kilauea eruption produced lava with these characteristics (Wright and Fiske, 1971) and the ongoing eruptions of Puu Oo also show some of these features (e.g., Garcia *et al.*, 1989).

6.07.12 Magmatic Systems

Earth's surface displays a rich diversity of igneous rock from which most other rocks are derived. The majority of igneous rocks are either oceanic-floor basalts or continental granitics. The processes that produce this strong bimodality are physical processes, buttressed by chemical processes, associated with a prevailing tectonic theme. Mantle convection gives rise to seafloor spreading and a distinct style of magma production and evolution in a steady-state standing magmatic mush column capped by a passive thin sill. No continental silicic material is produced. The seafloor is an enormous gabbroic batholith. Silicic noise is produced within the solidification fronts of basaltic systems on small local scales. The key to accentuating and enhancing this silicic signal is through systematic reprocessing. Remelting of the oceanic crust in subduction zones, during massive bolide impacts, in areas like Iceland, and in other immobile crustal welts, accumulates this silicic material into viable rock masses.

Magmatic processes in and of themselves operate within a vast array of tectonic environments, but the processes involved in the behavior and evolution of magma are finite and understandable within a clear physical and chemical framework. The key to analyzing magmatic systems is to gain an integrated physical perspective of the overall process of magma production, transport, and emplacement or eruption. Magmas chemically evolve through the gain and loss of crystals, which is governed by entrainment of exotic crystals in addition to those nucleated and grown within the magma itself. But it is the understanding of the intimate coupling of spatial physical relations and processes with phase equilibria that furnishes the greatest insight into the true processes that shape the magma and the Earth itself.

Acknowledgments

This work on magmatic processes is supported primarily by the National Science Foundation via grant OPP-0440718 to the John Hopkins University (BDM). Unless otherwise noted, all figures are from the book *Magma Physics* in preparation by the author.

References

Ariskin AA (1999) Phase equilibria modeling in igneous petrology: use of COMAGMAT model for simulating fractionation of ferro-basaltic magmas and the genesis of high-alumina basalt. *Journal of Volcanology and Geothermal Researach* 90: 115–162.

Baragar WRA (1960) Petrology of basaltic rocks in part of the Labrador Trough. *Bulletin of the Geological Society of America* 71: 1589–1644.

Barksdale JD (1937) The Shonkin Sag laccolith. *American Journal of Science* 33: 321–359.

Becker GF (1897) Fractional crystallization of rocks. *American Journal of Science* 4: 257–261.

Bergantz GW (1989) Underplating and partial melting: Implications for melt generation and extraction. *Science* 245: 1093–1095.

Bhattacharji S (1967) Mechanics of flow differentiation in ultramafic and mafic sills. *Journal of Geology* 75: 101–112.

Boudreau AE (1994) Mineral segregation during crystal aging in two-crystal, two-component systems. *South Africa Journal of Geology* 4: 473–485.

Bowen NL (1915) The later stages of the evolution of the igneous rocks. *Journal of Geology* 23: 1–89.

Bowen NL (1947) Magmas. *Bulletin of the Geological Society of America* 58: 263–280.

Brandeis G and Jaupart C (1986) On the interaction between convection and crystallization in cooling magma chambers. *Earth and Planetary Science Letters* 345–361.

Brandeis G and Marsh BD (1989) The convective liquidus in a solidifying magma chamber: A fluid dynamic investigation. *Nature* 339: 613–616.

Brandeis G and Marsh BD (1990) Transient magmatic convection prolonged by solidification. *Geophysical Research Letters* 17(8): 1125–1128.

Carmichael ISE, Turner FJ, *et al.* (1974) *Igneous Petrology*. New york: McGraw-Hill Book Company.

Carr MJ, Stoiber RE, *et al.* (1973) Discontinuities in the deep seismic zone under the Japanese Arcs. *Bulletin of the Geological Society of America* 84: 2917–2930.

Carslaw HS and Jaeger JC (1959) *Conduction of Heat in Solids*. Oxford: Clarendon Press.

Cartwright J and Hansen DM (2006) Magma transport through the crust via interconnected sill complexes. *Geology* 34(11): 929–932.

Coffin MF and Eldholm O (1992) Volcanism and continental break-up: A global compilation of large igneous provinces. In: Storey BC, Alabaster T, and Pankhurst RJ (eds.) *Magmatism and the Causes of Continental Break-up*, pp. 17–30. Boulder, CO: Geologial Society of America.

Dawson JB (1992) First thin sections of experimentally melted igneous rocks: Sorby's observations on magma crystallization. *Journal of Geology* 100: 251–257.

Dicken AP, Nguyen T, and Crocket JH (1999) Isotopic evidence for a single impact melting origin of the Sudbury Igneous Complex. In: Dressler BO and Sharpton VL (eds.) *Geological Society of America, Special Paper 339: Large Meteorite Impacts and Planetary Evolution II*, pp. 361–371.

Dobran F (2001) *Volcanic Processes, Mechanisms in Material Transport.* Kluwer Academic.

Drever HL and Johnston R (1967) Picritic minor intrusions. In: Wyllie P (ed.) *Ultramafic and Related Rocks*, pp. 71–82. New York: John Wiley and Sons, Inc.

Fleming TH, Elliott DH, *et al.* (1992) Chemical and isotopic variations in an iron-rich lava flow from the Kirkpatrick Basalt, north Victoria Land, Antarctica: implications for low-temperature alteration. *Contributions to Mineralogy and Petrology* 111: 440–457.

Fuijii T (1974) Crystal settling in a sill. *Lithos* 7: 133–137.

Garcia MO, Ho RA, *et al.* (1989) Petrologic constraints on rift-zone processes Results from episode 1 of the Puu Oo eruption of Kilauea volcano, Hawaii. *Bulletin of Volcanology* 52: 81–96.

Ghiorso MS, Carmichael ISE, *et al.* (1983) The Gibbs Free Energy of mixing of natural silicate liquids; an expanded regular solution approximation for the calculation of magmatic intensive variables. *Contributions to Mineralogy and Petrology* 84: 107–145.

Gibb FGF and Henderson CMB (1996) The Shiant Isles Main Sill: structure and mineral fractionation trends. *Mineralogical Magazine* 60: 67–97.

Gray NH and Crain IK (1969) Crystal settling in sills: A model for suspension settling. *Canadian Journal of Earth Sciences* 6: 1211–1216.

Gregory RT and Taylor HPJ (1981) An oxygen isotope profile in a section of Cretaceous Oceanic Crust, Samail Ophiolite, Oman: evidence for d^{18}O buffering of the oceans by deep (>5 km) Seawater-hydrothermal circulation at mid-ocean ridges. *Journal of Geophysical Research* 86(B4): 2737–2755.

Grieve RAF, Stoffler D, *et al.* (1991) ‘‘The Sudbury Structure: Controversial or Misunderstood?’’ *Journal of Geophysical Research* 96(E5): 22,753–22,764.
Gunnarsson B, Marsh BD, *et al.* (1998) Generation of Icelandic Rhyolites: Silicic Lavas from the Torfajokull Central Volcano. *Journal of Volcanology and Geothermal Research* 83: 1–45.
Hein JR, Scholl DW, *et al.* (1978) Episodes of Aleutian ridge explosive volcanism. *Science* 199: 137–141.
Helz RT (1986) Differentiation behavior of Kilauea Iki lava lake, Kilauea volcano, Hawaii: An overview of past and current work. *Geochemical Society Special Publication* 1: 241–258.
Helz RT, Kirschenbaum H, *et al.* (1989) Diapiric transfer of melt in Kilauea Iki lava lake, Hawaii: a quick, efficient process of igneous differentiation. *Geological Society of America Bulletin* 101: 578–594.
Hersum T, Hilpert M, and Marsh B (2005) Permeability and melt flow in simulated and natural partially molten basaltic magmas. *Earth and Planetary Science Letters* 237: 798–814.
Hess HH (1956) The magnetic properties and differentiation of dolerite sills – discussion of dolerite sills. *American Journal of Science* 254: 446–451.
Ho RA and Garcia MO (1988) Origin of differentiated lavas at Kilauea Volcano, Hawaii: Implications from the 1955 eruption. *Bulletin of Volcanology* 50: 35–46.
Holden GS and Hooper PR (1987) Petrology and chemistry of a Columbia River basalt section, Rocky Canyon, west-central Idaho. *Geological Society of America Bulletin* 87: 215–225.
Hon K, Kauahikaua J, *et al.* (1994) Emplacement and inflation of pahoehoe sheet flows: Observations and measurements of active lava flows on Kilauea Volcano, Hawaii. *Geological Society of America Bulletin* 106: 351–370.
Hort M (1997) Cooling and crystallization in sheet-like magma bodies revisited. *Journal of Volcanology and Geothermal Research* 76: 297–317.
Hort M, Marsh BD, *et al.* (1999) Convection and crystallization in a liquid cooled from above: An experimental and theoretical study. *Journal of Petrology* 40(8): 1271–1300.
Hsui AT, Marsh BD, *et al.* (1983) On melting of the subducted oceanic crust: effects of subduction induced mantle flow. *Tectonophysics* 99: 207–220.
Hurlbut CSJ (1939) Igneous rocks of the Highwood Mountains, Montana Part I The Laccoliths. *Bulletin of the Geological Society of America* 50: 1043–1112.
Imsland P (1984) *Petrology, Mineralogy and Evolution of the Jan Mayen Magma System*. Reykjavik, Prentsmidjan Oddi.
Jaupart C (1998) Gas loss from magmas through conduit walls during eruption. The Physics of Explosive Volcanic Eruptions. *Geological Society of London Special Publication* 145: 73–90.
Jaeger JC (1968) Cooling and solidification of igneous rocks. In: Hess HH and Poldervaart A (eds.) *Basalts: The Poldervaart Treatise on Rocks of Basaltic Composition*, vol. 2, pp. 503–536. New York: Interscience.
Jaeger JC and Joplin GA (1955) Rock magnetism and the differentiation of dolerite sill. *Journal of the Geological Society of Australia* 2: 1–19.
Jaeger JC and Joplin GA (1956) The magnetic properties and differentiation of dolerite sills - discussion. *American Journal of Science* 254: 443–446.
Jhaveri B and Homsy GM (1980) Randomly forced Rayleigh-Benard convection. *Journal of Fluid Mechanics* 98: 329–348.
Kadanoff LP (1991) Complex structures from simple systems. *Physics Today* 9–10.
Kerr RC, Huppert HE, *et al.* (1989) Disequilibrium and macrosegregation during solidification of a binary melt. *Nature* 340: 357–367.
Khurana A (1988) Rayleigh-Benard experiment probes transition from chaos to turbulence. 17–21.
Kincaid C and Sacks IS (1997) Thermal and dynamical evolution of the upper mantle in subduction zones. *Journal of Geophysical Researach* 102: 12295–12315.
Lightfoot PC, *et al.* (1997) Geochemical relationships in the Sudbury Igneous Complex: Origin of the Main Mass and Offset Dikes. *Economic Geology* 92: 2890397.
Maaloe S, *et al.* (1989) Population density and zoning of olivine phenocrysts in tholeiites from Kauai, Hawaii. *Contributions to Mineralogy and Petrology*.
Maaloe S, *et al.* (1992) The Koloa volanic suite of Kauai, Hawaii. *Journal of Petrology* 33(4): 761–784.
Makse HA, *et al.* (1997) Spontaneous stratification in granular mixtures. *Nature* 286: 379–382.
Mangan MT and Marsh BD (1992) Solidification front fractionation in phenocryst-free sheet-like magma bodies. *Journal of Geology* 100: 605–620.
Marsh BD (1979a) Island arc development: Some observations, experiments, and speculations. *Journal of Geology* 87: 687–713.
Marsh BD (1979b) Island-Arc Volcanism. *American Scientist* 67: 161–172.
Marsh BD (1982) On the mechanics of igneous diapirism, stoping, and zone melting. *Amerian Journal of Science* 282: 803–855.
Marsh BD (1988) Crystal capture, sorting, and retention in convecting magma. *Geological Society of America Bulletin* 100: 1720–1737.
Marsh BD (1989) On convective style and vigor in sheet-like magma chambers. *Journal of Petrology* 30: 479–530.
Marsh BD (1991) Reply to comments On convective style and vigor in sheet-like magma chambers. *Journal of Petrology* 32(4): 855–860.
Marsh BD (1996) Solidification fronts and magmatic evolution. *Mineralogical Magazine* 60: 5–40.
Marsh BD (1998) On the interpretation of crystal size distributions in magmatic systems. *Journal of Petrology* 39: 553–599.
Marsh BD (2002) On Bimodal Differentiation by Solidification Front Instability in Basaltic Magmas, I: Basic Mechanics. *Geochimica et Cosmochimica Acta* v66: 2211–2229.
Marsh BD (2004) A Magmatic Mush Column Rosetta Stone: The McMurdo Dry Valleys of Antarctica. *EOS Transactions American Geophysical Union* 85(4723): 497–502.
Marsh BD (2006) Dynamics of magmatic systems. *Elements* 2: 287–292.
Marsh BD (2007) Magma Physics. (in preparation).
Marsh BD, Gunnarsson B, *et al.* (1991) Hawaiian basalt and Icelandic rhyolite: Indicators of differentiation and partial melting. *Geologische Rundschau* 80(2): 481–510.
McBirney AR (1993) *Igneous Petrology*. Boston: Jones and Bartlett Publishers.
McBirney AR (1999) *Santorini and Its Eruptions*, by Ferdinand A. Fouqué (translated by A. R. McBirney), 495 pp. Baltimore, MD: Johns Hopkins University Press.
McKenzie D (1984) The generation and compaction of partially molten rock. *Journal of Petrology* 25: 713–765.
Melnik O, Barmin AA, and Sparks RSJ (2005) Dynamics of magma flow inside volcanic conduits with bubble overpressure buildup and gas loss through permeable magma. *Journal of Volcanology and Geothermal Research* 143: 53–68.
Murata KJ and Richter DH (1966) The settling of olivine in Kilauean magma as shown by lavas of the 1959 eruption. *American Journal of Science* 264: 194–203.
Nicolas A (1995) *The Mid-Oceanic Ridges Mountains Below Sea Level*. Berlin Heidelberg: Springer-Verlag.
Osborne FF and Roberts EJ (1931) Differentiation in the Shonkin Sag laccolith, Montana. *American Journal of Science* 22: 331–353.

Philpotts AR and Carroll M (1996) Physical properties of partly melted tholeiitic basalt. *Geology* 24(11): 1029–1032.

Pirsson LV (1905) Petrography and Geology of the Igneous Rocks of the Highwood Mountains, Montana. *United States Geological Survey Bulletin no. 237.*

Ryan MP (1994) Neutral-buoyancy controlled magma transport and storage in mid-ocean ridge magma reservoirs and their sheeted-dike complex: A summary of basic relationships. In: Ryan MP (ed.) *Magmatic Systems*, pp. 97–138. San Diego, California: Academic Press, Inc.

Savage SB and Lun CKK (1988) Particle size segregation in inclined chute flow of dry cohesionless granular solids. *Journal of Fluid Mechanics* 189: 311–335.

Scheidegger KF, Corliss JB, *et al.* (1980) Compositions of deep-sea ash layers derived from North Pacific Volcanic arcs: Variations in time and space. *Journal of Volcanology and Geothermal Research* 7: 107–137.

Simkin T (1967) Flow differentiation in the prictic sills of North Skye. In: Wyllie PJ (ed.) *Ultramafic and Related Rocks*, pp. 64–69. New York: John Wiley and Sons.

Sinton JM and Detrick RS (1992) Mid-ocean ridge magma chambers. *Journal of Geophysical Research* 97(B1): 197–216.

Smith AL and Roobol MJ (1982) Andesitic pyroclastic flows. In: Thorpe RS (ed.) *Andesites Orogenic Andesites Related Rocks*, pp. 415–436. New York: John Wiley and Sons.

Smith RL and Bailey RA (1968) Resurgent Cauldrons. In: Coats RR, Hay RL, and Anderson CA (eds.) *Studies in Volcanology A Memoir in Honor of Howell Williams* pp. 613–662. Geological Society of America.

Stoiber RE and Carr MJ (1971) Lithospheric plates, Benioff zones, and volcanoes. *Geological Society of America Bulletin* 82: 515–522.

Sugimura A (1968) Spatial relations of basaltic magmas in island arcs. In: Hess HH and Poldervart A (eds.) *Basalts The Poldervaart Treatise on Rocks of Basaltic Composition*, vol. 2, pp. 537–572. New York: Interscience Publishers.

Toksoz MN and Bird P (1977) Modeling of temperatures in continental convergence zones. *Tectonophysics* 41: 181–193.

Turcotte DL and Schubert G (1982) *Geodynamics*. New York: John Wiley and Sons.

Turner FJ and Verhoogen J (1960) *Igneous and Metamorphic Petrology.* McGraw-Hill.

Turner JS (1973) *Buoyancy Effects in Fluids*. New York: Cambridge University Press.

Upton BGJ and Wadsworth WJ (1967) A complex basalt-mugearite sill in Piton des Neiges volcano, Reunion. *American Mineralogist* 52: 1475–1492.

Viskanta R and Gau C (1982) Inward solidification of a superheated liquid in a cooled horizontal tube. *Warme-Stoffubertrgung* 17: 39–46.

Wager LR and Brown GM (1968) *Layered igneous rocks*. San Francisco: W.H. Freeman.

Wager LR and Deer WA (1939) Geological investigations in East Greenland, Part III: The petrology of the Skaergaard Intrusion. *Kangerdlagssuaq, East Greenland, Medd Eroenl* 105(4): 1–346.

Walker F (1956) The magnetic properties and differentiation of dolerite sills – Critical discussion. *American Journal of Science* 254: 433–443.

Wilch TI, Lux DR, *et al.* (1993) Minimal pliocene-pleistocene uplift of the dry valleys sector of the Transantarctic Mountains: A key parameter in ice-sheet reconstructions. *Geology* 21: 841–844.

Williams H (1941) Calderas and their origin. *Bulletin of the Department of Geologial Sciences, University of California* 25(6): 239–346.

Wright TL (1971) Chemistry of Kilauea and Mauna Loa lava in space and time. *Geological Survey Professional Paper* 735: 40.

Wright TL and Fiske RS (1971) Origin of the differentiated and hybrid lavas of Kilauea volcano, Hawaii. *Journal of Petrology* 12(1): 1–65.

Wright TL and Okamura RT (1977) Cooling and crystallization of tholeiitic basalt, 1965 Makaopuhi lava lake, Hawaii. *U.S. Geological Survey Professional Paper no. 1004.*

Zieg MJ and Marsh BD (2002) Crystal Size Distributions and Scaling Laws in the Quantification of Igneous Textures. *Journal of Petrology* 43(1): 85–101.

Zieg MJ and Marsh BD (2005) The Sudbury Igneous Complex: Viscous Emulsion Differentiation of a Superheated Impact Melt Sheet. *Bulletin of Geological Society of America* 117: 1427–1450.